ÉCOLE DE TECHNOLOGIE SUPÉRIEURE
UNIVERSITÉ DU QUÉBEC

A THESIS SUBMITTED TO
ÉCOLE DE TECHNOLOGIE SUPÉRIEURE

IN PARTIAL FULFILLMENT OF THE REQUIREMNTS
FOR THE DEGREE
DOCTOR OF PHILOSOPHY
Ph.D

BY
SLAVEN KINCIC

VOLTAGE SUPPORT OF TRANSMISSION NETWORK FROM DISTRIBUTION LEVEL

MONTRÉAL, 13 JUNE 2006

CETTE THÈSE A ÉTÉ ÉVALUÉE

PAR UN JURY COMPOSÉ DE :

M. Ambrish Chandra, directeur de thèse
Département de génie électrique à l'École de technologie supérieure

M.Boon-Teck Ooi, codirecteur
Département de génie électrique à McGill University

M. Pierre Jean Lagacé , président du jury
Département de génie électrique à l'École de technologie supérieure

M. Louis A. Dessaint,
Département de génie électrique à l'École de technologie supérieure

M. Vijay K. Sood, chercheur
Hydro-Quebec (IREQ)

ELLE A FAIT L'OBJET D'UNE SOUTENANCE DEVANT JURY ET PUBLIC

LE 12 MAI 2006

À L'ÉCOLE DE TECHNOLOGIE SUPÉRIEURE

VOLTAGE SUPPORT OF TRANSMISSION NETWORK FROM DISTRIBUTION LEVEL

Slaven Kincic

ABSTRACT

In this thesis a new concept is proposed and developed. The concept is named "Transmission Lines Voltage Support Decentralization". It is shown that, when transmission lines require sustained voltage support, it is more efficient and economically beneficial to provide it on distribution level with large number of smaller sized Static Var Systems (SVS) regulating distribution voltages rather then with fewer large bulk SVS on transmission level regulating transmission voltages.

The benefits of the proposed concept over the traditional voltage support of transmission lines on transmission level with bulk compensators are underlined. The benefits include lower var requirement, lower transformer MVA requirements, possibility of elimination of LTC transformer for load voltage regulation, lower stand by requirements to satisfy N-1 reliability criterion, enhanced reliability and better voltage regulation of distribution buses. These benefits are converted into the dollar value.

The feasibility and reliability of the proposed concept is demonstrated by detailed, dynamic, real time simulations. Simulation studies have shown that the distributed, distribution voltage support units operate harmoniously in recovery after different kinds of the faults including three phase-to-ground faults.

SUPPORT DE LA TENSION DE TRANSMISSION PAR DES COMPENSATEURS STATIQUES LOCALISÉS AU NIVEAU DE LA DISTRIBUTION

Slaven Kincic

RÉSUMÉ

Dans cette thèse, un nouveau concept de support de la tension du réseau électrique est proposé. Ce concept consiste à remplacer les compensateurs statiques traditionnels par des compensateurs de plus petite capacité, localisés au niveau de la distribution. Ses avantages sont mis en évidence. Le concept peut être avantageux surtout dans le cas d'une planification et d'une construction de nouvelles lignes de transmission.

Traditionnellement, la régulation dynamique de la tension de transmission est effectuée avec des compensateurs statiques ou des compensateurs synchrones de grande capacité qui sont installés au niveau de la transmission. Cette étude propose la restructuration de l'infrastructure destinée à la régulation de la tension de transmission et le transfert des compensateurs dynamiques du côté de la transmission (haute tension HT) vers le côté de la distribution (basse tension BT) de façon à ce que les compensateurs agissent seulement sur la tension au niveau de la distribution. Enfin, pour améliorer la fiabilité du système, les compensateurs sont répartis en plusieurs unités de petite taille. Il est démontré que ce concept est bénéfique, et présente des avantages considérables. Ses caractéristiques sont analysées en régime permanent. La faisabilité et la robustesse dans les régimes transitoires sont testées au moyen de nombreuses simulations numériques. Les simulations numériques sont effectuées en temps réel et en temps différé à l'aide du simulateur *Hypersim* développé par l'Hydro-Québec. L'avantage du simulateur *Hypersim* réside dans le fait que les simulations dynamiques de longue durée peuvent être exécutées

tout en permettant d'analyser à la fois la stabilité transitoire et les phénomènes à long terme. Un autre avantage de ce simulateur, est la disponibilité des modèles détaillés de l'ensemble des composantes d'un réseau électrique. L'analyse en régime permanent et l'analyse conceptuelle sont élaborées en utilisant les diagrammes vectoriels et la théorie des circuits électriques, notamment les lois de courant et de tension de Kirchhoff. Dans l'analyse conceptuelle, cette approche est plus appropriée que celle qui utilise les équations des écoulements de puissance, car les relations entre les courants, les tensions et les chutes de tension sont linéaires plutôt que quadratiques. De plus, les diagrammes vectoriels permettent la visualisation entre les tensions et la chute de tension.

Le premier chapitre de cette thèse analyse la problématique envisagée par l'industrie de l'électricité à l'heure actuelle, notamment le problème d'instabilité de la tension qui est une conséquence directe des nouvelles tendances dans l'industrie. En bref, cette problématique consiste en l'insuffisance de la capacité du réseau de transport, la déréglementation de l'industrie d'électricité ainsi que la qualité de tension fournie. La solution traditionnelle de ces problèmes se situe dans le support dynamique de tension localisé au niveau transmission, soit avec des compensateurs synchrones, soit avec des compensateurs statiques à grande capacité de compensation. D'autre part, de nouvelles tendances reliées au protocole de Kyoto, c'est-à-dire l'évolution de la conscience environnementale et le manque de grandes ressources énergétiques, ont forcé les planificateurs de réseaux à se tourner vers les ressources renouvelables et les réseaux de production décentralisée. L'intégration des petites sources dans le réseau d'électricité conventionnel se fait au niveau de la distribution. La génération de l'électricité elle-même peut être effectuée à l'aide de machine synchrones ou asynchrones, dépendamment de la nature de la source. La génération intégrée dans le réseau d'électricité conventionnel localisée au niveau de la distribution nécessite un contrôle dynamique de tension précisément au point de l'intégration de la source dans le réseau, c'est-à-dire au niveau de la distribution. Nous pouvons affirmer que les réseaux de production décentralisée nécessitent un contrôle dynamique de tension par des compensateurs décentralisés.

Dans ce contexte, il est justifiable d'examiner si le support de tension du réseau entier peut être effectué par des compensateurs statiques de petite capacité localisés au niveau de la distribution, sans contrôler directement la tension de transmission. Cette opération est-elle réalisable, économiquement justifiable et fiable? Serait-il plus bénéfique de fournir le support de tension par un large compensateur du côté transmission ou de fournir le support de tension par plusieurs petites unités du côté distribution ? Voici les grands enjeux qui sont explorés dans cette thèse.

Les causes de la chute de tension et l'action pour y remédier sont analysés dans le deuxième chapitre. Le courant alternatif, en passant par des lignes de transmission, produit le champ magnétique qui varie en fonction du temps. Dû à l'inductance de ligne, et en accord avec la loi de Farady-Lenz, la chute de tension est induite le long de la ligne de transport. L'action pour remédier à la chute de tension dite inductive consiste à injecter un courant (appelé le courant de compensation), qui induit la tension égale mais de signe opposé, en annulant la chute de tension inductive ce qui produit, en effet, le support de tension. À la fin du chapitre, il est démontré qu'en utilisant le principe de superposition, c'est-à-dire en fournissant le support de tension du côté distribution, la tension de transmission est supportée, et vice-versa.

Le troisième chapitre aborde les principes de fonctionnement d'un convertisseur basé sur les semi-conducteurs et son application comme source de puissance réactive. Un onduleur à niveaux multiples de topologie calé par diodes est présenté conjointement avec une commande à fréquence fondamentale (FFM). C'est une configuration attrayante pour des applications de haute tension, et surtout en tant que STATCOM. La commande à fréquence fondamentale appliquée avec cette configuration minimise les pertes et permet l'optimisation de forme d'onde de tension produite par le convertisseur. En effet, le convertisseur, avec l'action rapide des interrupteurs, forme une tension alternative, quasi-sinusoïdale à partir de la tension continue du côté CC du convertisseur. La loi de

commande permettant l'application du convertisseur en tant que compensateur (STATCOM) est alors conçue et testée.

Dans le chapitre quatre, il est démontré que la stratégie d'utiliser plusieurs compensateurs de petite taille pour le support de tension du côté distribution présente plus d'avantages que celle d'utiliser un compensateur de large taille du côté transmission. Les avantages incluent i) la diminution de réserve afin d'assurer la fiabilité ii) l'élimination du transformateur élévateur pour couplage de compensateur avec le réseau et, iii) la diminution de la capacité du compensateur pour assurer le support de la tension. L'étude, réalisée à l'aide de la simulation, a été effectuée sur un système test à l'aide du simulateur *Hypersim*. Le système test consiste en une ligne radiale de longueur de 300 km et de 315 kV. La puissance maximale transmise à travers la ligne est de 375 MW. Le support de tension est effectué au niveau de la distribution à l'aide de quatre compensateurs (STATCOM). Il est démontré que la perte d'un compensateur n'affecte pas le système. Par contre, si le support de tension est fourni par un compensateur du côté transmission, la perte du compensateur mène à l'effondrement de la tension. La simulation a démontré aussi que plusieurs compensateurs dynamiques (STATCOM) fonctionnent en synchronisme sans interactions néfastes lors des phénomènes transitoires.

Le chapitre cinq constitue une étude détaillée du concept proposé. Deux schémas sont comparés - le schéma traditionnel, c'est-à-dire la régulation dynamique localisée au niveau de la transmission par un compensateur de grande capacité versus le schéma proposé, la régulation dynamique de la tension au niveau de la distribution par plusieurs compensateurs de petite capacité. Un système général consistant en K lignes de transmission, fournissant N charges à travers N sous-stations reliées en parallèle, est considéré. Les lignes de transport sont modélisées à l'aide des paramètres distribués. Les diagrammes vectoriels sont utilisés pour démontrer la faisabilité et la fiabilité. Par la suite, les équations permettant le calcul de la puissance nominale du compensateur sont

déduites en présentant deux cas d'étude : le premier étant un compensateur localisé au niveau de la distribution, et le second, un compensateur localisé au niveau de la transmission. Le calcul en p.u. est utilisé. Les équations déduites sont générales, et offrent une application à tous les niveaux de tension sur différentes longueurs de lignes. À partir des équations déduites, la puissance nominale en vars est comparée dans deux schémas de support de tension. La comparaison est effectuée entre différentes longueurs de ligne et différentes puissances maximales transmises à travers la ligne. L'étude a démontré que, dans la majorité des cas, le positionnement de la compensation au niveau de la distribution présente plus d'avantages par rapport au positionnement localisé au niveau de la transmission en termes de vars requis pour le support de tension. Les avantages sont convertis en valeur approximative de dollars. Les pertes dues à la résistance de lignes sont comparées dans deux schémas de compensation. Il est montré qu'en général, les pertes sont en général moindres pour la compensation du côté distribution. Finalement, un système de test est étudié à l'aide d'une simulation dynamique.

Dans le chapitre six, les équations générales permettant le calcul du besoin réactif du réseau nécessaire pour la régulation de tension sont déduites à partir des diagrammes vectoriels. Les équations sont générales et applicables à l'ensemble de la distribution des compensateurs et à toutes les topologies du réseau. La validité des équations est confirmée avec trois méthodes indépendantes. L'avantage des équations déduites par rapport aux équations de l'écoulement de puissance réside dans le fait que les besoins réactifs des compensateurs peuvent être calculés explicitement dans le cas de la compensation localisée au niveau de la transmission. Le deuxième avantage de ces équations est que celles-ci permettent l'observation de la proximité du point d'effondrement de la tension.

L'objectif du chapitre sept est de surmonter l'écart entre le secteur de transmission et de distribution dans la planification du réseau électrique ainsi que la régulation de tension de

transmission et parallèlement, de mettre en évidence le concept avancé, notamment la décentralisation de la régulation de tension de transmission et son transfert du niveau de la transmission vers le niveau de la distribution. L'analyse portera sur une ligne radiale de 400 km de longueur et de 230 kV de tension nominale, fournissant 800 MW aux quatre centres situés le long de la ligne. Le système radial a été retenu pour cette étude, car les lignes radiales sont les plus vulnérables et les moins fiables. Présentement, une multitude de lignes radiales sont en service à travers le monde, et ces lignes exigent une régulation dynamique de la tension, d'où l'importance de cet exercice. De plus, les lignes radiales seront aussi utilisées afin de permettre l'électrification des communautés éloignées dans les pays du tiers monde aussi bien que dans les pays de grande superficie. La tension de la ligne est réglée dynamiquement par quatre compensateurs statiques de var (SVC) du côté distribution. La stabilité et la robustesse du concept proposé, en prenant en considération les différentes conditions de charge ainsi que certaines failles, sont démontrées à l'aide de la simulation numérique.

Finalement, les conclusions ainsi que les recommandations pour les travaux futurs sont présentées dans le chapitre huit. Les conclusions suivantes sont déduites, à partir du matériel présenté dans ce document:

1. La régulation dynamique et le support de tension du réseau de transmission peuvent être effectués d'une façon plus économique du côté distribution sans le contrôle direct de la tension de transmission.
2. Lorsque la tension de distribution est réglée dynamiquement, la qualité de tension fournie aux consommateurs est améliorée, et la possibilité d'effondrement de tension due à la dynamique de moteur à induction s'en trouve diminuée.
3. Si la tension de distribution est contrôlée directement, le transformateur changeur de prises n'est pas requis, par conséquent le coût du maintien est diminué.
4. Les compensateurs statiques installés du côté distribution peuvent être branchés directement. Le transformateur élévateur pour le couplage avec le réseau n'est pas

nécessaire, ce qui diminue le coût de compensation d'environ 20 %.

5. L'élimination du transformateur élévateur contribue à la fiabilité du réseau.
6. Si la compensation est effectuée avec plusieurs compensateurs installés du côté distribution, la perte d'un compensateur n'affectera pas le réseau de façon considérable. Par contre, si la compensation est effectuée avec un compensateur du côté transmission, la perte du compensateur pourra mener à l'effondrement de la tension.
7. Les pertes Joule sont, en général, diminuées si la compensation se fait du côté distribution.
8. La quantité de puissance réactive requise pour le support de tension du côté distribution est diminuée par rapport à celui effectué du côté transmission.
9. Le support de tension d'une ligne longue peut être effectué efficacement et économiquement du côté distribution.

Finalement, dans le cas des réseaux électriques de type radial constitués de très longues lignes de transport (de longueur 400 km et plus), les compensateurs statiques localisés au niveau de la transmission jouent un rôle important au niveau de la stabilité transitoire et des petits signaux. Les compensateurs statiques localisés au niveau de la distribution peuvent probablement assumer ce rôle en les remplaçant, mais cette thèse n'analyse que le problème d'effondrement et de support de la tension. En effet, l'aspect de la stabilité transitoire, ainsi que l'amortissement des oscillations électromécaniques n'est pas abordé dans cette étude et il représente une recommandation pour le travail futur.

ACKNOWLEDGMENTS

The thesis represents a fraction of the work that has been completed in the period between 2001 and 2004. The thesis is the compilation of some six conference papers that have been reviewed and presented in 2002 and 2003 on conferences in Halifax (LESCOPE 2002), Dubrovnik (EPE-PEMC 2002), Lisbon (IEEE Mediterranean Conference on control Automation), Montreal (CCECE 2003 and LESCOPE 2003) and Toronto (PES2003) together with journal papers that has been published or accepted for publication in IEEE Transaction on Power Delivery and IEE Proceedings on Generation, Transmission and Distribution.

The number of the people have helped me to complete this work and I want to thank to all of them.

First of all I want to express my deepest gratitude to my director Dr. Ambrish Chandra for the continuous support, funding, encouragement, time and confidence he gave to me. I have completed my master thesis under his direction too.

I want to express my deepest gratitude to Dr. Boon-Teck Ooi. I have been privileged to work under his close guidance and supervision. It was an illuminating and motivating experience. He has shown me how to fly through time and space as electromagnetic waves. He was the excitation and control circuit I generated under.

I want to express my deepest gratitude to Prof. Donald McGillis for his help and contribution. He has shared a part of his experience and time unselfishly with me.

I also want to thank to Dr. Z. Huang for his help with Hypersim and his friendship.

I would like to acknowledge to Ecole de technologie supérieure for providing me three fellowships (bourse aux mérités) for 2001, 2002 and 2003 and for giving me an opportunity to lecture different undergraduate and graduate courses.

Finally, special thanks go to my wife for her support and sharing her time with me throughout this research, before and after.

TABLE OF CONTENTS

LIST OF FIGURES

Page

LIST OF TABLES

Page

LIST OF SYMBOLS

$\mathbf{V_S}$	sending end voltage
$\mathbf{V_{Ri}}$	transmission side receiving end voltage of i^{th} node
$\mathbf{V_{Li}}$	distribution bus load voltage of i^{th} load center
X_i	transmission line reactance of i^{th} line section
X_{Ti}	power delivery transformer reactance of i^{th} substation
$\mathbf{I_{Ci}}$	compensating current i^{th} substation
$\mathbf{I_{Li}}$	load current of i^{th} substation
$\mathbf{I_i}$	line current through i^{th} section of the line
P	power delivered over one transmission line
N	number of units
M	number of transmission line sections
Q_{iD}	reactive power required to provide voltage support on distribution level
Q_{iHV}	reactive power required to provide voltage support on transmission level
$\mathbf{I_{Cl}}$	compensator current when voltage support provided on transmission side of power delivery substation with lumped compensator
$\mathbf{I_{Cd}}$	compensator current when voltage support provided on distribution side of power delivery substation with distribution compensator
P_{max}	maximum power delivered over one transmission line
P_{SIL}	surge impedance load (used as 1 p.u.)
M	ratio P_{max} / P_{SIL}
Qd	reactive power provided by distributed distribution side compensator(s)
Ql	reactive power provided by lumped transmission side compensator

CHAPTER 1

INTRODUCTION

Transmission systems are already highly stressed due to deregulation, rising demand, and difficulties in constructing new lines. As a result, these systems are prone to voltage instabilities. As the possibility of the voltage collapse limits the transmission capacity over the lines, reactive power compensation is required to provide voltage support. More and more reliance is placed on voltage support devices providing and absorbing vars, thus making power systems susceptible to voltage instabilities should some of these devices fail. In recent years, numerous voltage incidents have occurred around the world, resulting in complete or partial black out [1-4]. Voltage stability assessment and voltage regulation have become more important issues. Increased consciousness of the subject has resulted in some special publications over the last decade [5]-[7].

In addition, growing environmental concerns and the unavailability of large traditional natural resources have forced energy planners and the scientific community to turn towards renewable resources and distributed generation. An EPRI study has indicated that by 2010, 25% of new generation in North America will be distributed [8]. Distributed generation will include reliable energy sources as micro-turbine and fuel cells as well as wind and solar energy. The distributed generation sources will be embedded into the power system at the distribution level, scattered around main power grid. The generation itself may be carried out with synchronous or induction machines. Whatever the form of the distributed generation, it will require voltage control thus pushing voltage support from the transmission to the distribution level. In this context it seems timely to examine whether voltage support of transmission lines can be successfully shifted from the transmission to distribution level. Is it feasible, reliable and economically justifiable? This is the direction this thesis is heading toward.

1.1 Voltage Regulation

It is well known that voltage control issues in power systems are related to reactive power compensation. The usual approach to reactive power management is to minimize reactive power transfer between different voltage levels. On the transmission level, the flat voltage profile is achieved when the line is naturally loaded. In this case the reactive power produced by the line capacitance corresponds to the reactive power absorbed by the line inductance. Line current and voltage are in phase in every point of the line and the losses are the lowest for a given power transfer. When the line is overloaded/underloaded, the consumption and generation of the reactive power do not match causing variation of the voltage. The role of compensator on the transmission level is to change the line parameters in order to match consumption and generation of reactive power [9]. Traditionally, this is achieved by inserting inductance and capacitance into the system, by synchronous condensers, or with static var system (SVS).

On the distribution level, the philosophy of the voltage regulation differs from that on the transmission level. Traditionally, reactive requirements of the loads and the voltage control are provided by combination of switched capacitors, load tap changing (LTC) transformers or line regulators. However, it has been recognized that LTC transformer can be a principal cause of voltage instability leading to voltage collapse [1]. It is incapable of stepless variation of voltage and has slow response.

The role of the ideal compensator is to change dynamically the line parameters in order to match instantaneously production and consumption of the reactive power on the point of its coupling with the grid. During the high load periods the reactive power consumed by the line inductance is higher then that supplied by the line capacitance and the compensator has to supply reactive power. On the other hand, the compensator has to absorb reactive power to prevent overvoltages that arise during light loads. Therefore,

depending upon the line loading, the compensator has to function on either side: as a source of reactive power or as a sink of reactive power.

1.2 Needs for Dynamic Voltage Regulation

There are different reasons for fast, dynamic voltage regulation. Some of them are considered in the following subsections.

1.2.1 Fault Clearing

If the heavily compensated, overloaded line is subjected to sudden open circuiting due to the fault clearing, the line current is cut, so also is the voltage drop it causes. Because of the fast current change and line inductance, transient over-voltages arise. If the large number of slow acting compensation devices, previously providing reactive power, is still on line they also aggravate situation. A large amount of reactive power is released into the system tending to increase voltage to a dangerously high level. Therefore, under the fault conditions and the associated clearing process, the compensators must act fast to absorb reactive power to avoid insulation failures of the power system and compensation equipment.

1.2.2 Wind Farms

Larger numbers of wind farms, using induction generators, are being embedded into the distribution system, rising spectra of voltage issues on distribution feeders. The variable power output from induction generators is accompanied by variation in reactive power, causing voltage fluctuations which can seriously affect neighboring loads and even induction generators themselves. The wind farms often do not take part in voltage regulation, and they are being simply disconnected from the power system during the disturbances. To regulate voltage, the installation of dynamic voltage regulation device

that can provide or absorb reactive power is required. Increase in number of wind farms, coupled with distribution grid with low short circuit capacity, will require installation of larger number of smaller sized Static Var Systems (SVS) on distribution level capable to provide efficient voltage regulation. Looking into the future, one can foresee that increase in number of wind farms coupled with distribution grid will require adequate voltage support on distribution level. It can be said that distributed generation shows need for distributed, distribution level, voltage regulation.

1.2.3 Induction Motors

Transient voltage instability or induction motor instability is another form of voltage instability that can lead to fast voltage collapse. For its prevention, dynamic voltage regulation is required. A closer look shows that induction motor loads behave as follows: Large industrial motors normally have under-voltage protection by which they are tripped as soon as the voltage drops to 30% to over 65%) [1]. Once they are tripped, they cease to be a problem to voltage recovery. This leaves the smaller motors which have thermal overload protection only. During the short circuit fault, or some other voltage disturbance these smaller motors are decelerated by the loads to low speeds. Upon the clearing of the fault, the still connected motors all accelerate at the same time drawing large currents from the transmission line because of the large slip s (low speed). The large accelerating motor current cause high voltage drop causing voltage collapse in week system or in system with lack of reactive power. Loads having low inertia as air conditioners and refrigerators are the most onerous.

1.2.4 Prevention of Overvoltages

For minimizing overvoltages due to load rejection and switching operations the dynamic voltage regulation is required. It is done with SVC (TCR). The example of SVC to prevent overvoltages are ABB installations of SVC (four TCR 75 Mvar each) in the

Mexican power system (1982 Temascal), installation of SVC in Indian (Kanapur 1992)power system, installation of SVC in Namibia (520 km radial line -SVC 250 Mvar inductive-80 Mvar capacitive).

1.3 State of Art Devices

1.3.1 Reactive Power Management

Traditional means of reactive power management and voltage support/control, apart from generator itself, have been synchronous condensers switched/fixed capacitors and inductances. The synchronous condensers have been connected on transmission and sub-transmission voltage levels to improve voltage profile under varying load conditions and contingency situations over the last 80 years [9]. Their advantage is possibility to provide and absorb continuously reactive power enabling smooth voltage control over wide range of operating conditions. Their main drawbacks are rotational instabilities and high maintenance requirements due to rotational parts. For economical reason their application on sub-transmission voltage levels has been replaced by fixed/switched capacitor banks. In spite of their low cost, the capacitor banks have drawbacks of slow response, introduction of harmonics due to switching operation of the breaker and possibility of resonance with the rest of the power system. Moreover, they occupy a large amount of real estate and they cannot provide stepless voltage control. As the breaker has limited life (typically 2000 to 5000 switching operation) they are not suitable for systems where frequent capacitors switching is required.

Developments in solid-state technologies, micro-processor technologies and Flexible AC Transmission Systems (FACTS) have led to the application of power electronic based switching devices for reactive power management and voltage control. Due to their fast switching capability and voltage and current ratings they can provide fast and accurate dynamic voltage control at transmission and distribution levels. The power electronic

based FACTS devices can overcome the traditional compensators drawbacks and with their fast dynamics they can significantly improve power system stability and voltage profile. Power switching device can undertake a role of breaker and be used for fast switching in/out of capacitor banks and inductance. These devices called Static VAr Compensators (SVC) provide advantage of fast response and no wear and tear. They consist of Thyristor Switched Capacitor (TSC) /Fixed Capacitors (FC)/Switched Capacitors (SC) and Thyristor Control Reactor (TCR).

Power electronic converter can be applied to provide voltage support. They shape DC voltage and produce AC voltage of controllable amplitude and phase. In this case they simulate AC source and we talk about Static Synchronous Compensator or STATCOM. The voltage support can be also provided with HVDC back to back configuration if the power converters forming HVDC consist of full controllable power switching devices.

1.3.2 Shunt FACTS Controllers

The Thyristor Switched Capacitors – Thyristor Control Reactor (TSC-TCR) is a mature FACTS controller [9-16] based on proven and reliable technology. The first installation date from 1978 near Rimuski, Quebec. The compensator is used for performance evaluation and is applied for regulation of 230 kV transmission voltage. The installation consist of 93.6 Mvar fixed capacitors bank wye-connected and 93.6 Mvar TCR delta-connected. Later the same principles are applied to provide dynamic voltage regulation and voltage support at five intermediate points along 1000 km of Hydro-Quebec's long transmission lines enabling delivery of James Bay power [12]. Today, TCR-TSC/SC/FC are routinely installed on transmission level to provide transmission voltage regulation of long lines [17,18]. TSC-TCRs have fast response, but they have some serious drawbacks as high cost, possibility of resonance with the rest of the power system, introduction of harmonics and larger installation area. Moreover, they behave as a variable admittance.

Their reactive power output is largely dependent on the system voltage. Therefore, if the line voltage goes down, the reactive power supplied by the shunt capacitors also reduces.

One of the most versatile FACTS devices is a STATCOM [20-28]. It is basically alternative voltage source behind reactance. Its application can vary depending on the needs of power system where it is to be installed. In transmission system, it can be considered as transmission expansion alternative to provide big savings. It can be used to stabilize the system and improve damping, or to support the voltage profile [16-28]. In distribution system, STATCOM can be applied for power factor correction of the load, or for voltage regulation. Moreover, it can be used as dynamic supplement to shunt capacitors because of high price of switching devices for high MVA ratings, or it can act alone as individual unit. The STATCOM itself, in spite of numerous advantages over traditional compensators, has some serious limitations. The main building block of the STATCOM is Voltage Source Converter (VSC). When applied in transmission system, the rating of switching devices can be a problem. Moreover, in order to produce output voltage and current low in distortion, the switching frequency has to be increased which implies higher switching losses. The numerous efforts have been undertaken in order to overcome these limitations. The solution of this problems has been seen in different multi-pulse arrangements of power converters, putting switching devices in series [29] or in the various multilevel topologies [30-40]. The power switching devices evolve in the direction of increased voltage and current ratings, and switching frequency with decrease in switching losses. The promising power electronic switching devices for high voltage and high power applications are GTO (Gate Turn Off Thyristor) and IGBT (Insolated Gate Bipolar Transistor). Their present voltage and current ratings are about 6 kV, 6 kA for GTO and 1.7 kV and 0.8 kA for IGBT. Switching frequency is of order 5 and 20 kHz for GTO and IGBT respectively. Development target maximum voltage and current rating of GTO is about 10 kV and 8 kA while for IGBT is of order 3.5 kV and 2 kA.[41]. It is anticipated that higher frequency switching modulation strategies will be applicable on transmission level in recent future [42-46]. That would make their application in

power system even more attractive, especially on transmission level making STATCOM an attractive alternative to new transmission line installation. The main advantage of STATCOM over its traditional counterparts (TSC-TCR) is in its intrinsic possibility to provide voltage independent reactive output so that voltage profile of line can be supported even up to higher power level as compared to TSC-TCR of the same rating. In case if the maximum rating of the STATCOM has been reached, the STATCOM will continue to supply rated reactive power while TSC reactive output decreases proportionally to square of the line voltage.

1.3.3 Static Var Systems

In this work the term Static VAr System (SVS) is treated as a continuously controllable source of reactive current. It represents a combination of switched capacitors (SC), switched inductance (for economy), thyristor switched capacitor (TSC), thyristor control reactors (TCR) and SVCs or STATCOMs (to give continuously adjustable control between the capacitor steps). Some of above mentioned configurations are displayed on the Fig. 1. The power electronic switching devices allow fast action and fast adaptation to current loading condition in order to alleviate transients and to relax power system.

Figure 1 Different arrangements of static var compensators: a) TCR with switched capacitors, b) TCR-TSC.

1.3.4 Positioning of SVS

Historically, synchronous condensers, connected at the sub-transmission and transmission buses, have been used to supply the continuously adjustable capacitive or inductive

currents to support the voltages at the load centers [9]. Because of the precedence set by synchronous condensers, the SVSs which have largely supplanted them, still tend to be situated at the sub-transmission and transmission buses. Even the term FACTS tends to impose application on transmission level. However, SVSs are suited to distribution bus voltages and sizes. This is because they are based on solid-state technologies, which have grown from the application of thyristors, gate-turn-off thyristors (GTOs) and insulated gate bipolar transistors (IGBTs) to variable speed AC motor drives. The controllers of SVS such as the Static VAR Compensators (SVCs) and the STATic COMpensator (STATCOM), are solid-state switch technologies pushing upwards to the higher MVA ratings of power utilities. In fact, this has been one motivation of multi-level converter research. A few manufacturers have already mastered the technology of connecting GTOs or IGBTs in series to increase the voltage ratings of STATCOMs to distribution voltage levels. Recent examples are following ABB installations (SVC light - that is ABB trade mark for STATCOM): *Hagfors, Sweeden* -STATCOM (based on IGBT technology together with PWM) rated 44 Mvar directly connected at voltage 10.5 kV via its phase reactor and *Moselstahlwerk* in Trier -STATCOM rated at 20 kV, 38 Mvar is directly connected at 20 kV votage via its phase inductor [47,48].

1.3.5 Distribution Level SVS

Developments in solid-state technologies has enabled the SVSs to have fast voltage control at distribution levels. Smaller sized SVCs and distribution STATCOMs (D-STATCOMs) have been successfully developed, tested and applied, providing voltage regulation for large, fast fluctuating loads, such as, arc furnaces, arc welders, rolling mills and very large motors which start and stop frequently [49],[50]. In [51], it has been demonstrated that fast acting SVC can prevent voltage collapse due to induction motor instability. In [26] and [52], results of feasibility studies of distribution STATCOM application on Commonwealth Edison's power system have been described showing that performance of a STATCOM can benefit the system if STATCOM properly coordinated

with existing voltage control equipment. The benefits include enhanced power quality, increased loadability while number of switching operations and LTC operations has been decreased, reducing maintenance requirement. Many companies have put D-STATCOM on the market, available with or without energy storage as option. Recent installation of D-STATCOM in BC Hydro System is described in [53], and installation of Distributed Superconducting Magnetic Storage System (D-SMES) in Entergy System for improvement of Voltage Stability has been reported in [54]. Most of the papers discussing application of distribution side dynamic voltage control consider only one SVS. The merits of removing voltage support from transmission side to distribution side of power delivery substation and dispersing it in the form of small size units have been investigated in [55-59].The preliminary findings based on reliability, lower VAr and transformer requirement favor distributed, distribution compensation.

1.4 Research Objectives

This research addresses voltage issues in modern power system. The main goal of this thesis is to investigate avenues that can lead toward economical and reliable voltage regulation of overall power system. Based on current state of development and actual problematic, as described above, the objectives of this research are as follows:

1. Enhancement of voltage stability of electric power grid.
2. Enhancement of voltage quality on distribution feeders.
3. Increase of transmission capacity of transmission system
4. Development of new control techniques for application of power electronic converter in voltage control (STATCOM)
5. Investigating the impact of shunt compensation on reliability
6. Investigating optimal positioning of voltage support devices

These issues are considered in detail in the work that follows.

1.5 Research Tools

As a music is made of tones and the poem from words, this thesis is made of the basic laws of circuit theory, namely, Kirchhoff's current and voltage laws together with vector diagrams. They are used as main research tools. For the realization of the dynamic study and enumerated objectives, standard simulation packages such as MATLAB, together with the newest available in power industry, HYPERSIM, software and simulator developed by IREQ, Hydro-Quebec's research institute, for real time, dynamic simulation of power systems. The simulator is state of the art equipment based on parallel processors. HYPERSIM is based on EMTP software mostly. The main advantage of HYPERSIM is availability of high precision models of lines, loads and SVCs based on many years of experience of R&D at IREQ. In this thesis HYPERSIM is used because it was available, not because it is required. However, importance of real time dynamic simulation is in fact that long term dynamic stability study can be performed to insure that there are no long term instabilities following contingency situations.

1.6 Outline of Thesis

The main contribution of this thesis is in proposing a new concept, namely, "Transmission Voltage Support Decentralization and Sustained Voltage Support of Transmission Lines from Distribution Level". It is demonstrated in this thesis that sustained voltage support of transmission lines can be provided, more efficiently, with large number of smaller sized distribution, distributed SVS scattered all around the main grid compared to smaller number of lumped SVS on transmission level. The term "more efficiently" means better voltage regulation for smaller cost or "to get more for less money". Finally, the obtained conclusions are verified with real time dynamic simulation using detailed modeling and professional, state of the art tool for simulation of power systems.

The structure of the thesis is as follows:

In Chapter 2 the principle of voltage drop and voltage support are discussed. In Chapter 3 the principles of operation of STATCOM are reviewed together with its control circuit. In Chapter 4 the advantages of removing voltage support from transmission level to distribution level are quantified on radial system using simplified model of the line. In Chapter 5 detailed modeling of lines is undertaken and voltage support on distribution level with N compensator is discussed. In Chapter 6, general equations allowing reactive power requirements are deduced. In Chapter 7 the voltage support required by a long, radial transmission line in feeding several remote load centers spaced along its length is addressed. It has been shown that it is feasible to use Static Var Systems (SVS) located on distribution buses of each of the load centers. Finally, in Chapter 8, the conclusions are drawn and suggestions for future work are given.

CHAPTER 2

VOLTAGE DROP ANALYSIS

2.1 Introduction

This chapter is concerned with maintaining the voltage profile of a system by means of reactive power management. The mechanism causing voltage drop across the transmission line and the remedy action to cancel voltage drop is identified. Of the various test scenarios that have been examined the radial system has been chosen due to variety of reasons: 1) it gives clear insight into the mechanism of the voltage drop and the voltage boost; 2) every power system, regardless of its topology, seen from the point of coupling with power delivery substation, is seen as a radial system since it can be modeled as simple Thévenin equivalent circuit; 3) the radial systems are known to have lowest reliability and highest vulnerability and 4) the radial systems are most likely to develop voltage problems.

The chapter begins with a discussion of some basic concepts related to power transmission over the line leading toward identification of voltage drop causes and action to remedy it. Afterwards, an analysis of a non compensated line is undertaken followed by the effect of power factor correction of the load and then the analysis of a compensated line where the compensation is on the receiving-end high-voltage buses or low-voltage buses is effected. These analytical treatment of voltage regulation is the key to understanding the focus of this thesis and the conclusions which follow.

2.2 Phenomenology of Power Transfer

The power industry offers to its clients energy in the form of the electricity. The voltage and current are principal entities the industry operates with. The potential difference

(voltage) is created in power plants using magnetic forces, transferred over the line and offered to consumes. Physical significance of potential difference is possibility to do a work by electrical forces between the points the potential difference exist. This work consists in moving free charges through conducting medium between two points the difference of potential is imposed (conduction current), allowing conversion of electrical energy performance. The work is energy in conversion process. The work effected by electrical forces in moving a charge q between points P_1 and P_2 the difference of the potential U exist is:

$$W = \int_{P_1}^{P_2} \vec{F} d\vec{l} = q \int_{P_1}^{P_2} \vec{E} d\vec{l} = qU \tag{2.1}$$

where U [V] is voltage (potential difference) between point P_1 and P_2. and E(V/m) is electrical field in conductor and q [C] is one charge carrier that participate in electrical current. When consumer load connected on utilities output within points the potential difference exists, it draws a current. It can be said that current is medium for energy conversion. The conduction current is drift motion of the free charges (free electrons), under the influence of the electrical forces (Coulomb's forces) and free charges in solids are consequence of metallic bonds.

This potential difference (voltage) provided by utility is created in magnetic field of generator using magnetic forces to redistribute free charges in the conductor, the armature of the generator is made from. The magnetic force per unit charge q in motion is given by:

$$\frac{\vec{F}_m}{q} = \vec{v} \times \vec{B} \tag{2.2}$$

where **B** is magnetic flux density created by excitation circuit and ferromagnetic material the generator rotor and stator are made of, and $\boldsymbol{v}$ is a velocity armature conductors

move(in fact the conductors are stationary but field created by excitation circuit is moving). Under the influence of the magnetic forces, free charges are drifted toward one end of the conductor living the other end positively charged. The separation of the charges create electric field and potential difference. The electric forces balance magnetic forces according to:

$$\vec{F}_m + \vec{F}_e = q\left(\vec{v} \times \vec{B} + \vec{E}\right) \tag{2.3}$$

The potential difference created between two points is given as circulation of electric field between this two point act as the source of *emf* according:

$$\int_{P_1}^{P_2} \vec{E} d\vec{l} = V_2 - V_1 = U = -\int_{P_1}^{P_2} \left(\vec{v} \times \vec{B}\right) d\vec{l} \tag{2.4}$$

The equation (2.4) is referred as a motional *emf*. The generator of *emf* is number of conducting loop in rotating magnetic field, connected in series so that potential difference, obtained using magnetic forces to separate free charges, is added. Due to sinusoidal distribution of magnetic field in the generator and the generator geometry, the potential difference obtained pulsates following sinusoidal law. This potential difference is offered at distribution feeders to consumers. When consumer is connected on potential difference with its load, it draws current. The current flowing through the armature of generator creates its magnetic field (armature reaction). Interaction of the excitation magnetic fields and current through the armature (armature magnetic field) produces mechanical forces opposing to rotation according to:

$$d\vec{F} = Id\vec{l} \times \vec{B} \tag{2.5}$$

and mechanical work has to be invested to continue to rotate generator rotor to support potential difference that results in current flow. It is a process of conversion of mechanical energy into electrical energy.

The potential difference offered on distribution feeders has to be transferred through the line or, as it is said, line has to be energized or charged to function. As the potential difference pulsate, line is continuously charged and discharged. The charging of the line can be seen as charging current. As soon as difference of potential exist (charge is deposed) between two lines or between line and ground, the electric field exists surrounding the line suggesting that line can be modeled as capacitance per unit of length and current i(t) is charging current as shown in Fig.2. As the voltage pulsate, electromagnetic field surrounding the line pulsates too. The charging energy is provided by the source (generator) and the charging energy is continuously exchanged between electromagnetic field surrounding the line and generator magnetic field. The charging current is medium for the transfer of charging energy. The line charging energy can be termed reactive because it is not dissipated but exchanged between line and generator. It is consistent with the fact that, when generator has to supply reactive power the excitation current has to be increased in order to boost magnetic field. The reaction of the line against voltage changes is capacitive current:

$$i_C = C\frac{dU}{dt} \tag{2.6}$$

The line opposes to voltage changes. To change the potential difference, the charging of the line has to be changed first resulting in current that lead to voltage. During the line charging, charging current leads the voltage by 90 degrees as indicated in (2.6). Whether loaded or not, line has to be charged to function and charging energy has to be supplied. The charging energy depends on line length and voltage level.

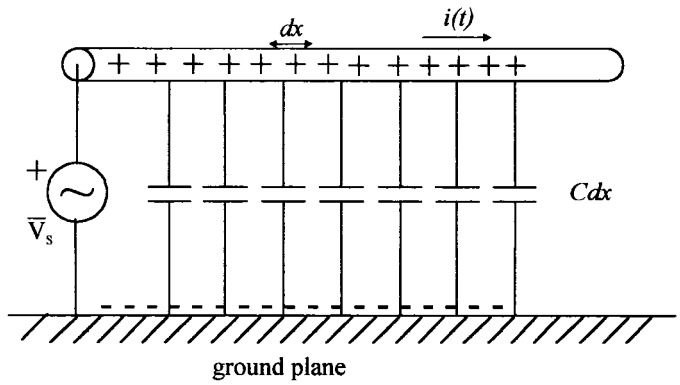

Figure 2 Open circuit transmission line during charging

When the line is loaded as shown in Fig.3, the load draws pulsating sinusoidal current that superpose to charging current. The pulsating current will cause pulsating magnetic field passing through the loop between two conductor (or conductor and ground) as illustrated in Fig.3.

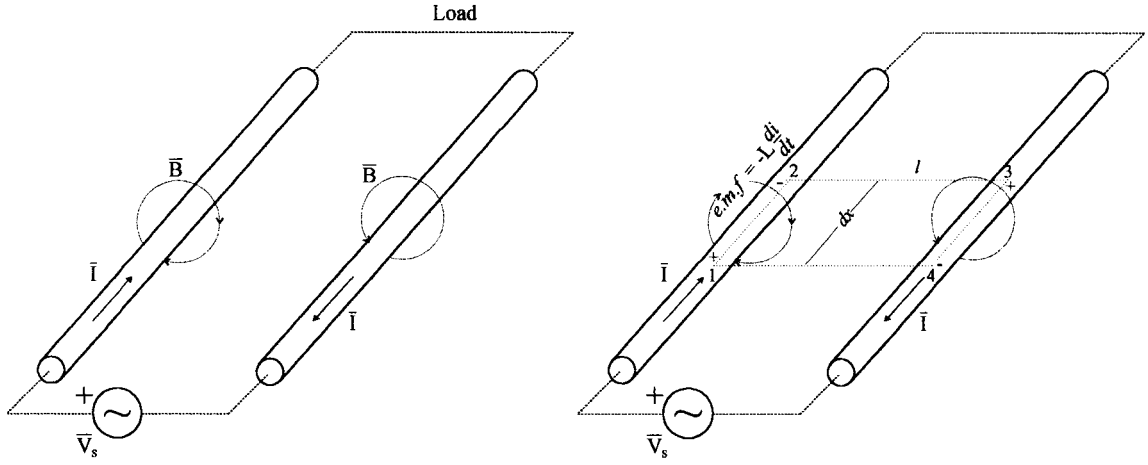

Figure 3 Simplified representation of transmission line

The pulsating magnetic field, in accordance with Faraday-Lenz's law, induce electric field opposing to its cause:

$$\oint_l \vec{E}d\vec{l} = -\int_S \frac{\partial \vec{B}}{\partial t} d\vec{S} = -\frac{d}{dt}\int_S \vec{B}d\vec{S} = -\frac{d\Phi}{dt} = -\frac{d\Phi}{di}\frac{di}{dt} = -L\frac{di}{dt}[V] \qquad (2.7)$$

It is possible to calculate *emf* induced along the line considering imaginary closed contour *l* along the line that is shown dotted on Fig.2.b. The circulation of vector **E** along the closed contour *l* is proportional to negative rate of increase of the magnetic flux linking the circuit. The induce *emf* along the contour *l* have the polarity that opposes to current change. The induced emf superpose to *emf* imposed by the source causing phase shift of voltage along the line. As it can be seen from (2.7), the induced *emf* can be expressed using self-inductance L of the line suggesting that infinitesimal lent of the line dx can be seen as inductance per unit of length. The self inductance L is defined as ratio of the magnetic flux linkage in the loop itself and current that created it. As the line is made from nonmagnetic material it is justified to assume that $\frac{d\Phi}{di} = \frac{\Phi}{I} = L$ where $L=2L_i+L_e$.where $L_i = \frac{\mu_0}{8\pi}\left[\frac{H}{m}\right]$ is internal inductance per unit length of the conductor and L_e is the external inductance per unit length that depends on geometry of the conductor dispositions. As the flux linkage depend on surface between two lines, and the line radius, the line inductance L is lower if the spacing between the conductors is lower and the radius is higher. The spacing between conductors is limited with permitivity of the dielectric between the conductors to prevent flashover. So every differential lent dx of lossless line can be represented using inductance and capacitance per line length as shown in Fig.4.

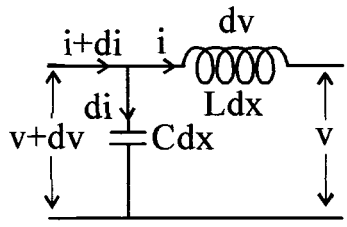

Figure 4 Transmission line model for lossless line

Considering open line with charging current only, at every point of the line charging current leads voltage by 90 degrees. The charging current creates pulsating magnetic field around the line. The pulsating field induces emf in accordance with Faraday-Lenz law:

$$emf = -L\frac{di_C}{dt} \tag{2.8}$$

Combining (2.6) and (2.8) gives:

$$emf = -L\frac{di_C}{dt} = -LC\frac{d^2U}{dt} \tag{2.9}$$

As voltage imposed by the source is sinusoidal:

$$U(t) = U_{\max}\cos\omega t \tag{2.10}$$

$$emf = LC\omega^2 U_{\max}\cos\omega t \tag{2.11}$$

It can be seen that (2.10) and (2.11) are in phase. At every point of the line, the induced emf due to charging current is in phase with emf generated by the source raising the voltage along the line. With increase in loading of the line, the load current increases superposing the charging current. Supposing the resistive load, load current is in phase with voltage:

$$i_l(t) = \frac{U(t)}{R} = \frac{U_{\max}}{R}\cos\omega t \tag{2.12}$$

$$i(t) = i_C(t) + i_l(t) = C\frac{dU}{dt} + \frac{U(t)}{R} = -CU_{\max}\omega\sin\omega t + \frac{U_{\max}}{R}\cos\omega t \tag{2.13}$$

With increase in load, pulsating magnetic field created by load current increases too (R decreases) together with induced *emf* along the line. Induced *emf* due to load current is added to induced *emf* due to pulsating charging current as:

$$emf = -L\frac{di}{dt} = -L\frac{d\left(i_C + i_l\right)}{dt} = -LC\frac{d^2U}{dt^2} - \frac{1}{R}\frac{dU(t)}{dt} = \\ = CLU_{\max}\omega^2 \cos\omega t + \omega L\frac{U_{\max}}{R}\sin\omega t \tag{2.14}$$

The first term on the right side of equation (2.14) is in phase with source voltage along the line and is responsible for voltage boost and the second term on the right side of equation (2.14) is responsible for voltage drop because it is phase shifted by 90 degrees. With increase in loading of the line, the term responsible for voltage drop increases while term providing voltage boost is constant. It depends on charging current and charging current depends on voltage level and line parameters.

For the short line, the charging current is small. Therefore the term providing voltage boost can be neglected and term responsible for voltage drop is predominant. It is in accordance with line modeled as series inductance. Long lines require higher charging current. The induced *emf* due to charging current add along the line leading to increase in voltage along the line resulting in highest voltage at line end (Ferranti effect). It shows that voltage profile along the line is function of spatial coordinate as well as a function of time. It is in accordance with wave equation for voltage and current that can be deduced from Fig.4

$$\frac{\partial^2 u}{\partial x^2} = LC\frac{\partial^2 u}{\partial t^2} \tag{2.15}$$

$$\frac{\partial^2 i}{\partial x^2} = LC\frac{\partial^2 i}{\partial t^2} \tag{2.16}$$

The (2.15) and (2.16) are partial differential equation. The solution of the wave equation for voltage and current (D'Alambert solution) is in the form:

$$\begin{aligned} u(x,t) &= u(x+ct) + u(x-ct) \\ i(x,t) &= i(x+ct) + i(x-ct) \end{aligned} \tag{2.17}$$

where $c^2 = \frac{1}{\sqrt{LC}}$ is velocity of propagation of the wave, L is inductance per unit of length and C is capacitance per unit of length. The solution (2.17) represents forward and backward traveling waves.

When the line is naturally loaded (matched-or loaded with natural impedance) the voltage and the current are in phase along the line. In this case, only forward wave exist indicating the fact that energy is transferred only in one direction, from the source towards the load.

Based on the above discussion the following explanation can be given. For functioning, the transmission line has to be charged. To charge the line, the work has to be done by the source of *emf* (generator) and this work is converted into the energy stored into the electromagnetic field surrounding the charged line. This energy is given by:

$$W = W_e + W_m = \frac{1}{2}\int_{space} \varepsilon E^2 dv + \frac{1}{2}\int_{space} \frac{B^2}{\mu} \tag{2.18}$$

where W_e is energy stored into the electric component of electromagnetic field and W_m is energy stored in magnetic component of electromagnetic field.

When energized with sinusoidal voltage, line is constantly charged and discharged. The intensity of electromagnetic field surrounding the line pulsates with line voltage and

current, and the energy stored in electromagnetic field pulsates too. The charging energy is provided and absorbed by the source and transferred along the line and back due to change in voltage polarity. This energy is transferred through the line using the charging current as a medium. When the load is connected at the end of the line it draws the current, and the current creates magnetic field in the space surrounding the conductor superposing to magnetic field created by charging current. The magnetic field is pulsating (sinusoidal) because the current is pulsating and the magnetic field the energy is stored in. Due to pulsating magnetic field, electric field is induced in the space surrounding the line creating voltage drop along the line length according to Faraday-Lenz law. This voltage drop is sinusoidal, phase shifted compared to voltage imposed by the source and it superpose with voltage imposed by the source resulting in voltage that is changed in magnitude and phase. When the line is naturally loaded, the charging energy, ones supplied by the source, does not have to be exchanged between the line and source but rather is locally exchanged in electromagnetic field surrounding the line. Or, more precisely, the charging energy is locally exchanged between component of *electromagnetic* field surrounding the line that is consequence of charging current and the component of *electromagnetic* field that is consequence of load current. Or the voltage boost created by charging current is canceled by the voltage drop created by load current. It is worth noting that in both cases, voltage drop and voltage boost are consequence of phenomenology of Faraday-Lenz law. In this case, it can be said that line compensate itself.

If the line is not naturally loaded, the component of electromagnetic field created by charging current and the component of electromagnetic field created by load current do not match and, due to their pulsating nature, at least the part of the energy has to be exchanged with source. To avoid this energy exchange between source and line, the line has to be compensated at intermediate points along the line with capacitors/inductance that are used as energy storages that exchange the energy with line locally on the points of

its connection with line. Obviously, ideal compensation of the transmission line should be uniformly distributed, flexible dynamic energy storages at every point of the line.

2.3 Phase Shift

The cause of phase shift between voltage and current has been discussed above. When voltage and currents are in phase as shown in Fig.5 a) the instantaneous power (product of voltage and current) do not change sign as it can be seen on Fig.5.a) (lower trace). The physical meaning of the above mentioned fact is that power flow is only in one direction (from the source to the load). When the voltage and current through the line are phase shifted as shown on Fig.5 b) (upper trace) then instantaneous power change the sign four time over the one period of nominal frequency indicating the fact that the power flow changes direction four time over the one period, from the source to the load and from the load to the source. If the phase shift is 90^{o} the net power flow is zero meaning that the quarter of the period power flows from the source to the load and next quarter period in opposite direction, from the load to the source. The net power transferred over the line (average power) is given by (2.19):

$$P = \frac{1}{T}\int_{0}^{T} p(t)dt \tag{2.19}$$

Geometrically, the average power is the surface the instantaneous power curb $p(t)$ forms with ωt axis. In case of the zero phase shift as in Fig.5.a) the surface is always above ωt axis (positive). In the case of phase shift between voltage and current the part of the surface the instantaneous power curb $p(t)$ makes with ωt axis is above and part is bellow ωt axis.

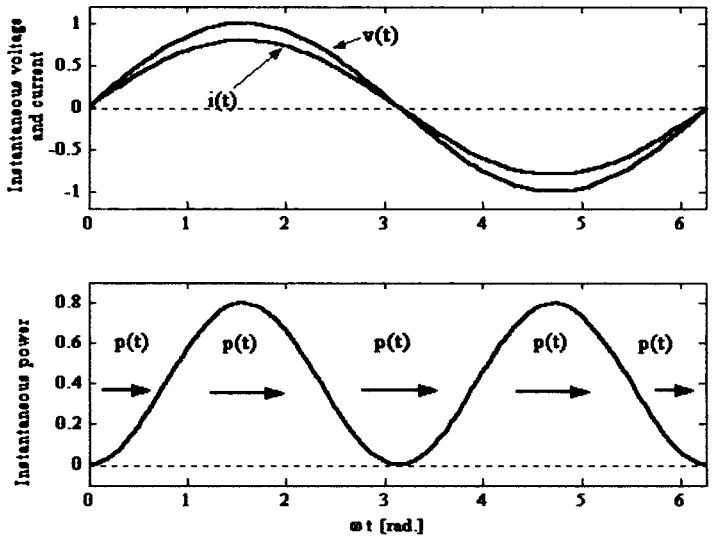

(a)

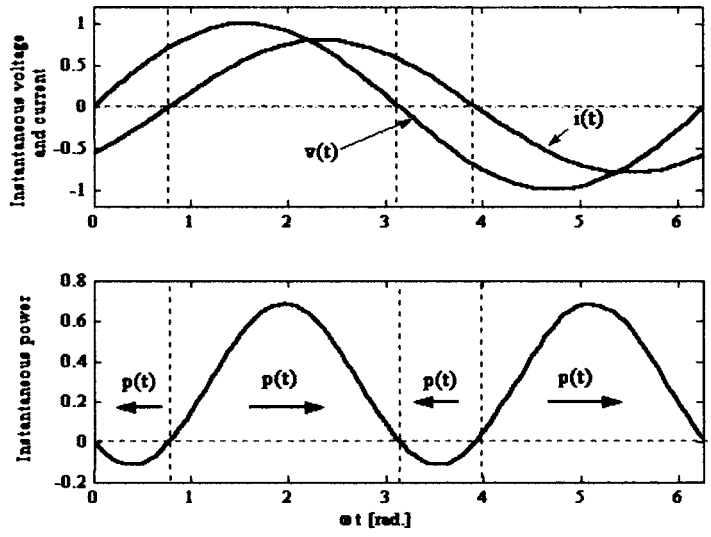

(b)

Figure 5. a) When instantaneous voltage and current are in phase (upper trace) the instantaneous power flow is in one direction only (lower trace), b) when voltage and current are phase shifted (upper trace) the instantaneous power flow change direction four time over the one cycle (lower trace).

The part of the surface that is bellow ωt axis is considered to be negative and is subtracted from the part of the surface above ωt axis. It means that, for the same amplitude of the voltage and current, the net power transferred from the source to the load is lower for the phase shifted voltage and current. Because of the phase shift, for the constant voltage, to provide the same average power, the current has to be increased. Increased current means higher losses and higher inductive as well as resistive voltage drop.

The same principles apply to three phase circuit. The advantage of the three phase balanced system over the one phase system is in the fact that instantaneous power is not pulsating but constant physical entity.

2.4 Nature of Voltage Boost

Consider simple circuit shown in Fig.6. illustrating the bus voltage *v(t)* that is to be regulated and a compensator, that is represented as a voltage source $v_c(t)$ behind inductance L. The inductance L can be a transformer leakage reactance.

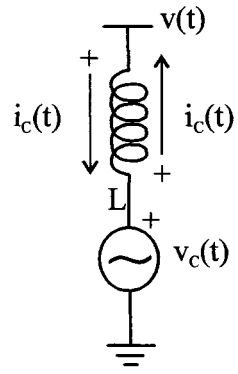

Figure 6 Voltage support of line voltage is provided with voltage source behind inductance L.

If the compensator voltage $v_c(t)$ is synchronized (in phase) with the bus voltage *v(t)* that is to be regulated, the net (average) active power flow between two of them is zero. As two voltages are in phase, the current $i_c(t)$ flowing between two of them is consequence of the

voltage gradient only (difference in magnitude). If the both voltages are of the same magnitude there is no current flow between them. The change in the magnitude of the compensator voltage $v_c(t)$ change the current polarity. When the current polarity is changed, the polarity of the voltage drop across the inductance L is changed too, as shown in Fig.6, so the voltage drop across the inductance L can change from voltage boost to voltage drop and vice versa, depending on polarity of the current $i_c(t)$:

$$v(t) = L\frac{di_c(t)}{dt} + v_{c(t)} \tag{2.20}$$

One may be tempted to think that voltage boost (drop) depends upon inductance value L. The compensator current $i_c(t)$ can be calculated as:

$$i_c(t) = \frac{1}{L}\int (V_{\max} - V_{c\max})\cos\omega t dt = \frac{1}{\omega L}(V_{\max} - V_{c\max})\sin\omega t \tag{2.21}$$

as consequence:

$$L\frac{di_c(t)}{dt} = L\frac{d\left(\frac{1}{\omega L}(V_{\max} - V_{c\max})\sin\omega t\right)}{dt} = \left((V_{\max} - V_{c\max})\cos\omega t\right) \tag{2.22}$$

as it can be seen from (2.22), the voltage boost does not depend upon L if the source of compensating current i_c is voltage source behind inductance because the current through the inductance depends on inductance itself.

2.4.1 Phasor Approach

As the voltages and currents are sinusoidal it is helpful to use phasor notation.

$$v(t) = V_{\max}\cos\omega t = \mathrm{Re}\left\{V_{\max}e^{j\omega t}\right\} \tag{2.23}$$

$$v_C(t) = V_{C\max}\cos\omega t = \mathrm{Re}\left\{V_{C\max}e^{j\omega t}\right\} \tag{2.24}$$

$$\begin{aligned} i_c(t) &= \frac{1}{L}\int(V_{\max} - V_{c\max})\cos\omega t dt = \frac{1}{L}(V_{\max} - V_{c\max})\int\mathrm{Re}\left\{e^{j\omega t}\right\}dt = \\ &= \frac{1}{L}(V_{\max} - V_{c\max})\,\mathrm{Re}\left\{\frac{e^{j\omega t}}{j\omega}\right\} = \frac{1}{\omega L}(V_{\max} - V_{c\max})\sin(\omega t) = \\ &= \frac{1}{\omega L}(V_{\max} - V_{c\max})\cos(\omega t - 90^\circ) \end{aligned} \tag{2.25}$$

or, using phasor notation

$$\bar{I}_C = -\frac{j}{\omega L}(V_{\max} - V_{c\max}) \tag{2.26}$$

From (2.23) it can be seen that if $V_{max} > V_{Cmax}$ the current $i_c(t)$ lagging after the voltages $v_c(t)$ and $v(t)$ by 90^0 (inductive current) and if $V_{max} < V_{Cmax}$ the current $i_c(t)$ is leading the voltages $v_c(t)$ and $v(t)$ by 90^0 (capacitive current). The two cases are represented by Fig.7.a) and b).

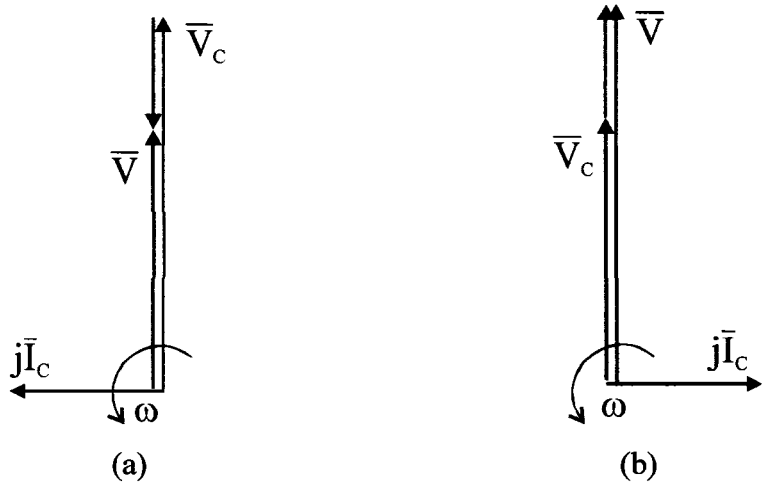

Figure 7 a) Vector diagram showing creation of voltage boost and b) voltage drop across inductance L.

2.5 Voltage Drop Analysis

2.5.1 Equivalent Circuit

Every power system, regardless of its topology, seen from the point of coupling with power delivery substation can be represented as Thévenin equivalent circuit as illustrated in Fig.8. The Thévenin voltage V_{Th} and impedance Z_{Th} can be readily obtained from short circuit current I_{SC}, short circuit capacity S_{SC} and X/R ratio of the supply system as:

$$S_{sc} = \overline{V}_{Th}\overline{I}^{*}_{SC} = \frac{\overline{V}^{2}_{Th}}{Z^{*}_{Th}} \tag{2.27}$$

$$\tan\phi_{sc} = \frac{X}{R}$$

where Z_{Th}=R+jX

These parameters are well known in engineering practice. The equivalent impedance Z_{Th} is usually inductive in meshed system, however it can be capacitive in case of long lines. The Thévenin impedance Z_{Th} can be considered as fictional, radial transmission line. The Thévenin voltage V_{Th} can be considered as sending end voltage V_S. V_R and V_L stand for receiving end and load voltage respectively while X_T is power delivery substation reactance and I_L load current.

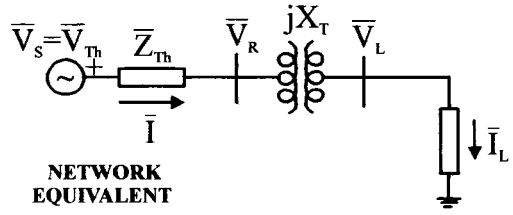

Figure 8 Power system seen from point of coupling with power delivery substation.

2.5.2 Non-Compensated Line

In order to get better insight in voltage drop in the lines and action to remedy it, it is useful to represent the line and the transformer as lumped inductance and consider simple, one line transmission system with one bulk power delivery transformer and load as shown in Fig.9 a). As it has been shown in the previous subsection it is very general case.

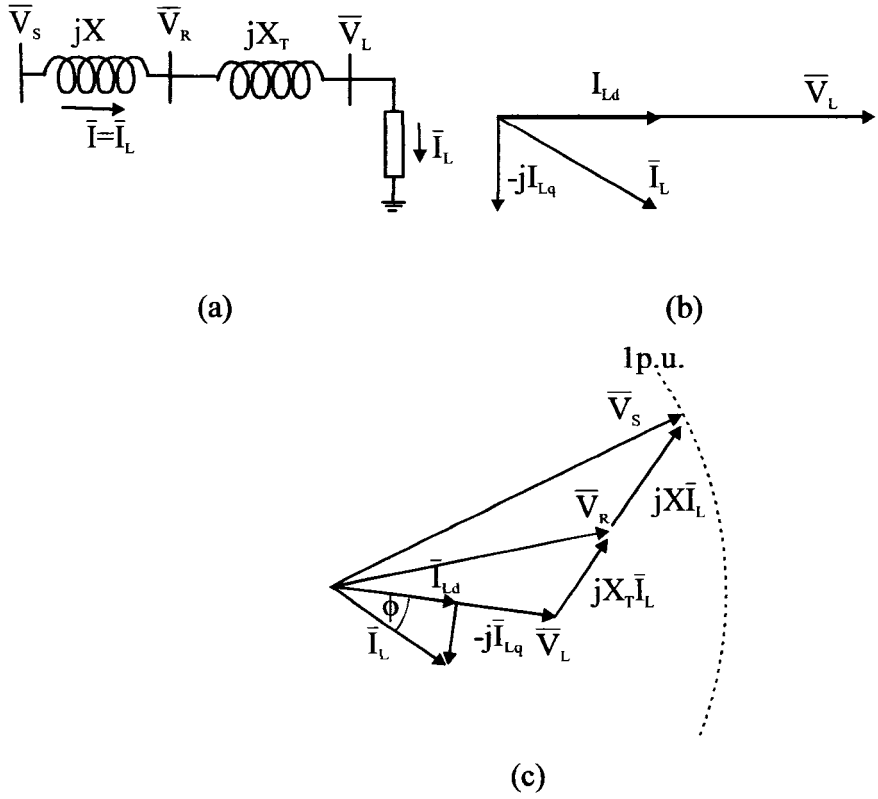

Figure 9 a) Single line diagram of radial transmission line (jX). Line is connected to infinite bus with voltage $\mathbf{V_S}$ = 1p.u. Transformer X_T connects line to load, b) Current phasor c) complete phasor diagram. Voltage drop is caused by the load current $\mathbf{I_L}$ across line reactance jX and supply transformer jX_T.

To highlight the essentials, following is assumed:

1. The line is connected to infinite bus.

2. The line is short and it can be represented by its series reactance jX.

First we consider the non compensated line from Fig. 9. The current $\mathbf{I_L}$ drawn by the load is inductive and can be decomposed into two components, one that is in phase I_{Ld}, and another inductive $-jI_{Lq}$ in quadrature with load voltage $\mathbf{V_L}$ (Fig.9.b). The load current causes the voltage drop $j(X+X_T)(I_{Ld}-jI_{Lq})$ in the transformer and line reactance, decreasing receiving end voltage $\mathbf{V_R}$ and load voltage $\mathbf{V_L}$, as shown in Fig.9.c).

2.5.3 Power Factor Correction

The power factor correction indicate that all reactive requirements of the load are satisfied locally. The power factor of the load is mostly corrected with switched/fixed capacitors installed in parallel with load. After the power factor of the load is corrected locally by injecting capacitive current $+jI_{Lq}$, the inductive component of the load current $-jI_{Lq}$ and the voltage drop $\Delta\mathbf{V_L} = (X+X_T)I_{Lq}$ it causes are cancelled, as shown in Fig.10 b). The voltage drop caused by the I_{Ld} component of the load current still persists, preventing load voltage from being 1pu.

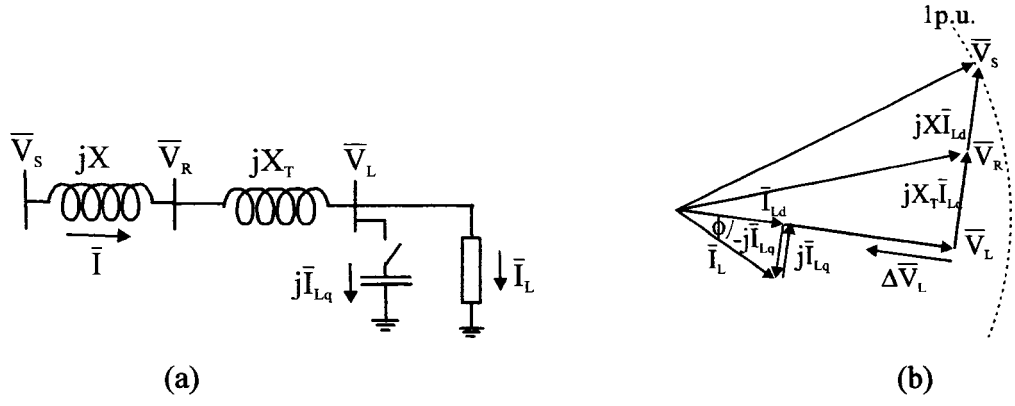

Figure 10 a) The reactive requirement of the load are supplied locally. b) After power factor correction, voltage drop is partially mitigated.

2.5.4 Voltage Regulation

The compensator is treated as reactive current source. To cancel voltage drop and to keep load voltage $\mathbf{V_L}$ at nominal value, the additional capacitive current has to be injected into the system. The capacitive current can be injected on distribution or on transmission level as illustrated in Fig. 11. If the voltage support is provided on distribution level (switch S_2 on and S_1 off) the injected capacitive current is perpendicular to distribution voltage $\mathbf{V_L}$. If voltage support provided on transmission level(switch S_2 off and S_1 on) the injected capacitive current is perpendicular to nodal transmission voltage $\mathbf{V_R}$. In both cases the line current **I** is vector sum of load current and compensation current.

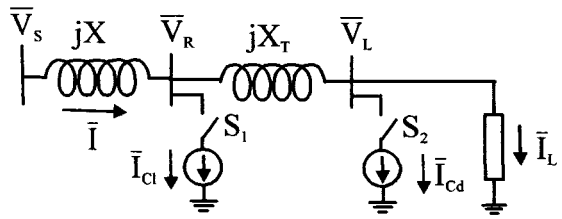

Figure 11 Single line diagram of radial transmission line (jX). Line is connected to infinite bus with voltage V_S = 1p.u. Transformer X_T connects line to load. Voltage support can be provided on transmission level (S_1 on, S_2 off) or on distribution level (S_1 off, S_2 on).

First we consider the non compensated line (Fig. 11 with switches S_1 and S_2 off). The power factor of the load is assumed to be corrected as shown previously. The current drawn by the load depends on load itself and the voltage $\mathbf{V_L}$. The current causes the voltage drop in the transformer and line reactance. It results in decrease in transmission voltage $\mathbf{V_R}$ and the load voltage $\mathbf{V_L}$. The load voltage $\mathbf{V_L}$ is in phase with current drown by the load. This is represented by the vector diagram as shown in Fig.12.

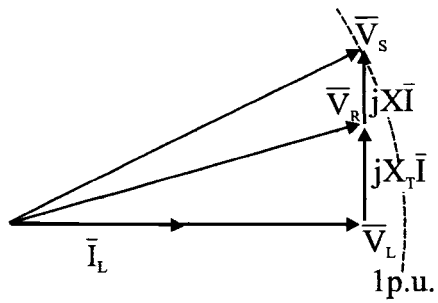

Figure 12 Voltage drop caused by the load current $\mathbf{I_L}$ across the line reactance jX and distribution transformer jX_T

Linearity of the circuit in Fig.11 makes it possible to apply superposition theorem in order to compare contributions of each compensator in voltage support. The circuit in Fig.11 can be represented as a sum of three circuits shown in Fig. 13. a), b) and c).

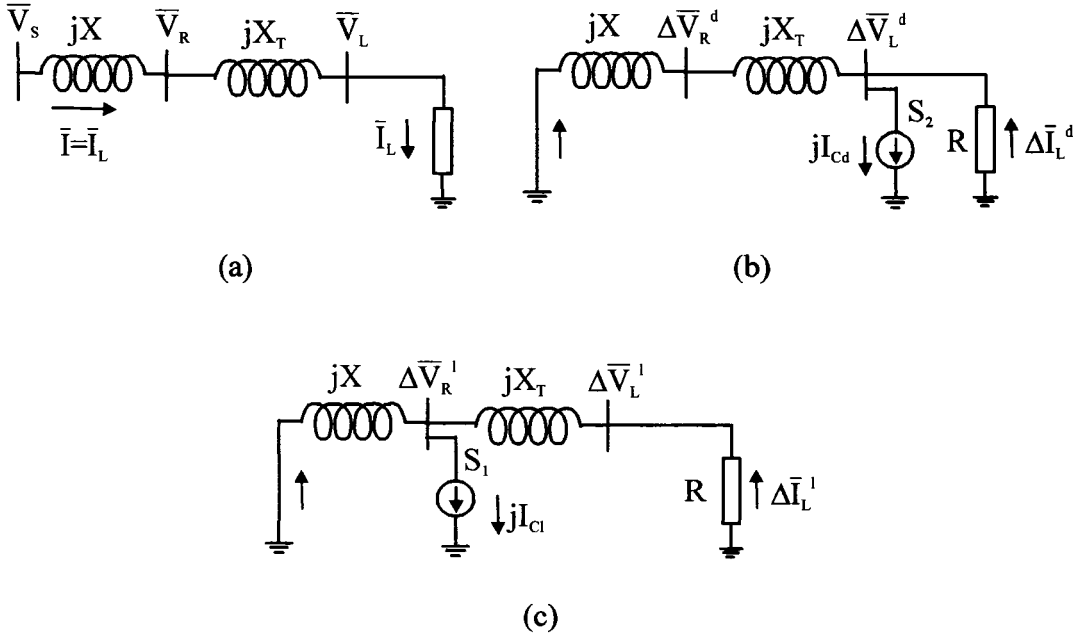

Figure 13 Circuit from Fig.11 decomposed according to the principle of superposition (a) without compensation, (b) voltage support provided on distribution side of power delivery substation, (c) voltage support provided on transmission side of power delivery substation

From Fig.13. b) it is possible to evaluate value of the voltage support due to reactive current injection $\mathbf{I_{Cd}}$ on the distribution side of substation:

$$\Delta\bar{I}_L^d = \frac{jI_{Cd}j(X+X_T)}{R+j(X+X_T)} \tag{2.28}$$

$$\Delta\bar{V}_L^d = -R\Delta\bar{I}_L^d = \frac{RI_{Cd}(X+X_T)}{R+j(X+X_T)} \tag{2.29}$$

ΔV_L^d is voltage boost of the load voltage $\mathbf{V_L}$ due to current $\mathbf{I_{Cd}}$ injected by the compensator on the load side. The plus sign indicate that it is voltage drop, but due to the fact that the voltage drop given by (2.28) is in opposite direction according to the voltage drop caused by the load current $\mathbf{I_L}$ in transformer and line reactance $\mathbf{I}j(X+X_T)$ in Fig.11, it is actually the voltage boost.

Influence of injected compensating current $\mathbf{I_{Cd}}$ on distribution side of the substation on transmission voltage is given by:

$$\Delta\bar{V}_R^d = \frac{RjI_{Cd}jX}{R+j(X+X_T)} = -\frac{RI_{Cd}X}{R+j(X+X_T)} \tag{2.30}$$

Equation (2.30) give voltage boost on the transmission side of the substation. (Minus sign depicts the fact that voltage drop is negative (negative voltage drop is boost), and the part of the compensator current flowing through the line impedance jX has the same direction as total current flowing through the line - the current I in Fig.11.

If the compensation current is injected on transmission side of substation as shown in Fig.13 c)

$$\Delta\bar{I}_L^l = \frac{jI_{Cl}jX}{R + j\left(X + X_T\right)} \tag{2.31}$$

$$\Delta\bar{V}_L^l = -R\Delta\bar{I}_L^l = \frac{RI_{Cl}X}{R + j\left(X + X_T\right)} \tag{2.32}$$

$$\Delta\bar{V}_R^l = \frac{\left(R + jX_T\right)jI_{Cl}jX}{R + j\left(X + X_T\right)} = -\frac{XI_{Cl}\left(R + jX_T\right)}{R + j\left(X + X_T\right)} \tag{2.33}$$

if both injected currents are equal in magnitude $|I_{Cd}| = |I_{Cl}|$ then from (2.29) and (2.30)

$$\frac{\Delta\bar{V}_L^d}{\Delta\bar{V}_L^l} = \frac{\left(X + X_T\right)}{X} \tag{2.34}$$

From (2.34) it can be seen that both placement of compensators provide voltage boost on distribution side of the transformer X_T, but the voltage boost is more pronounced when compensator sat on distribution side due to transformer reactance X_T.

The influence of two compensating schemes on transmission side voltage $\mathbf{V_T}$ can be compared from (2.30) and (2.33). Again, for same magnitude of the compensating currents

$$\frac{\Delta\bar{V}_R^d}{\Delta\bar{V}_R^l} = \frac{R}{R + jX_T} \tag{2.35}$$

From (2.35) it can be seen that in both cases transmission voltage $\mathbf{V_R}$ is supported, but the support of transmission voltage is more efficient in case of compensator on high voltage side of the transformer X_T.

2.6 Conclusion

In this chapter the mechanisms of power transfer, voltage drop and voltage boost has been discussed. It has been shown that the nature of the inductive voltage drop and voltage boost is in the phenomenology of electromagnetic field and Faraday-Lenz law. Moreover, it has been shown that voltage drop across the inductance can be changed into voltage boost if the polarity of the current through inductance is changed.

Finally, a simple power system consisting of the infinite bus, radial transmission line, power delivery transformer and load has been analyzed using principle of superposition. The influence of the voltage support provided on transmission and distribution level has been analyzed. It has been shown that, when voltage support is provided on distribution level the transmission voltage is supported too and vice versa.

CHAPTER 3

VOLTAGE SOURCE CONVERTER AS A STATCOM

3.1 Introduction

Benefits of reactive power compensation are well known: increased stability, increased transmission capacity over existing lines, better voltage profile and decreased losses. As it has been mentioned in chapter one, the management of reactive power by traditional means has its drawbacks, depending on compensation technique used. These include a possibility of resonance, slow response, introduction of harmonics, rotational instability or management of reactive power in discrete steps. Moreover, if capacitor banks are used (with or without thyristors), they occupy a considerable amount of real estate. The new generation of static compensator based on converter circuits can successfully overcome those problems and allow reactive power compensation without using bulky capacitors. Unfortunately, the voltage rating of semiconductor switching devices is not high enough for high voltage application. To cope with this problem, a few switching devices must be put in series, or different multilevel topologies are to be used. Multilevel topologies have their advantages over simply putting switching devices in series. These include a better output voltage waveform while FFM (fundamental frequency modulation) switching strategy is used so that filters can be avoided and switching losses decreased. Voltage stress dv/dt in the switching devices is limited to one level of voltage so that converter rating can be increased, allowing direct coupling with AC system without step up transformer. However, the application of power electronic converters are suited to distribution bus voltages and sizes. This is because they are based on solid-state technologies, which have grown from the application of thyristors, gate-turn-off thyristors (GTOs) and insulated gate bipolar transistors (IGBTs) to variable speed AC motor drives. The controllers of SVS such as the Static VAR Compensators (SVCs) and the STATic COMpensator (STATCOM), are solid-state switch technologies pushing upwards to the

higher MVA ratings of power utilities. In fact, this has been one motivation of multi-level converter research. Some manufacturers have already mastered the technology of connecting GTOs or IGBTs in series to increase the voltage ratings of STATCOMs to distribution voltage levels so that they can now be connected directly, without transformers, to the electric utility[47,48].

In this chapter a review of STATCOM principles are presented. The original STATCOM control strategies for voltage control of power system is tailored and tested. Numerical simulation using Hypersim is used to validate proposed control strategy. The positioning of the STATCOM in transmission line is discussed too.

3.2 Voltage Source Converter

STATCOM is basically AC voltage source behind the reactance as illustrated in Fig.6. Voltage source converter (VSC) is used as a voltage source. Fig. 14 a) illustrates one converter leg of basic three phase converter circuit and Fig.14 b) illustrates three phase six pulse converter topology. The VSC is an array of power electronic switching devices, that, with their fast switching action, can shape DC voltage to AC and AC to DC. While doing it, the phase and magnitude of AC voltage can be controlled, so as the power flow through the converter. While doing conversion, the harmonics are introduced into the power system also. The output square waveform is shown in Fig. 14 a). It consist of fundamental component and spectra of odd harmonics. In three phase configuration, due to 120^{o} phase shift between three output AC voltages third harmonic and its multiple will get canceled for balanced circuit in line to line voltage.

The advantage of the STATCOM over traditional synchronous compensator is lack of inertia providing fast response without introduction of oscillation and lack of rotational parts lowering maintenance requirements. The disadvantage is introduction of harmonics, rating of switching devises and switching losses and high initial cost. To decrease

harmonic content in the output voltage waveform, PWM or some other fast switching strategies has to be used but that may lead to increase in switching losses. Moreover, power switching devices has limited voltage and current ratings, so the switches have to be put in series and in parallel which may lead to gating problems.

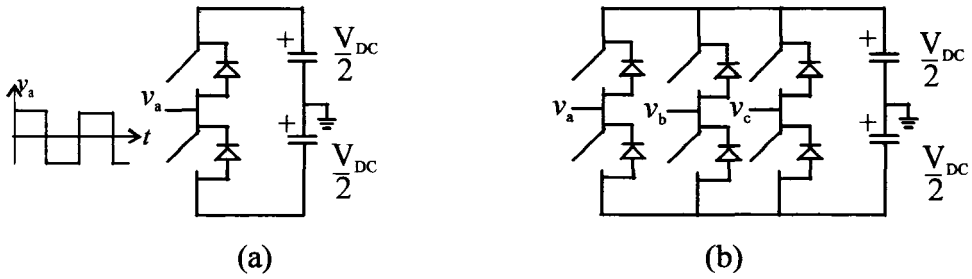

Figure 14 Basic six pulse converter circuit. a) one converter leg with its output AC voltage waveform, b) three phase circuit.

To decrease switching losses, increase rating and improve output voltage waveform, the six pulses converters are combined as shown in Fig.15, cascaded or multilevel topologies are used for power system applications.

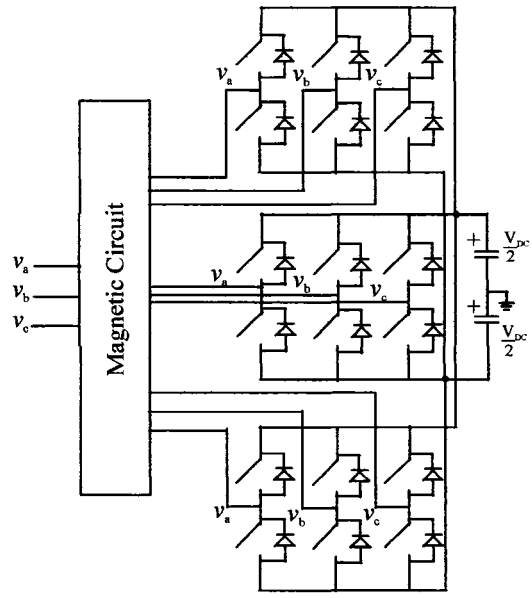

Figure 15 Inverter coupling with magnetic circuit

3.3 Diode Clamped VSC

One of the most popular multilevel converter topologies for high voltage application is so called "diode clamped" topology. Fig.16 shows one phase of five-level diode clamped VSI together with its output voltage waveform. The topology that was proposed by Nabae et al. [30] had initially only three levels controlled by PWM modulation strategy. The three-level diode clamped VSI gained a lot of attention for high voltage applications and, very soon, has been upgraded with the new levels [31] and enhanced [32]. Because of its advantages such as decreased THD, off-line optimization of switching angles, increased voltage rating and diminished dv/dt stress, the topology has been suggested for different high voltage applications such as STATCOM, UPFC and back to back DC link [35-38]. However, there are some important drawbacks such as complicated construction, unequal current stress on switching devices and capacitor voltage balancing problem. The capacitor voltage unbalance depends upon switching angles and net active power transferred between AC and DC side of inverter. If this transfer is zero, than the problem disappears. Because of the capacitor balancing problem, the most suitable application for diode clamped multilevel VSI is STATCOM. In the case of ideal STATCOM, the net active power exchange between AC and DC side of inverter circuit is zero during steady state operation. The capacitor balancing problem has been solved in [60].

3.3.1 Topology description

Fig.16 shows one phase of five-level diode clamped inverter. The DC bus of the N level inverter consists of N-1 capacitors that allow N taps for N levels of voltage. The capacitors are common for all three phases. One phase of power circuit has (N-1)x2 power switches and (N-2)x2 clamping diodes. Each switching devices has to stand one voltage level.

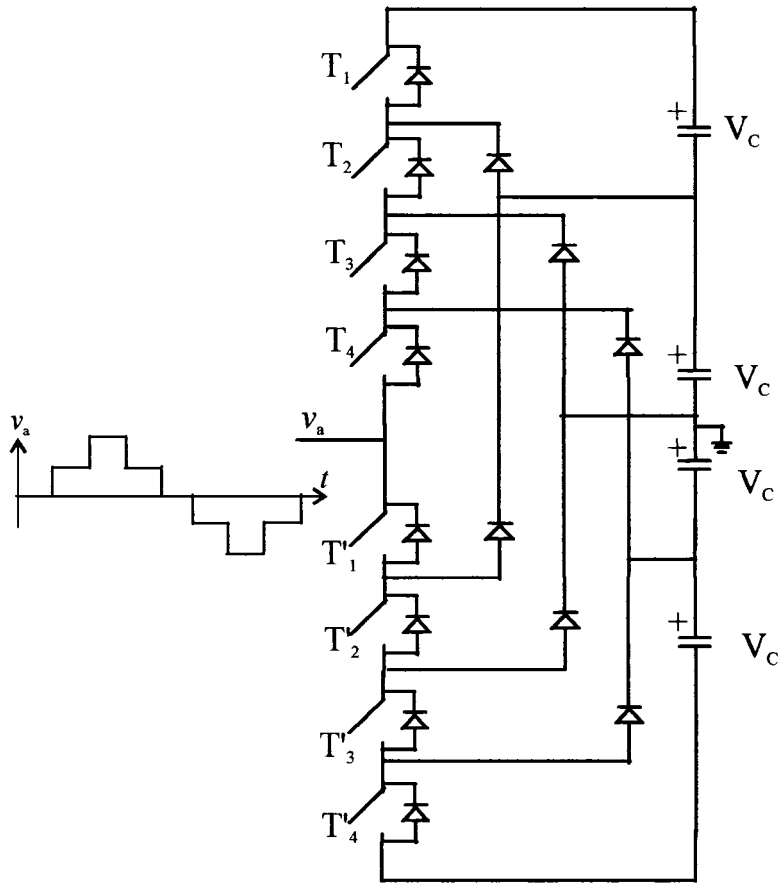

Figure 16 One leg of five level diode clamped voltage source converter

3.3.2 FFM Switching Strategy and Switching Functions

The FFM switching strategy is conceived on a premise that each switch commutes only twice over one cycle of fundamental frequency (once on and once off). This strategy of modulation may be difficult to accept in the case of six pulses inverter because of large amount of pollution in output voltage waveform. But in the case of multilevel inverter, if the number of level is sufficiently high, the distortion present in output voltage is small enough. Moreover, FFM is crucial for high voltage application because it allows a considerable decrease in switching losses. Fig.17 shows switching functions that allow generation of five-level staircase output voltage.

Switching devices T_1, T_2, T_3 and T_4 have for their complements T_1', T_2', T_3' and T_4'. If T_1 is forced to close, T_1' is forced to open and vice versa. The same is true for the other devices. The voltage on the DC side of the converter V_{DC} consists of four equal voltages V_C, where V_C is voltage across one of the four capacitors that form DC bus. The switching devices are controlled by switching function given by Fig 17. The shaded areas show that transistors are in conduction. Output voltage waveform consists of five-level $2V_C$, V_C, 0, $-V_C$ and $-2V_C$.

- to obtain voltage level $2V_C$, transistors T_1, T_2, T_3 and T_4 are closed and their complements T_1', T_2', T_3' and T_4' are open.
- to commute to voltage level V_C, transistor T_1 is forced to open an T_1' to close
- to commute to voltage level 0, T_2 is forced to open an T_2' to close.
- to commute to voltage level $-V_C$, T_3 is forced to open and T_3' to close
- to commute to voltage level $-2V_C$, T_4 is forced to open and T_4' to close.

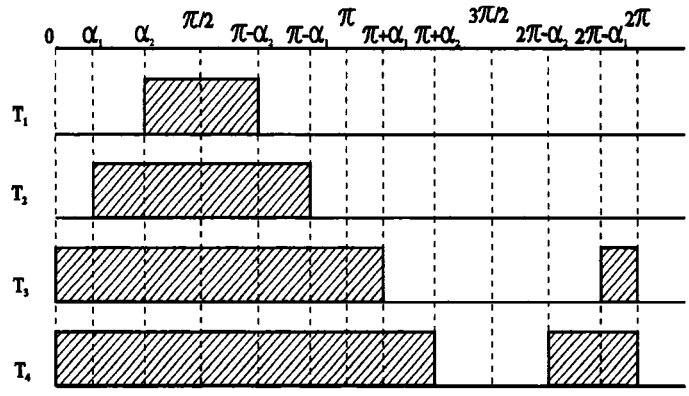

Figure 17 Switching function for five-level voltage source converter

By returning in reverse direction the full cycle is described. Repeating given pattern, the staircase quasi-sinusoidal voltage output waveform is obtained. The voltage stress on transistors dv/dt is limited to one level that is voltage V_C across one of the capacitor on the DC side of converter. The current path through converter depends on the voltage level and sign of the current. The current stress is not equally distributed among switching

devices and that it is more pronounced for inner switching devices (T_4 and T_1') than for outer switching devices (T_1 and T_4'). As a consequence, the rate of charging and discharging inner capacitors C_2 and C_3 is higher than that of outer capacitors C_1 and C_4, so that the voltage across the inner capacitors will tend to increase or decrease more than the voltage across outer capacitors, depending on the mode of operation (capacitive or inductive). The voltages across capacitors must be balanced in order to prevent distortion of the output voltage and to ensure the even voltage stress dv/dt in the switching devices. Equalizing DC capacitors voltages can be achieved by additional hardware [31] or within control algorithm [38],[60]. The voltage balance problem does not exist in case of ideal reactive operation (converter currant lead or lag converter voltage by 90 degrees).

3.3.3 Voltage Output Waveform: Optimization

In general, one N-level diode clamped VSI can produce N-level output voltage waveform (Fig.18) and the line-to-line voltage can consist of 2N-1 levels. If the FFM switching strategy is applied, then each switching device commutes twice per cycle, diminishing switching losses.

N-level output voltage waveform produced using FFM switching strategy (Fig.18) is symmetric and can be represented by series of Fourier:

$$v(t) = \sum_{k=1}^{\infty} \frac{4V_C}{\pi k} \left[\cos k\alpha_1 + \cos k\alpha_2 + \ldots + \cos k\alpha_{\frac{N-1}{2}} \right] \sin k\omega t \tag{3.1}$$

$$k = 2n+1, \quad n \in N$$

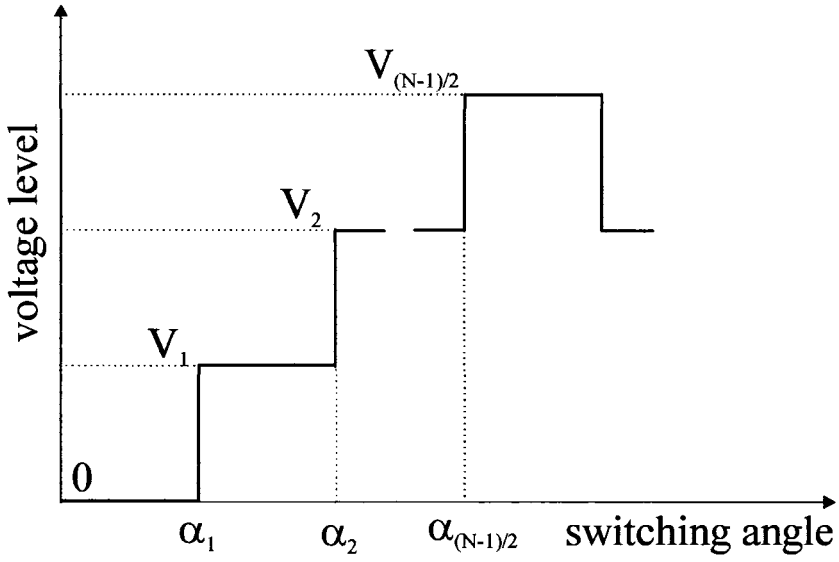

Figure 18 N-level output voltage waveform

From Fig. 18 it can be seen that for N-level output voltage waveform (N-1)/2 switching angles α_1, α_2 to $\alpha_{(N-1)/2}$ can be chosen in order to eliminate (N-1)/2 dominant harmonics or to minimize (total harmonic distortion) THD. In other words, N-level converter has (N-1)/2 degrees of liberty. The amplitude of k^{th} harmonic is given by (3.2).

$$A_k = \frac{4V_C}{\pi k}\left[\cos k\alpha_1 + \cos k\alpha_2 + \ldots + \cos k\alpha_{\frac{N-1}{2}}\right] \tag{3.2}$$

In the five-level output voltage waveform, two dominant harmonics can be eliminated (5^{th} and 7^{th}) by solving a set of equations given by (3.3), where A_i are Fourier coefficients given by (3.2) for i=5,7.

$$\begin{aligned} A_5 &= 0 \\ A_7 &= 0 \end{aligned} \tag{3.3}$$

After finding solutions from (3.3), THD of phase voltage is 21.7%. The third harmonic and its multiples are eliminated in the line-to-line voltage. The line-to-line voltage is given by (3.4) and THD of line-to-line voltage is 8.56%.

$$V_{line} = \sum_{k=1}^{\infty} A_k \left[\sin(k\omega t) - \sin k\left(\omega t - \frac{2\pi}{3} \right) \right] \tag{3.4}$$

The other solution, appropriate for one phase converter, is to minimize THD. The function of THD for the five-level inverter is given by (3.5) where $f(\alpha_1, \alpha_2)$ is given by (3.6).

$$THD\% = 100\sqrt{\frac{V_{RMS}^2}{V_1^2} - 1} = 100\sqrt{f(\alpha_1, \alpha_2) - 1} \tag{3.5}$$

$$f(\alpha_1, \alpha_2) = \frac{\pi}{4} \frac{\left(2\pi - \alpha_1 - 3\alpha_2\right)}{\left(\cos\alpha_1 + \cos\alpha_2\right)^2} \tag{3.6}$$

After minimizing the function $f(\alpha_1, \alpha_2)$, THD of the phase voltage is 16% and THD of line voltage is 10.8%. In both case the line voltage consists of nine levels. The RMS value of phase N-level output voltage is given by (3.7) and RMS of fundamental is given by (3.8).

$$V_{RMS}^2 = \frac{2V_C^2}{\pi} \left[\left(\frac{N-1}{2} \right)^2 \frac{\pi}{2} - \alpha_1 - 3\alpha_2 - 5\alpha_3 - 7\alpha_4 + \ldots + (N-2)\alpha_{\frac{N-1}{2}} \right] \tag{3.7}$$

$$V_{1RMS}^2 = \frac{8V_C^2}{\pi^2} \left[\cos\alpha_1 + \cos\alpha_2 + \ldots + \cos\alpha_{\frac{N-1}{2}} \right]^2 \tag{3.8}$$

It is worth noting that magnitude of the inverter output voltage, if the off-line optimization applied, depends exclusively on the value of the voltage V_C across the capacitor on the DC side of inverter. If the off-line optimization is not applied, then this magnitude can be controlled by changing switching angles α_i .More details an be found in [61]. Some other modulation strategies such as pulse width modulation (PWM) or selective harmonics elimination (SHEM), which result with even better output voltage waveform, can be used, but they impose higher speed of switching, which may not be acceptable in high voltage applications.

3.4 VSC Equivalent Circuit

Fig.19 illustrates three phase Voltage Source Converter equivalent circuit. The AC side of the converter is modeled by voltage sources v_a, v_b and v_c while DC side of the converter is modeled as current source I_{DC} and capacitance [46]. The DC current I_{DC} is converter DC current. To model the switching and capacitive losses the resistance can be added in DC side of the converter. The AC and DC side of the converter are related through power balance equation:

$$P = V_{DC} I_{DC} = v_a i_a + v_b i_b + v_c i_c \tag{3.9}$$

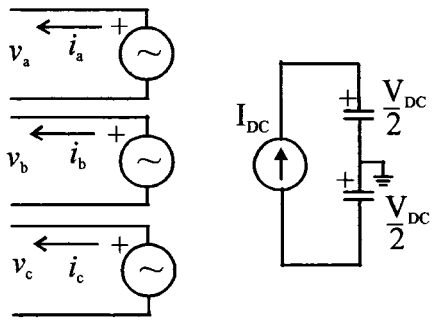

Figure 19 VSC equivalent circuit

3.5 Proposed Control Strategy for STATCOM

Fig.20 shows block diagram of the STATCOM control circuit. The primary objective of the control system is to provide the adequate voltage support. This is achieved by controlling the amplitude of STATCOM output voltage as described in section 2.6. When voltage support is needed, the STATCOM output voltage is increased, and STATCOM provides reactive power. During period of light loading of transmission line, when voltage has tendency to arise, the STATCOM output voltage decreases, STATCOM absorbs reactive power (or supply less reactive power), and controls the line voltages as illustrated on vector diagrams in Fig. 7 a) and b). A detailed description of control strategy is given in [62,63]. In this work the control strategy is conceived on low frequency PWM modulation. The DC voltage on DC bus of the power converter is kept constant. The relation between amplitude of STATCOM output voltage $V_{STAT.}$, and the voltage on the DC bus V_{DC} is given by:

$$V_{STAT.} = m\frac{V_{DC}}{2} \tag{3.10}$$

where m is modulation index. In order to control $V_{STAT.}$, the modulation index m is varied and DC bus voltage is kept constant. The outer control loop allows active power control. The PLL (phase lock loop) allows synchronization of the STATCOM output voltage with the AC system. Its robustness is crucial for the performance of the STATCOM. The PLL must be able to lock up the phase of line voltage immediately after disturbances. Its output is phase angle. DC bus voltage of the STATCOM is measured, filtered and compared to the reference value. The error is processed through Proportional-Integral (PI) block. The output of PI block is used as phase shift reference δ that is added to PLL output. The sum of the two signals gives phase angle reference for the STATCOM output voltage allowing the flow of active power from line into the STATCOM in order to meet its losses. The inner control loop has faster dynamic and allows reactive power control.

The instantaneous values of the three phase voltages v_a, v_b and v_c on the supported bus are measured and RMS value of midpoint voltage V_{RMS}. is computed using

$$V_{RMS} = \sqrt{\frac{1}{3}(v_a^2 + v_b^2 + v_c^2)} \tag{3.11}$$

The computed value is compared with V^*_{RMS} the desired value of the line voltage. The error signal is processed in PI block and applied as modulation index. The distinct advantages of this type of control are following:

1. There is no need to measure current, therefore, getting rid of the current transformers.
2. The active and reactive power control are completely decoupled.

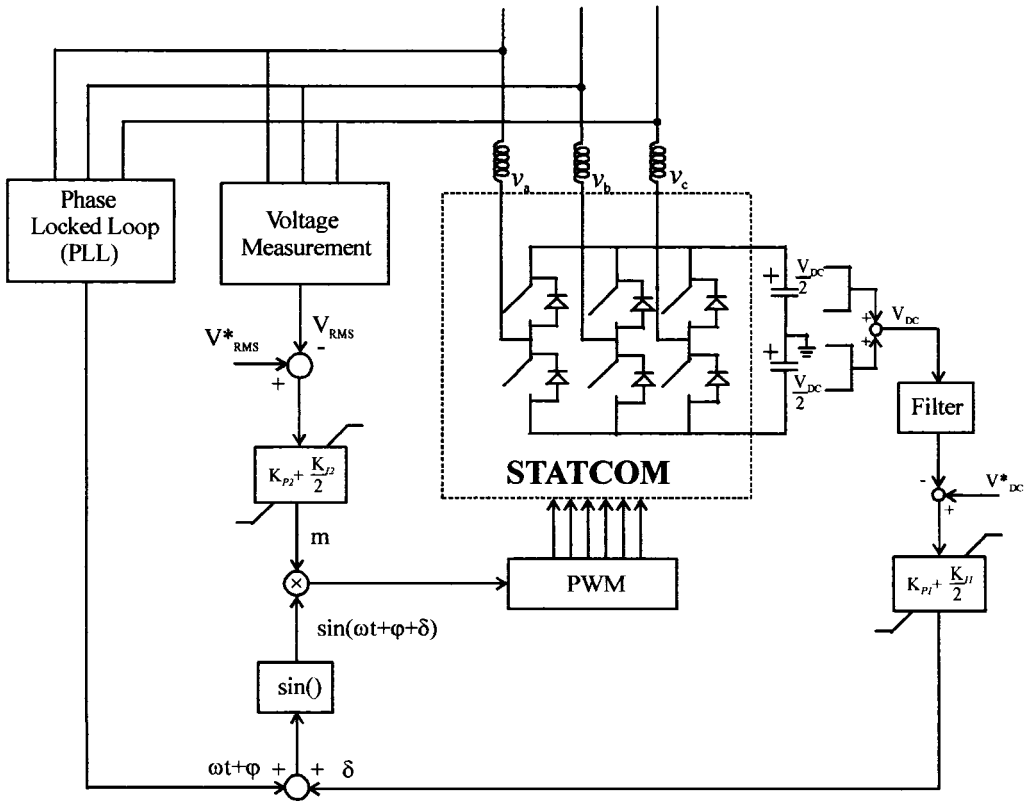

Figure 20 STATCOM control circuit

3.5.1 Phased lock loop (PLL)

Fig. 21 shows the structure of PLL. The PLL is designed for three phase operation.

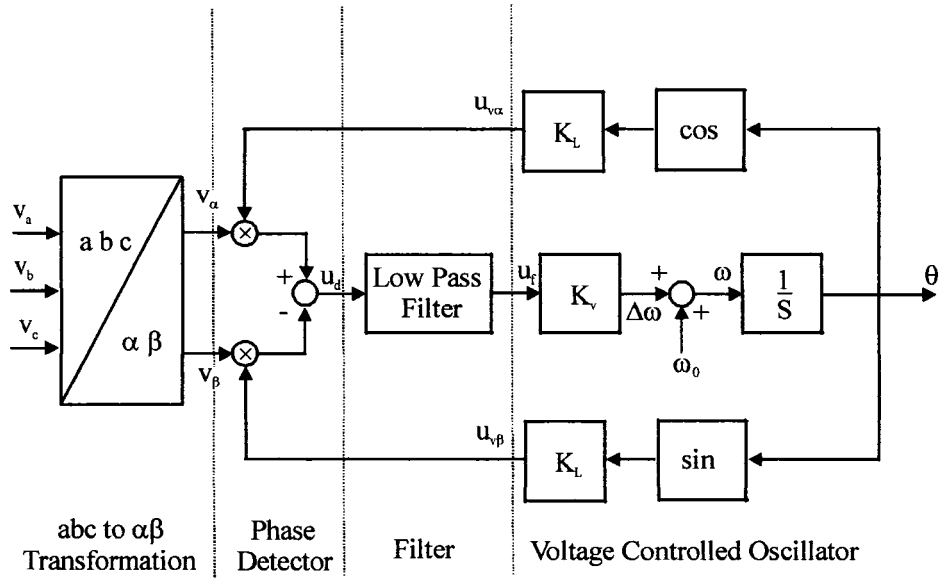

Figure 21 Phased lock loop-block diagram

The instantaneous line voltages v_a, v_b and v_c are measured and transformed in α–β reference frame. The PLL consist of three parts: phase detector, filter and voltage controlled oscillator. The line voltages are given by:

$$\begin{aligned} v_a &= V_{max.} \sin(\omega t + \varphi) \\ v_b &= V_{max.} \sin(\omega t + \varphi - \frac{2\pi}{3}) \\ v_c &= V_{max.} \sin(\omega t + \varphi + \frac{2\pi}{3}) \end{aligned} \tag{3.12}$$

After the transformation in in α–β reference (3.12) becomes (3.13).

$$v_\alpha = V_{\max.} \sin(\omega t + \varphi)$$
$$v_\beta = V_{\max.} \cos(\omega t + \varphi) \tag{3.13}$$

The phase angle of the line voltage is ωt+φ. The output of the phase detector is given by (3.14):

$$u_d = v_\alpha u_{v\alpha} - v_\beta u_{v\beta} = V_{\max} K_L \left[\sin(\omega t + \varphi)\cos\theta - \cos(\omega t + \varphi)\sin\theta\right] = V_{\max} K_L \sin(\omega t + \varphi - \theta) \tag{3.14}$$

Angle θ can be written as $\theta = \omega t + \varphi_1$ therefore (3.14) becomes:

$$u_d = V_{\max} K_L \sin(\varphi - \varphi_1) \tag{3.15}$$

Assuming that PLL is locked, (3.15) can be linearized and rewritten as:

$$u_d = V_{\max} K_L (\varphi - \varphi_1) \tag{3.16}$$

Signal obtained from (3.15) is passed through low pass filter that is PI block whose proportional and integral gains are K_P and K_I respectively so the output of the filter is:

$$U_f(S) = V_{\max} K_L (\varphi - \varphi_1)\left(K_P + \frac{K_I}{S}\right) \tag{3.17}$$

$\Delta\omega = K_V u_f$

$\omega = \omega_0 + \Delta\omega$

where ω is PLL frequency and finally phase angle is:

$$\theta = \omega_0 t + \int_{-\infty}^{t} \Delta\omega dt \tag{3.18}$$

3.5.2 Positioning of STATCOM

The optimal positioning of voltage support devices in transmission line has been investigated in [9,63],[65-67]. It has been stated in [9,65] that, when dynamic voltage support devices positioned in mid point of the transmission line power transfer can be doubled. The voltage profile of the line is given with solution of the wave equation:

$$\frac{d^2V}{dx^2} = \left[(r + j\omega l)(g + j\omega c)\right]V \tag{3.19}$$

Assuming lossless line the solution is given by:

$$\bar{V} = \bar{V}_R \cos\beta x + jZ_c\bar{I}_R \sin\beta x \tag{3.20}$$

Z_C is characteristic impedance of the line

$\beta = \omega\sqrt{lc}$ is wave number

l-line inductance (H/km)

c-line capacitance (F/km)

If the active and reactive power of the load are P+jQ, the sending end voltage(source voltage) is (3.21):

$$V_S = V_R \cos\theta + jZ_C \frac{P - jQ}{V_R} \sin\theta \tag{3.21}$$

V_R receiving end voltage

V_S sending end voltage

$\theta=\beta l$, l line length (km),

θ - electrical line length

The voltage $\mathbf{V_R}$ can be taken as reference, $\mathbf{V_S}$ can be written as (3.22)

$$\mathbf{V_S} = |\mathbf{V_S}|(\cos\delta + j\sin\delta) \qquad (3.22)$$
$$\mathbf{V_R} = |\mathbf{V_R}|$$

Combining (3.21) and (3.22) yield (3.23)

$$V_S \sin\delta = Z_C \frac{P}{V_R} \sin\theta \qquad (3.23)$$

From (3.23) the power transfer between two ends of the line is given by (3.24)

$$P_R = \frac{V_S V_R}{Z_C \sin\theta} \sin\delta \qquad (3.24)$$

where V_S is sending end voltage, θ is the electrical length of the line ($\theta=\beta l$) and δ is power angle. From (3.24) it is obvious that maximum power transfer occurs when δ is 90 degrees. If we assume that $|V_R| = |V_S| = |V|$, then steady state stability limit is (3.25).

$$P_{MAX.} = \frac{|V|^2}{Z_C \sin\theta} \qquad (3.25)$$

If the line voltage is supported by mid point sitting voltage source then the line can be considered to be made of the two section each having electrical length $\theta/2$. In this case (3.24) becomes:

$$P_R = \frac{V_S V_M}{Z_C \sin\frac{\theta}{2}} \sin\frac{\delta}{2} \tag{3.26}$$

where $| V_M | = |V|$ is mid-point voltage.

In this case the steady state stability limit is given by (3.27)

$$P_{MAX.COMP} = \frac{|V|^2}{Z_C \sin\frac{\theta}{2}} \tag{3.27}$$

The increment in steady state maximum power transfer depends upon the line length and is expressed as (3.28):

$$P_{MAX.COMP} = P_{MAX.} \frac{\sin\theta}{\sin\frac{\theta}{2}} \tag{3.28}$$

where $P_{MAX.COMP.}$ is maximum steady state transferable power of mid-point compensated line and $P_{MAX.}$ is maximum steady state transferable power of the non-compensated same line. In case of short line $\sin\theta \sim \theta$ and $\sin(\theta/2) \sim \theta/2$ and (3.28) becomes (3.29)

$$P_{MAX.COMP} = 2P_{MAX.} \tag{3.29}$$

In the reality, the maximum power that can be transferred over the transmission line is limited by transient stability of the power system. The transient stability limit can be determined by using equal-area stability criterion. The stable operation of mid point compensated line with controllable voltage source is extended in the second quadrant ($90^0 < \delta < 180^0$).

3.6 Simulation Studies

The objectives of the simulation are to evaluate dynamic response of the proposed control strategy and to evaluate how much one can increase power transfer over existing, long transmission line with mid point sitting of STATCOM for voltage support, using detailed models of all components. The simulated network consists of a 400 km long radial 735 kV transmission line. The line is energized by 10,000 MVA hydro-turbine. The simulation parameters are given in Appendix A. Other end of the line is attached to infinite bus so that we have a classical, one machine system, swinging around infinite bus. The STATCOM is positioned in the midpoint of the transmission line as illustrated in Fig.22.

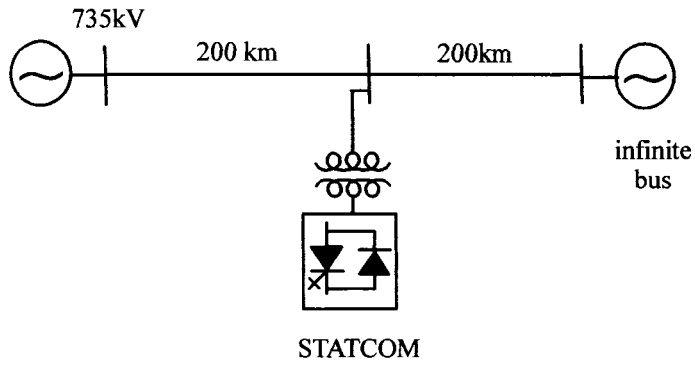

Figure 22 Single line diagram of the test network

3.6.1 STATCOM Dynamic Response

Figures 23 and 24 show STATCOM dynamic response for 10% step change of reference signals. Fig.23 (upper trace) shows system response for 10% step down and 10% step up (lower trace) change of reference voltage V_{RMS}. At the same time, Fig.23 illustrates STATCOM regulation capabilities. Fig.24 a) and b) shows STATCOM response for 10% step up and 10% step down change on DC reference V_{DC}.

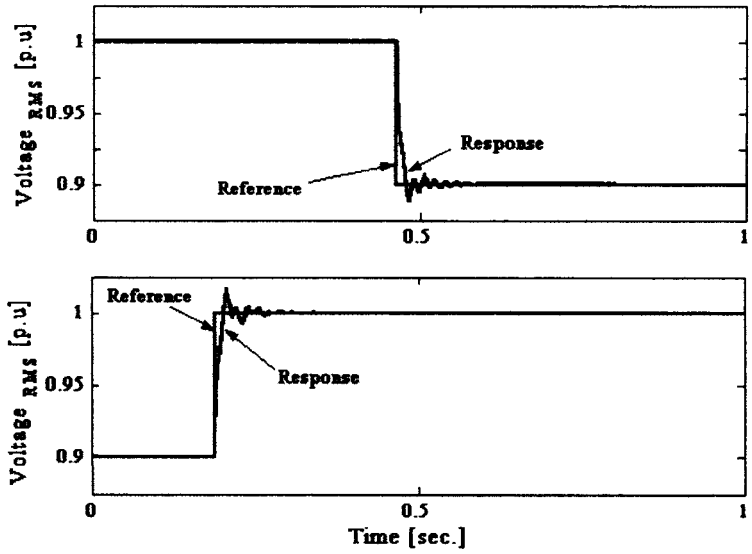

Figure 23 STATCOM dynamic response for 10% step down change in reference voltage and 10% step up change in reference voltage

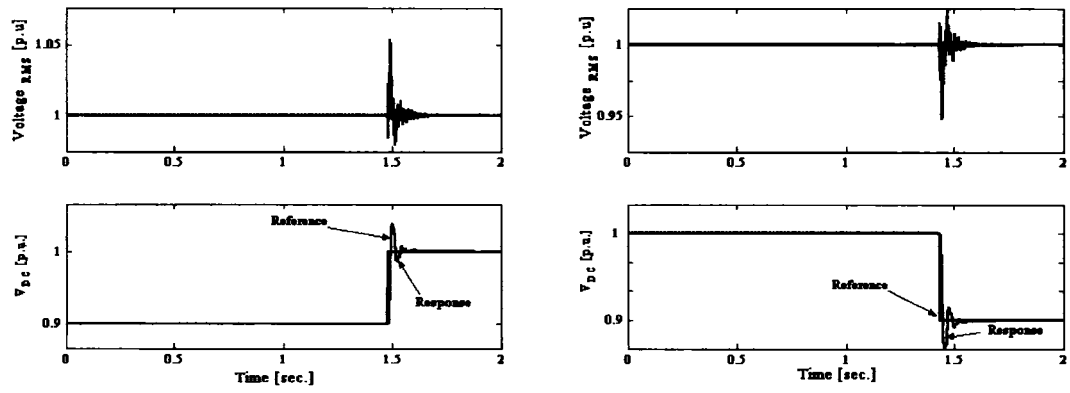

(a) (b)

Figure 24 a) STATCOM dynamic response for 10 % step up change in DC reference. Upper trace shows measured AC line voltage and lower trace shows DC bus voltage. b) STATCOM dynamic response for 10 % step down change in DC reference.

3.6.2 Steady State Stability

In order to investigate the power transfer steady state and transient stability limits, the system described above is simulated without and with STATCOM. For the analysis of steady-state performance, the power supplied by the generator-turbine unit is increased gradually. After each power increment, the simulated system is allowed to regain the stable point of operation. The power transferred over the line is measured. The maximum power that can be stably transferred without mid-point sitting STATCOM for voltage support is 4300 MW. When the STATCOM installed, the maximum power increases to 7450 MW. One can see that power transfer is increased during the steady-state by the factor of 1.732. The power transfer is not increased by the factor of two as expected in [65]. The reason is while power is increased, the line and transformer losses increase because of higher current. The second reason is that the line voltage is already naturally supported by line distributed shunt capacitance as shown in (3.28).

3.6.3 Transient Stability

The same system is subjected to transient stability test. The power loading is increased gradually and system is allowed to stabilize. Then three phase short circuit is applied in the vicinity of the generator unit (30 km from generator) and is cleared after 100 ms. The system must reestablish to the same power transfer level as before the short circuit in order to remain stable. The maximum power that can be transferred stably is 4000 MW without the STATCOM and 6400 MW with STATCOM sat in the middle of the line, which is an increase by a factor of 1.6.

3.7 Conclusion

The STATCOM based on power converter has been discussed in this chapter. An original control strategy for voltage support of transmission lines by STATCOM has been

presented and evaluated using a test system. The results of case analysis obtained by detailed numerical simulation have shown that STATCOM can significantly increase steady state and transient stability limits and hence transmission capacity of existing lines, while providing voltage support. When STATCOM put in the middle of the 400 km, 735 kV line, it is known to be optimal placing for the radial line, the steady state stability limit is increased by 73% and transient stability limit is increased by 60%. The power transfer can not be doubled due to the line length, losses and transformer and generator impedances. At the same time, voltage of the line is kept constant, independently of the loading which contributes significantly to power quality. It makes STATCOM attractive and cost effective alternative to building new line.

CHAPTER 4

VOLTAGE SUPPORT BY DISTRIBUTED STATIC VAR SYSTEMS (SVS)

4.1 Introduction

In this chapter it is shown that when load centers require Static VAR Systems (SVS) for regulated voltage control, the strategy of using many, small, distributed SVS located at distribution buses is more advantageous than a few large bulk SVS located at the transmission or sub-transmission bus. The advantages are: (i) standby to meet N-1 reliability criterion is reduced; (ii) costly high voltage transformers are no longer needed because the SVS can be connected directly to the low voltage distribution buses; (iii) distribution-side voltage support is more effective because the total MVAr requirement of the distributed SVS is less. Simulation studies have demonstrated that the distributed SVS units operate harmoniously together.

Faced with the difficulty of securing rights-of-way for new transmission lines, increasing reliance is placed on Static VAR Systems (SVS) to provide voltage support to the increasingly overloaded existing lines. In this chapter the term SVS is treated as a continuously controllable source of reactive current. It represents a combination of switched capacitors, switched inductance (for economy) and thyristor SVCs or STATCOMs (to give continuously adjustable control between the capacitor steps).

Presently, large bulk SVSs are located at the transmission or sub-transmission buses. This raises the specter of voltage collapse should the SVS fail. N-1 reliability criterion requires a redundant set of SVS. This chapter presents a preliminary evaluation of the alternative of using many small SVSs located at the low voltage distribution buses. With distributed SVSs, when any one of the M units fails, there are still M-1 units remaining to

provide voltage support. Apart from satisfying the reliability criterion better, distributed SVS bring other savings as well.

Historically, synchronous condensers, connected at the sub-transmission and transmission buses, have been used to supply the continuously adjustable capacitive or inductive currents to support the voltages at the load centers. Because of the precedence set by synchronous condensers, the SVS which have largely supplanted them, still tend to be situated at the sub-transmission and transmission buses. With the availability of STATCOMs or SVCs (cheaper) which can be connected at distribution level voltages without the need of transformers [47,48,68], it is timely to examine whether regulated voltage support should be by:

(1) a single or a few bulk SVSs connected at the transmission or sub-transmission buses.

or

(2) many small-sized distributed SVSs units connected at distribution buses.

This chapter presents the reasoning and some preliminary quantitative evaluations which support the case for distributed SVS. The objective is to arrive at positive interim conclusions which justify further in-depth studies further. The conceptual design of a substation serving a load center is given at the end of the chapter. Lastly, simulations have been used to show that many SVS units do not interact adversely to cause instability.

4.2 Model of Transmission Line to Load Center

A number of assumptions befitting a preliminary study have been used. Per-unit base referred to the transmission voltage side is used in the study and resistive losses are neglected.

In order to highlight the mechanism of "voltage drop" and conversely "voltage support", the radial transmission line is represented by an inductive reactance jX between the sending-end voltage $\mathbf{V_S}$ and receiving-end voltage $\mathbf{V_R}$ as illustrated in Fig. 25. The "telegraph line equations" could have been used, but the purpose of this chapter is to highlight the "mechanism" of voltage support using simple phasor diagrams. In presenting a Conceptual Design in Section 4.8, the "telegraph line equations" will be used to predict the inductive and the capacitive MVArs required to prevent overvoltage and undervoltage when loading below and above the Surge Impedance Level (SIL), respectively. For the present, the formula of the transmission reactance for different line length is X=0.0013 *l* p.u. of the surge impedance, where *l* is the length in km. M equal loads taking load currents $\mathbf{I_L}$/M each is supplied from the bus of $\mathbf{V_R}$. Transformers, whose leakage reactances are jMX_T, bridge the high transmission line voltage $\mathbf{V_R}$ to low the distribution voltage $\mathbf{V_L}$ of the loads. The transformer reactance is assumed to be X_T=0.10 p.u. The distributed SVS supply current $\mathbf{I_{Cd}}$/M directly at the load buses without transformers because the distribution voltage is within the capability of existing SVS technology.

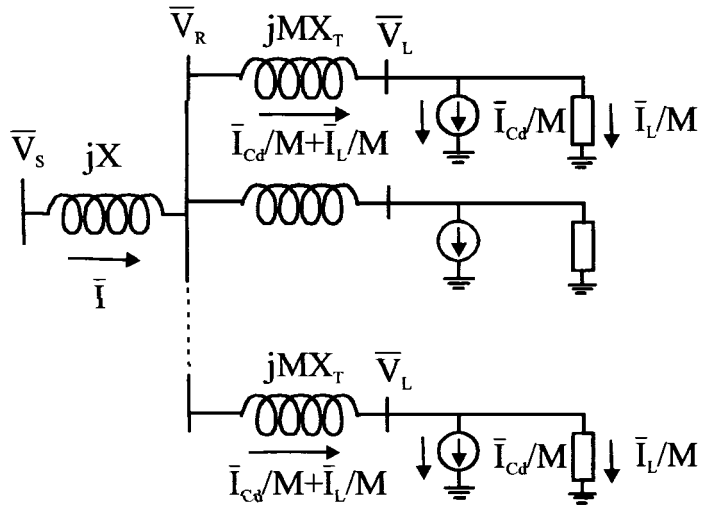

Figure 25 Single line diagram of transmission line (jX) between $\mathbf{V_S}$ and $\mathbf{V_R}$. M transformers (jMX_T) connect transmission line to M loads. Distribution SVS currents $\mathbf{I_{Cd}}$/M provide voltage support of load voltage $\mathbf{V_L}$.

The M transformers and the loads of Fig. 25 have been replaced by single transformer of reactance jX_T and a single load current $\mathbf{I_L}$ in Fig. 26. Fig. 26 a) and b), respectively, show the bulk SVS compensation current $\mathbf{I_{Cb}}$ at the transmission voltage bus side and the distributed SVS compensation current $\mathbf{I_{Cd}}$ at the distribution voltage bus side. Fig. 26 a) includes an additional transformer which is required to raise the voltage output of the SVS to the transmission line voltage of $\mathbf{V_R}$.

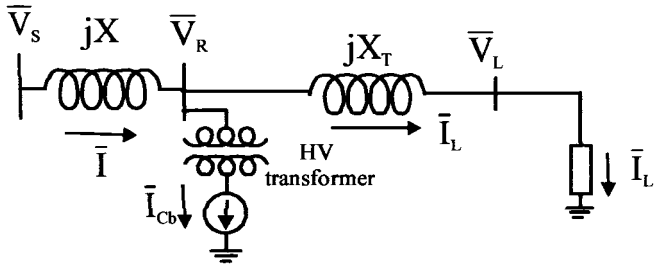

(a)

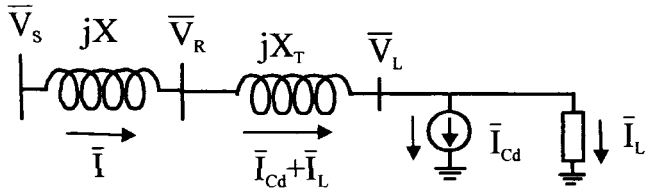

(b)

Figure 26 Single line diagram with M loads of Fig.1 equivalenced as a single load carrying current $\mathbf{I_L}$. (a) Bulk SVS connected to bus of $\mathbf{V_R}$ by additional transformer; (b) Distributed SVS located at bus of $\mathbf{V_L}$.

4.3 Case For Distributed SVS

The findings of this preliminary study point to potential cost savings arising from: (i) reduction of standby MVAr needed to satisfy N-1 reliability criterion; (ii) reduced MVAr

rating in the distributed SVS of Fig. 26 b); (iii) not needing the high voltage transformer of Fig.26 a).

4.3.1 Reliability

The loss of the bulk SVS in Fig. 26 a) affects the entire load center. N-1 reliability criterion requires there must be K units, K=2,3,4,..,, on standby and each unit has to be rated at the 1/(K-1) times the full MVAr required. The total cost is expressed as K/(K-1) times the full MVAr required.

In the system of Fig. 26 b), there are already M sets of distributed SVSs. It is a matter of rating each SVS at 1/(M-1) times the full MVAr required.

4.3.2 Effectiveness of Compensation

The "mechanism" of voltage control is complex and the details are outlined in the analysis in Section 4.4. However the basic idea is simple: as viewed from the load, an inductive current $\mathbf{I}= -jI_i$ flowing across transmission line inductive reactance jX produces a voltage drop of $-XI_i$ and a capacitive current $\mathbf{I}= jI_C$ produces a voltage boost of $+XI_c$. In Fig. 26 a), the bulk SVS current $\mathbf{I_{Cb}}$ passes through the transmission line reactance jX only. In Fig. 26 b) the capacitive current $\mathbf{I_{Cd}}$ passes through a larger reactance $j(X+X_T)$ since the load transformer reactance jX_T is added in the capacitive current path. Because of the larger reactance $j(X+X_T)$, the compensation produces a higher voltage boost/drop in Fig.26 b) than in Fig. 26 a). This simple-minded picture has been used as a guide only. Rigorous circuit theory analysis in Section 4.4 is applied to compare the MVAr requirements of Fig. 26 a) and Fig.26 b).

4.3.3 Potential Cost Saving of High Voltage Transformer

The bulk SVS in Fig. 26 a) requires a transformer to raise its output to transmission voltages. Additional transformers are not required in Fig.26 b) because the distributed SVS can be connected directly, without transformers, to the low voltage distribution buses. Therefore, there is a potential saving in cost.

4.4 Voltage Regulation Analysis

Voltage support analysis has mostly been approached at the quadratic level of complex power **S**=P+jQ. As will be shown below, the linear circuit theory approach using complex phasors of voltages and currents is more insightful.

The base line used in the comparative studies is that the load is a unity power factor load, i.e the load current $\mathbf{I_L}$ is in phase with the voltage of the load bus $\mathbf{V_L}$. As is well known, lagging power factor load depresses the load bus voltage further. The VARs required to correct the poor power factor will be accounted separately from the VARs required for voltage support of unity power factor loads. This is in line with the approach taken in the classic reference. Following this approach, the objective is to derive the formulae of the MVAr required for voltage support exclusively.

4.4.1 Bulk VAr Compensation at High Voltage Bus of $\mathbf{V_R}$

The phasor diagram of Fig. 27 is for the study of voltage regulation by bulk SVS located at the bus of $\mathbf{V_R}$ in Fig. 26 a). When the bulk SVS regulates the receiving-end voltage $\mathbf{V_R}$ at 1.0 p.u. voltage, V_L the magnitude of the load voltage $\mathbf{V_L}$ must be less than 1.0 p.u. (The per unitization is based on the voltage-base of the transmission line side.) The voltage drop is due to the voltage across the transformer reactance jX_T.

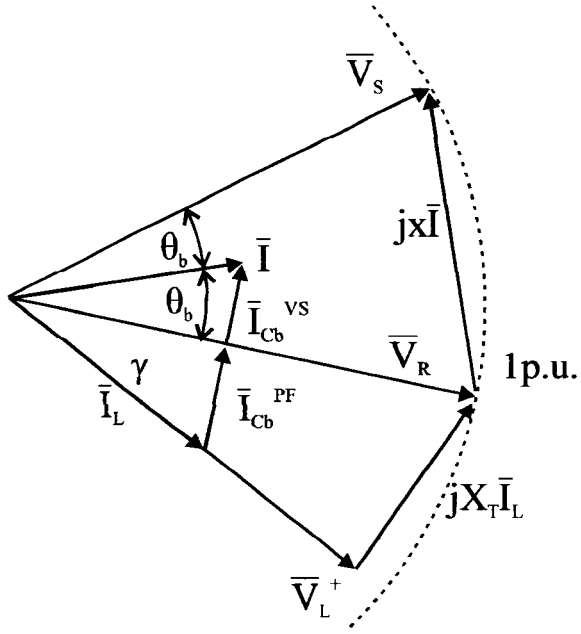

Figure 27 Phasor diagram--system of Fig. 26 a), Bulk SVS at Transmission Bus.

4.4.1.1.Phasor Diagram of Load Transformer

Fig. 27 shows $\mathbf{V_L}$ and $\mathbf{I_L}$ in phase for unity power factor operation, i.e. $P=V_L I_L$. It is necessary to compute the load voltage magnitude V_L for any load power P. For $|\mathbf{V_R}|=1.0$, applying Pythagoras Theorem to the right angle triangle formed by $\mathbf{V_R}$, $\mathbf{V_L}$ and $jX_T\mathbf{I_L}$

$$\left(X_T I_L\right)^2 + \left(V_L\right)^2 = 1 \tag{4.1}$$

Substituting $I_L=P/V_L$, (4.1) yields a quadratic equation of $(V_L)^2$. Solving the equation and choosing the solution which is nearest to 1.0 gives,

$$\left|\overline{V}_L\right| = \sqrt{\frac{1+\sqrt{1-4\left(X_L P\right)^2}}{2}} \tag{4.2}$$

The value of V_L^+ is defined as the solution of (4.2) for P=1.0. V_L^+ will be kept for the analysis of distributed SVS below. Although V_L^+ is less than 1.0 p.u., by choosing the transformer turns ratio, the distribution bus voltage can be 35 kV or 25 kV of the standard. The angle opposite to $jX_T\mathbf{I_L}$ is γ. From the properties of right angle triangle,

$$\gamma = \arccos\left(V_L^+\right) \tag{4.3}$$

4.4.1.2 Phasor Diagram of Transmission Line

In the triangle formed by $\mathbf{V_S}$ and $\mathbf{V_R}$ enclosing the angle $2\theta_b$, the power equation is

$$P = \frac{|\bar{V}_S||\bar{V}_R|}{X}\sin 2\theta_b \tag{4.4}$$

For $V_S=V_R=1.0$

$$\theta_b = \frac{1}{2}\arcsin(PX) \tag{4.5}$$

The transmission line current $\mathbf{I}$ is perpendicular to $j\mathbf{XI}$ and bisects the angle $2\theta_b$. The current of the bulk SVS is:

$$\bar{I}_{Cb} = \bar{I} - \bar{I}_L \tag{4.6}$$

$\mathbf{I_{Cb}}$ lies along the constant power line so that

$$|\bar{I}|\cos\theta_b = |\bar{I}_L|\cos\gamma \tag{4.7}$$

$\mathbf{I_{Cb}}$ consists of two parts: $\mathbf{I_{Cb}^{VS}}$ for transmission line compensation (voltage support) and $\mathbf{I_{Cb}^{PF}}$ for transformer compensation (power factor correction). The SVS current decomposed into the two components is

$$\left|\bar{I}_{Cb}\right| = \left|\bar{I}\right| \sin\theta_b + \left|\bar{I}_L\right| \sin\gamma \tag{4.8}$$

Dividing (4.8) either the LHS or RHS of (4.7) and multiplying throughout by P, it can be shown that the reactive power of the bulk SVS is

$$Q_b = P\left(\tan\theta_b + \tan\gamma\right) \tag{4.9}$$

In (4.9), P tan θ_b is for compensating the reactance jX of the transmission line and P tan γ is for the reactance jX_T of the transformers.

4.4.1.3 MVA Requirements of Transformers

In addition to the M load transformers, the bulk SVS requires a transformer to step up its low voltage to high transmission line voltage.

4.4.1.3.1 MVA Rating Requirement of Load Transformers

The high voltage side of the load transformers must be rated at $|\mathbf{V_R}| = 1.0$ p.u. The current requirement is $I_L = 1/V_L^+$. The MVA requirement of all the M load transformers is $|\mathbf{S_{b\,Load}}| = 1/V_L^+$, for V_L^+ taken from (4.2) for the case P=1.0.

4.4.1.3.2 MVA Rating Requirement of Transmission Bus SVS Transformer

The MVA rating of the high voltage transformer must be $|\mathbf{S_{bSVS}}| = P\ (\tan\theta_2 + \tan\gamma)$ for γ given by (4.3) and θ_b given by (4.5).

4.4.2 Distributed VAR Compensation at bus of V_L

Fig. 28 is the phasor diagram of Distributed SVS compensation. In order that the comparison is on the same foot, the load voltage is regulated at $|\mathbf{V_L}| = |\mathbf{V_L}^+|$ and the load power P is delivered at unity power factor. The closing side of the voltage triangle formed by $\mathbf{V_S}$ and $\mathbf{V_L}^+$ is $j(X+X_T)\mathbf{I}$. **I** lies perpendicular to $j(X+X_T)\mathbf{I}$ and makes an angle θ_d with $\mathbf{V_L}^+$. The angle δ lies between and $\mathbf{V_S}$ and $\mathbf{V_L}^+$.

The real power P is

$$P = \frac{|\bar{V}_L^+||\bar{V}_S|}{X + X_T}\sin\delta \tag{4.10}$$

For $V_S=1$,

$$\delta = \arcsin\left(\frac{P(X + X_T)}{|\bar{V}_L^+|}\right) \tag{4.11}$$

The angle, which **I** makes with $\mathbf{V_L}$, is θ_d. The angle, which **I** makes with $\mathbf{V_S}$, is $(\delta-\theta_d)$. The power transmitted at $\mathbf{V_S}$ is $P=|\mathbf{I}|\cos(\delta-\theta_d)$. The power received at $\mathbf{V_L}^+$ is $P=|\mathbf{V_L}^+||\mathbf{I}|\cos\theta_d$. Equating the two powers,

$$\cos(\delta - \theta_d) = |\bar{V}_L^+|\cos\theta_d \tag{4.12}$$

Substituting the trigonometry identity $\cos(\delta-\theta_d)=\cos\delta\cos\theta_d + \sin\delta\sin\theta_d$ in (4.12), it can be shown that

$$\theta_d = \arctan\frac{|\bar{V}_L^+| - \cos\delta}{\sin\delta} \tag{4.13}$$

The current of the distributed SVS is

$$\bar{I}_{Cd} = \bar{I} - \bar{I}_L \tag{4.14}$$

This current vector lies on the constant power line so that

$$|\bar{I}|\cos\theta_d = |\bar{I}_L| \tag{4.15}$$

The magnitude of the SVS current is

$$|\bar{I}_{Cd}| = |\bar{I}|\sin\theta_d \tag{4.16}$$

The reactive power of the distribution SVS is

$$Q_d = P\tan\theta_d \tag{4.17}$$

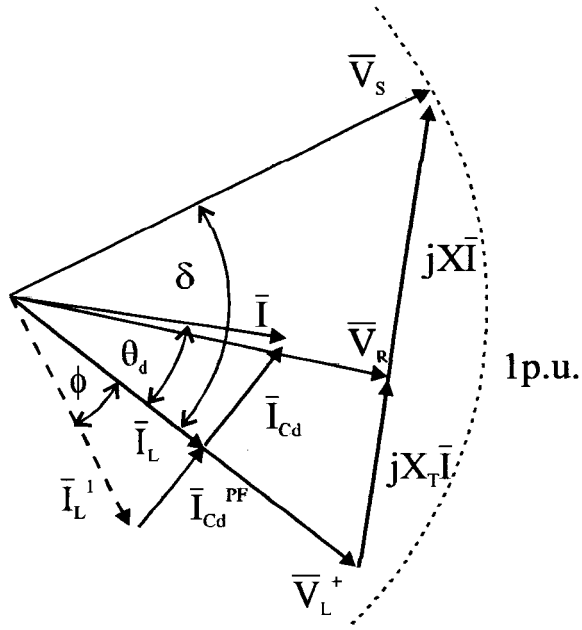

Figure 28 Phasor diagram—system of Fig.26 b), Distributed SVS at load bus.

4.4.2.1 Load with Lagging Power Factor

Normally the load current lags $\mathbf{V_L}$ by a power angle ϕ. Fig. 28 illustrates this case by the broken line phasor of the load current $\mathbf{I_L}^1$. When the load receives the same real power P, $\mathbf{I_L}^1$ must lie along the same constant power locus so that

$$\left|\bar{I}_L^1\right|\cos\phi = \left|\bar{I}_L\right| \tag{4.18}$$

Therefore in order to correct the lagging power load, the distributed SVS should take another capacitive current component $\mathbf{I_{Cd}}^{\mathbf{PF}}$ whose magnitude is $I_L{}^1\sin\phi$ and whose direction is the same as $\mathbf{I_{Cd}}$. In this case $\mathbf{I}= \mathbf{I_L}^1 + \mathbf{I_{Cd}} + \mathbf{I_{Cd}}^{\mathbf{PF}}$. The total current of the VAR compensator is $\mathbf{I_C}= \mathbf{I_{Cd}} + \mathbf{I_{Cd}}^{\mathbf{PF}}$.

The VAR required for power factor compensation is

$$Q_d^{PF} = P\tan\phi \tag{4.19}$$

Since the load can have different power factors, the systematic approach is to consider that $Q_d{}^{PF}$ is for power factor correction. For the remainder of this chapter, the focus is placed on $Q_d = P \tan\theta_d$, the requirement for voltage support.

4.4.2.2 MVA Rating Requirement of Load Transformers

The voltage rating of the load transformers must be $V_L{}^+$ p.u. The load current is $I_L = 1/ V_L{}^+$. From (4.15) the magnitude of the transformer current **I** is $I = I_L / \cos\theta_d$. Therefore the MVA requirement of the load transformers is $|\mathbf{S_{d\ Load}}| = V_L{}^+ I = 1/\cos\theta_d$.

4.5. Comparison of MVAr Requirement of SVS

For comparisons to be meaningful, the same real powers, P=1p.u., are drawn from the load bus at unity power factor and the load voltage $|\mathbf{V_L}| = V_L^+$. For distributed SVS the MVAr is calculated from $Q_d = P \tan\theta_d$, where θ_d is computed from (4.13). For bulk SVS at the transmission line voltage $\mathbf{V_R}$, $Q_b = P(\tan\theta_b + \tan\gamma)$ where θ_b and γ are taken from (4.5) and (4.3) respectively. $P\tan\gamma$ compensates jX_T of the load transformers and resembles an overhead requirement irrespective of transmission line length. $P\tan\theta_b$ compensates the line reactance jX and since X=0.0013 x km it increases with the length of the transmission line.

Fig.29 presents Q_d and Q_b in per-unitized MVAr plotted against the line length in km. The savings Q_b-Q_d, in adopting distributed SVS in preference over bulk SVS, varies from 5% to 10%, depending on the length of the transmission line. The 10% corresponds to X_T, the transformer leakage reactance.

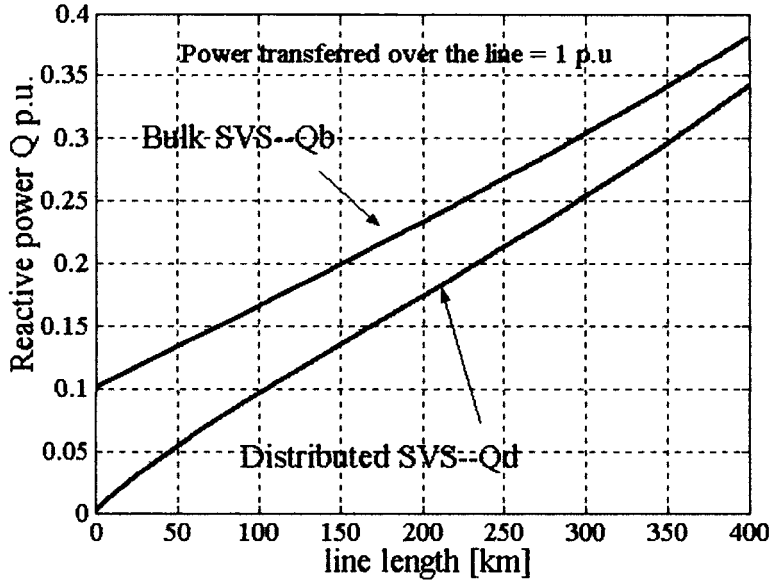

Figure 29 MVAr (p.u.) requirement of SVS plotted against transmission distance (km). Bulk SVS--Q_b ; Distributed SVS--Q_d. (X=0.0013 *l* km, X_T=0.10 p.u.)

4.6 Comparison of MVA Requirements of Transformers

For real power, P=1, for distributed SVS, the MVA rating of all the M load transformers is $|S_{d\ Load}| = 1/\cos\theta_d$, where θ_d is computed from (4.13). For bulk SVS, the MVA rating of all the M load transformers is $|S_{b\ Load}| = 1/V_L^+$ with V_L^+ computed from (4.2). The additional transformer to step up the voltage of the bulk SVS to transmission line voltage must have an MVA rating of : $|S_{b\ svs}| = (\tan\theta_b + \tan\gamma)$ where θ_b and γ are taken from (4.5) and (4.3) respectively.

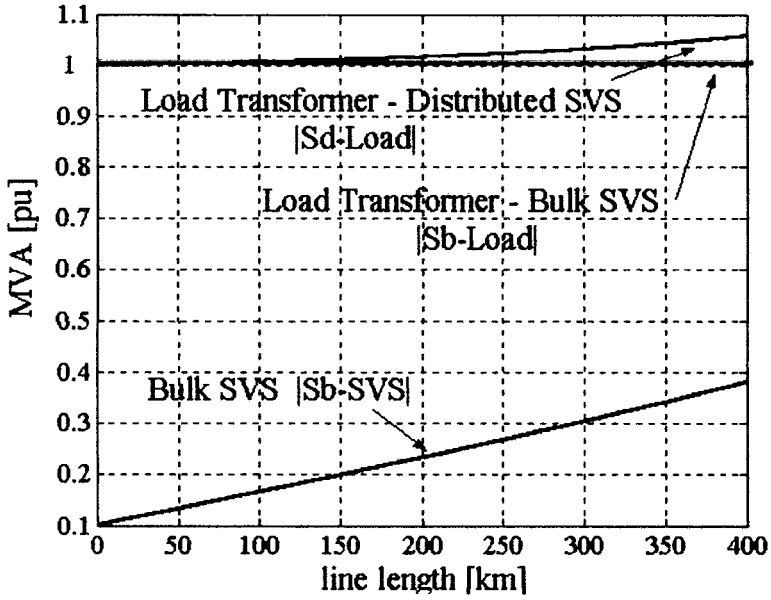

Figure 30 MVA (p.u.) of transformers plotted against transmission distance (km). $|S_{b\ svs}|$ ---transformer connecting Bulk SVS to power system. Load Transformers: $|S_{b\text{-}Load}|$ --Bulk SVS; $|S_{d\text{-}Load}|$ --Distributed SVS. (X=0.0013 l km, X_T=0.10 p.u.)

Fig. 30 presents the per-unitized MVA of load transformers: $|S_{d\ Load}|$ of distributed SVS and $|S_{b\ Load}|$ of bulk SVS plotted against the line length. Bulk SVS requires its own transformer of $|S_{b\ svs}|$ rating. In using distribution SVS, the compensating currents pass

through the load transformers so that their MVA have to increase especially when transmission line is long.

4.7 Discussion

4.7.1 Cost of VAR Compensators - Bulk Size vs. Distribution Size

The savings, Q_b-Q_d, in MVARs shown in Fig. 29 translate to lower costs in the Static VAR Compensators or STATCOM and switched capacitors for distributed SVS. However there is a cost component related to controls. Since every unit has its own controls, this cost component of distributed SVS increases with M, the number of units.

4.7.1.1 Estimate in Savings

As it is difficult to obtain cost of equipment from manufacturers, the authors have presented in Table I, the estimates of savings based on the MVAR of *SVS* saved multiplied to $/kVAR of SVC or STATCOM which have been listed in [69,70]. The MVAr saved is based on a conservative estimate of 5% (taken from Fig.29). Cost estimates for STATCOM and SVC are: STATCOM 50$/kVAr and SVC 40$/kVAr. Although the references were dated in 1996, the numbers provide reasonable guidance in 2004.

4.7.2 Cost of Transformers

In distributed SVS, there is a potential saving because the high voltage transformer of the bulk SVS of Fig. 26 a) is not required. However, the compensating currents from the distributed SVS of Fig. 26 b) must still pass through the M load transformers. Therefore their total MVA rating must be increased as $|S_{d\ Load}|$ shows in Fig.30. As the voltage

rating is kept regulated at V_L+, it is the current rating which is increased thus requiring thicker copper windings.

Bulk SVS requires an additional transformer with MVA rating of $|\mathbf{S_{b\,SVS}}| = (\tan\theta_2 + \tan\gamma)$. As the transformer carries Q_b of the bulk SVS, the plot of $|\mathbf{S_{b\,SVS}}|$ in Fig.30 is the same as Q_d in Fig.29. Not having to pay for a high voltage transformer of this MVA rating is an important saving knowing that it can make up to 20% of overall cost of SVC [69,70]. However, this has to be compared with the increase in the MVA of load transformers of distributed SVS. Since reactive power is added vectorially to the real power of the load, i.e. $|\mathbf{S_{d\,Load}}| = [1+Q_d^2]^{0.5}$, the increase only by about 7% for 400 km in Fig.30.

Table I

Savings from reduced Mvar of SVS

Nominal Voltage l-l [kV]V_{BASE}	230 [kV]	345 [kV]	500 [kV]	735 [kV]
$P_{SIL} = S_{BASE}$ [MVA]	140	420	1000	2280
savings [pu]	0.05	0.05	0.05	0.05
savings [MVAr]	7	21	50	114
savings [$] voltage support provided entirely by STATCOM	350000	$1.05 million	$2.5 million	$5.7 million
savings [$] voltage support provided entirely by SVC	280000	840000	$2 million	$4.56 million

4.7.3 Cost of AC Circuit Breakers

Each SVS has its AC Circuit Breaker. The cost of M Circuit Breakers at distribution voltage level and each having MVA rating at $PM/(M-1)\cos\theta_1$ is to be compared with the

cost of K Circuit Breakers of bulk SVS each rated at $PK(\tan\theta_2 + \tan\gamma)/(K-1)$ MVA rating at transmission or sub-transmission voltage level.

4.7.4 Cost of Redundancy

In bulk SVS of Fig. 26 b), N-1 reliability criterion requires K SVS for standby. Expressed in terms of MVAr, the cost of redundancy is $KQ_b/(K-1)$

In distributed SVS, the cost is $MQ_d/(M-1)$.

4.7.5 General Note

It should be noted that V_L^+ is defined and required for this work only. It fulfils the function of ensuring that the bulk SVS and distributed SVS are evaluated on equal footing. In other studies of distributed SVS where comparisons are not needed, the load bus voltage will be set as V_L=1.0 p.u. This will simplify Fig. 28 as $\mathbf{V_L}$ will lie on the unit circle and $\delta=2\theta_d$.

4.8 Conceptual Design of Power Delivery Substation

This section presents the conceptual design example of a 315/25 kV substation receiving power in the range of 50 MW to 375 MW from a 300 km long, 315 kV line. The desired voltage profile in the line is: at the sending end $|\mathbf{V_S}|$=315 kV and at the receiving end at the 25 kV busses of the substation, the load voltage is regulated at $|\mathbf{V_L}|$=25kV. The substation load is assumed to be at 90 percent power factor. The SVS units are located on the 25 kV bus of the substation.

4.8.1 MVAR Requirements of Substation

In the preceding sections, for simplicity in presenting the comparative merits of the transmission voltage vs. distribution voltage locations of the SVS, the lossless lumped inductance has been used to model the transmission line. Unfortunately, such a model cannot predict overvoltages when the load is below the Surge-Impedance Loading (SIL). In this section, the distributed parameter model is used. As the method is familiar to most readers, it is necessary only to recall that the single-conductor line is characterized by:

z, impedance per km (z = 0.474 ohm/km, from [71])

y, admittance per km ($y = 3.33\text{x}10^{-6}$ S/km, from [71])

$Z = z \cdot l$ and $Y = y \cdot l$, where l is the length of the line in km. $Z_S = \sqrt{z/y} = 377\ ohms$, $\mathbf{V_S}$ is 315 kV hence the Surge-Impedance Loading (SIL) of the line ($= |\mathbf{V_S}|^2/Z_S$) is 250 MW.

At the receiving end, it can be shown that the real and reactive powers are given by:

$$P = \frac{|V_S||V_R|}{B}\sin\delta \tag{4.20}$$

$$Q_R = -\frac{|V_R|^2 A}{B} + \frac{|V_S||V_R|}{B}\cos\delta \tag{4.21}$$

where $|\mathbf{V_S}|$ is the sending-end voltage, $|\mathbf{V_R}|$ is the receiving-end voltage, δ is the angle between $|\mathbf{V_S}|$ and $|\mathbf{V_R}|$, $A = \cosh\sqrt{ZY}$ and $B = Z\dfrac{\sinh\sqrt{ZY}}{\sqrt{ZY}}$.

$$l\sqrt{zy} = 1.256x10^{-3}(300) = 0.377 radians = 21.6^\circ$$

$$A = \cosh\sqrt{ZY} = \cosh l\sqrt{zy} = \cos 21.6^\circ = 0.9298$$

$$B = Z\frac{\sinh\sqrt{ZY}}{\sqrt{ZY}} = zl\frac{\sinh l\sqrt{zy}}{l\sqrt{zy}} = 0.474x300\frac{\sin 21.6^\circ}{0.377} = 138.85$$

Integrating the transmission line equations with the step-down transformer leakage reactance, the Q_R required by the transmission line, to meet the voltage constraint $|V_S|$=315 kV and $|V_L|$=25kV at both ends of the line, is shown in Fig. 31 under the label "Line". Inductive MVARs are required to counter overvoltage for light loads and capacitive MVARs for heavy loads. The cross-over takes place at the Surge Impedance Loading (SIL) of 250 MW.

Before proceeding further, a brief digression is in order. In Section 4.3, mention has been made that the transformer reactance jX_T contributes to the effectiveness of voltage support when the SVS is on the 25 kV side. This has been demonstrated by the quantitative comparison appearing in Fig.29 by which the capacitive MVARs of Distributed SVS is less than that of Bulk SVS. This raises the question as to whether the transformer reactance jX_T can contribute to reducing the -50 MVAR (inductive) required to prevent overvoltage when operating under low load condition. In transmitting 375 MW at 0.9 pf, the MVA base is 375/0.9=416.6 MVA. For 25 kV, it can be shown that the Z_{base} phase is 0.50 ohm. Assuming that –50 MVAR is provided by jX_{SVC} the inductive reactance of SVCs, the equivalent value of X_{SVC} =4.16 or 8.32 pu. The transformer reactance is taken as X_T=0.1 pu. Therefore, the size of X_{SVC} can be reduced to (8.32-0.1=) 8.22 pu. As this reduction is small, it is neglected for the remainder of this chapter.

There is a second requirement for capacitive MVARs. This is for unity power factor correction of the loads. For load operating at 0.9 pf, Q_{pf} the capacitive MVARs required is shown in Fig.31 under the label "Load". The total MVARs required at the substation is $Q_T=Q_R+Q_{pf}$ is shown under the label "Operating range of the SVS". In this chapter the term "SVS" covers a combination of switched inductor, switched capacitors and power electronic VAR controllers such as SVSs or STATCOMs.

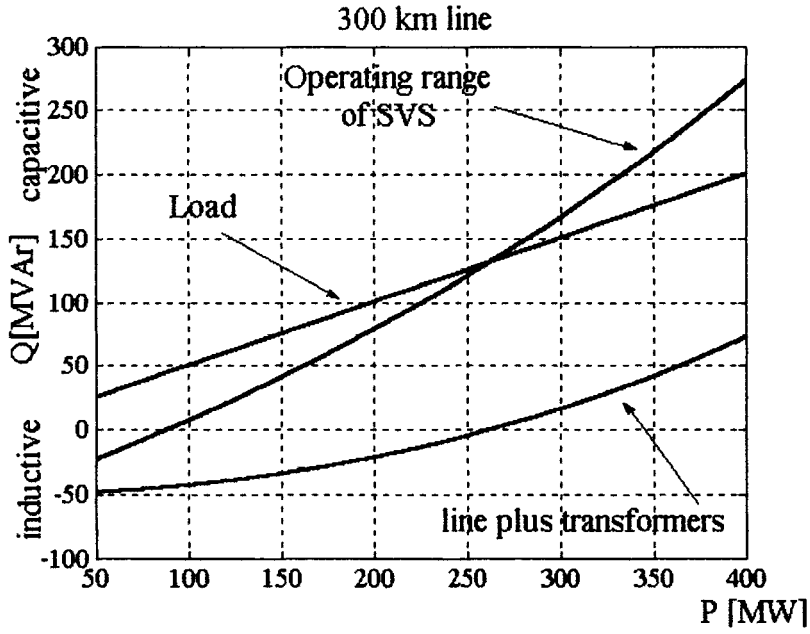

Figure 31 Operating range of SVS. (requirement for load from 50MW to 375 MW)

4.8.2 Substation

As shown in Fig. 32, the conceptual design of the substation consists of: high-voltage line terminations, high-voltage busbars, power transformers, low-voltage busbars and low-voltage line terminations. Breaker-and-a-half is used for both voltage levels main-buses in order to fulfill the reliability of power supply. Three 125 MW power transformers are chosen for the total power of 375 MW. One spare transformer is also used to increase the reliability. The total power distribution at 25 kV level is divided by 4 buses, each is around 125 MW. Each bus has one SVS with five terminations of 25 MW each. The SVS, located on the 25 kV bus of the substation, control the reactive power (unity power factor) so as to regulate the bus voltage at 25 kV.

4.8.3 Rating of Transformers

The 181 MVAR capacitive required for power factor correction does not cross the transformers. Thus the transformers must be rated to carry the maximum real power of 375 MW and the capacitive reactive power Q_R =60 MVAR (according to Fig. 31), which is required to support the receiving end voltage of the transmission line from dropping. The total MVA of the transformers should be $(375^2+60^2)^{0.5}$=379 MVA. In choosing 3 transformers, the MVA required for each is 127 MVA. For (N-1) reliability, 4 transformers, each rated at 125 MVA, are chosen in the substation layout as illustrated in Fig.32.

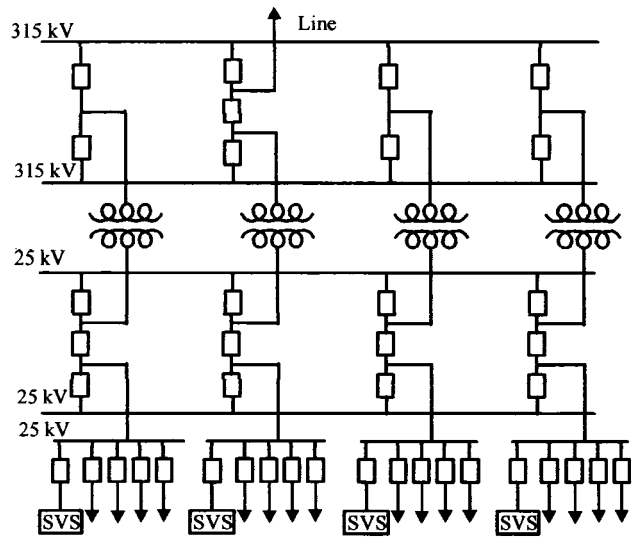

Figure 32 Single Line Diagram for 315/25 kV, 375 MW substation

4.8.4 Rating of SVS

From Fig. 31, the total MVAR requirement of the SVS ranges from -50 MVAR (inductive) to 240 MVAR (capacitive) (60 MVAR for voltage support +180 MVAR for pf

correction). For (N-1) reliability, the requirements for each of the four SVS are: -16.7 (=-50/3) MVAR (inductive) and 80 (=240/3) MVAR (capacitive). As there is one SVS for each of the four 25 KV busses, failure of any one SVS leaves a total of -50 MVAR (inductive) to 240 MVAR (capacitive), so that N-1 reliability is satisfied. The SVS can be realized by the Static VAR Compensator (SVS) using thyristor technology or the STATCOM using GTO or IGBT technology.

4.8.4.1 Rating of SVC

For the realization by SVCs as illustrated by Fig. 33, each of the four 25 kV busses will have: one SVC with inductive VAR= 20 MVAR

4 sets of Switched Capacitors rated at 20 MVAR each

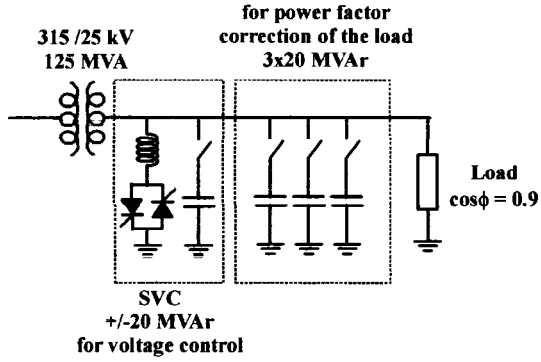

Figure 33 Single Line Diagram of SVS realized with SVC for voltage control and switched capacitors for power factor correction of the load

4.8.4.2 STATCOM

For the realization by STATCOMs as illustrated by Fig. 34, each of the four 25 kV busses will have: one STATCOM rated at ±20 MVAR

3 sets of Switched Capacitors rated at 20 MVAR each.

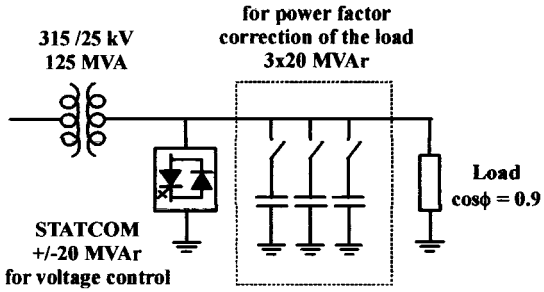

Figure 34 Single Line Diagram of SVS realized with STATCOM for voltage control and switched capacitors for power factor correction of the load

4.9 Dynamic Performance

As the preceding analysis is meaningless if the distributed SVSs will interact adversely against each other during transients, simulations studies have been performed which should put to rest such concern. The simulations have been carried out using HYPERSIM [72], a real-time simulator based on parallel computers developed by Hydro-Quebec. The value of HYPERSIM in comes from the availability of default models of transformers, induction motors and transmission lines (distributed line inductance and capacitance) based on many years experience of Hydro-Quebec researchers. All models are very accurate of high order. The real-time capability of HYPERSIM is not important in the simulations carried out.

The system which has been simulated consists of system from Fig. 32 which is connected to an infinite bus by a 300 km long 315 kV line. The power transferred over the line is 375 MW. Half of the load is resistive. The other half is induction motor driving constant torque load (compressor load of air-conditioning and refrigeration). The SVS is based on STATCOMs. Each STATCOM has its own control circuit. Only local feedback is used. Fig. 35 shows the case of the sudden loss of STATCOM #2 in the system of Fig. 32. The simulated instantaneous voltages at each ac bus have been converted to RMS voltages and displayed in Fig. 35 a) against the reference voltages. The waveforms show that the

transients disappear within 0.05s and the maximum voltage deviation is only about 0.1 kV (0.7% of rated 25 kV). Fig. 35 b) records the simulated instantaneous phase currents of the STATCOMS which lead the phase voltages by 90^0. The sudden loss of STATCOM #2 is apparent in the disappearance of the current. The other three STATCOMs respond by increasing their currents to make up for the lost one. The simulation clearly shows that any fear that instability arising from the STATCOMs interacting adversely with each other is groundless.

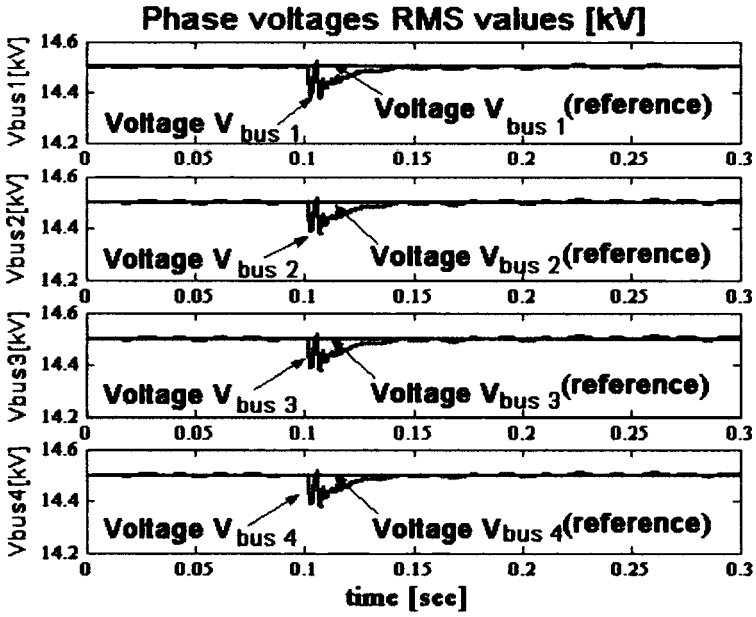

Figure 35 a) Phase voltages of 25 kV bus of Fig.32 when STATCOM #2 is lost

Fig. 36 shows the case of the sudden disconnection of one load bus as happens when its circuit breaker trips. Fig. 36 a) shows RMS values of phase voltages of supported buses. Fig. 36 b) shows phase-a current of every STATCOM. The lowest trace on Fig 36 b) shows power transferred over the transmission line. Once again, the results demonstrate that the STATCOMS operate harmoniously.

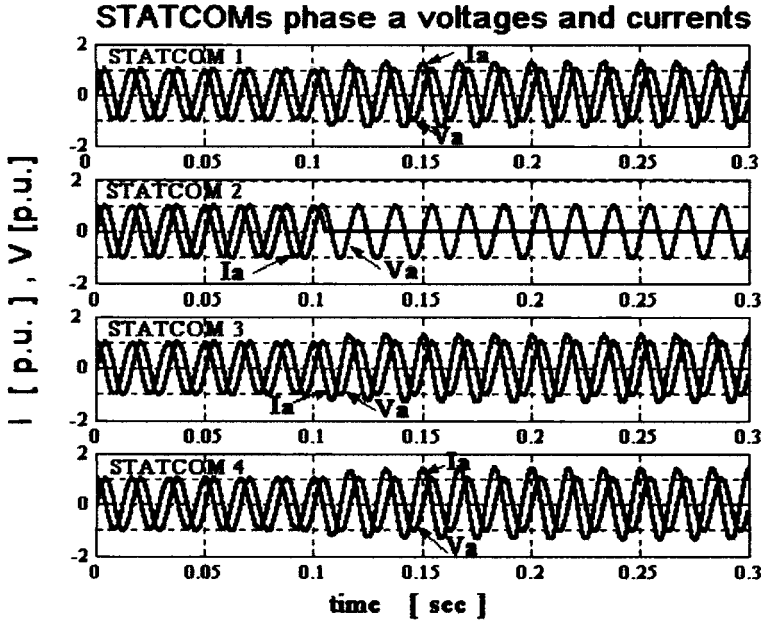

Figure 35 b) Voltages and current of one phase of every STATCOM of Fig.32. Current disappears when STATCOM #2 is lost (Q_{base} = 25 MVAr)

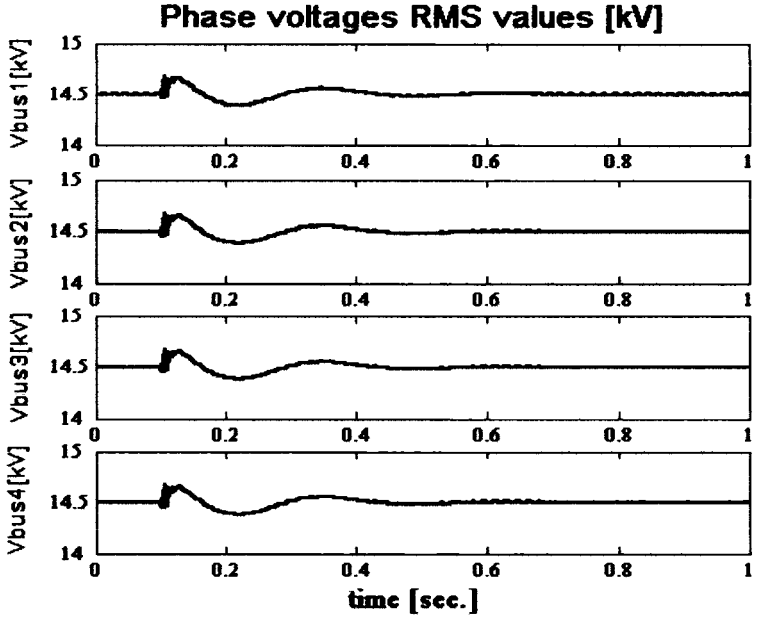

Figure 36 a) Phase voltages (rms) of 25 kV bus of Fig.32 when circuit breaker trips thus disconnecting load and STATCOM #2.

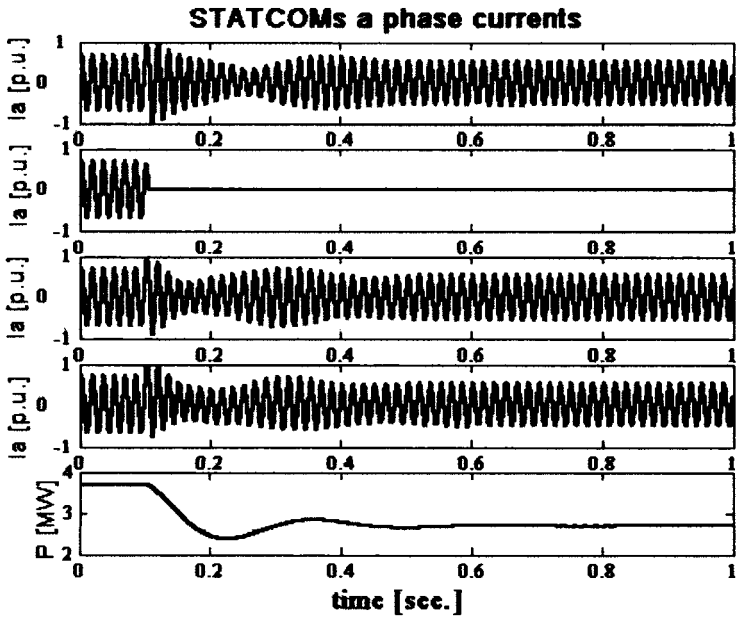

Figure 36 b) Phase-a current of every STATCOM. The lowest trace shows the power transferred over the transmission line.

4.9.1 Bulk vs Distributed SVS

Fig. 37 repeats the simulations of Fig. 35 with the important difference that all the distributed STATCOMS are lumped together as a single bulk STATCOM (as would be used if the compensation is on the high voltage side without satisfying the N-1 reliability criterion). After the sudden loss of the STATCOM, all the load bus voltages drop instantaneously for about 15 % as shown in Fig. 37 a). Fig.37 b) shows the phase-a current of the STATCOM, the reactive power flow of the load substation, the induction motor power and the induction motor slip (lowest trace). As the load has a large induction motor component, the large inductive var causes the load bus voltages to continue dropping as are evident from the gradual descending slopes in Fig. 37 a). This is because the lowering of the terminal voltage slows the induction motors further, increasing their slip and inductive var, as shown in Fig. 37 b). The positive feedback aggravation

eventually leads to voltage collapse. Fig. 37 shows that when bulk SVS is used on the high voltage side, N-1 reliability criterion requires at least 2 units.

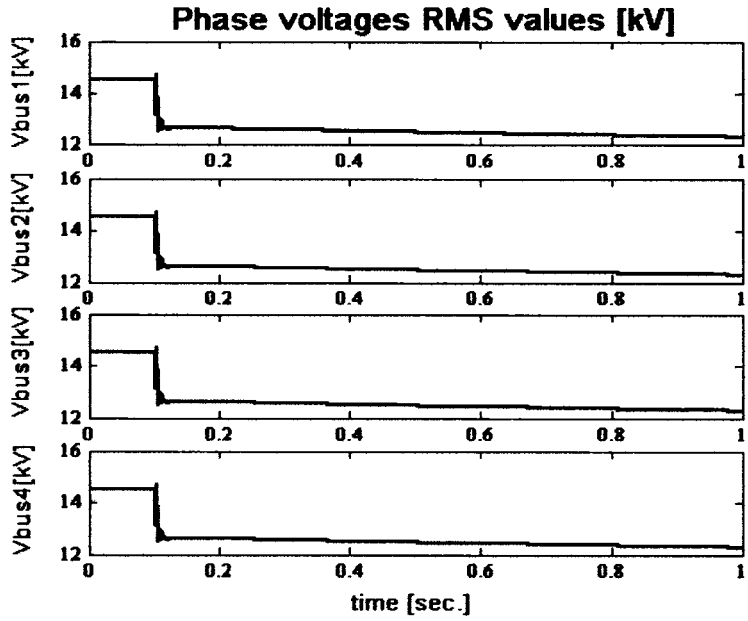

Figure 37 a) Phase voltages (rms) of 25 kV bus when single bulk STATCOM providing voltage support to 315 kV bus is lost

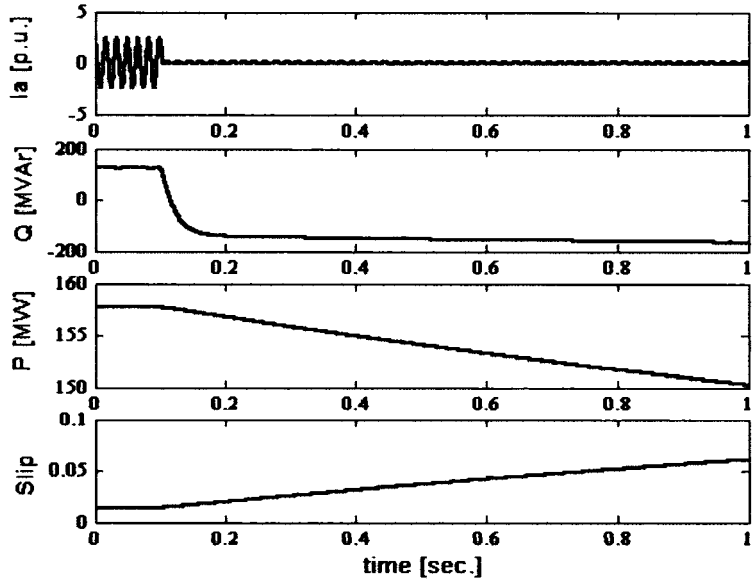

Figure 37 b) Phase-a current of bulk STATCOM, reactive power flow through the substation, active power drawn by the induction motor and motor slip

4.10 Conclusion

The preliminary evaluation, based on: (1) savings in MVArs required of the SVS and (2) savings in MVAs of the transformers, has shown that distributed SVS is more advantageous than bulk SVS located at the transmission line bus. Saving from the cost of reduced redundancy to meet N-1 reliability criterion will require knowing K, the number of SVCs or STATCOMs for standby, which will be used for bulk SVS. The designers of bulk SVS will likely divide the installation after the pattern of Fig.4.8.

Preliminary transient studies have demonstrated that the many SVS units operate harmoniously together. From the positive conclusions, further in-depth studies are justified. These studies will identify unforeseen problems in load centers regulated by distributed SVS and solve them when they surface.

CHAPTER 5

DISTRIBUTED, DISTRIBUTION STATIC VAR SYSTEMS VS. LUMPED STATIC VAR SYSTEMS: AN IN-DEPTH STUDY

5.1 Introduction

In the previous chapter it has been shown that, when a load center requires SVS for voltage support, the strategy of using many smaller sized SVS located at distribution bus is advantageous over lumped compensation on transmission level. In this chapter a step further is made toward generalization of the proposed concept showing that, when a few load centers are in parallel, providing voltage regulation with many smaller sized widely distributed Static VAr Systems (SVSs) at distribution level has more advantages than a few large lumped SVSs on transmission level. The benefits obtained from distributed, distribution voltage support scheme are quantified. The feasibility and reliability of distributed voltage support scheme with SVSs based on SVCs and STATCOMs are demonstrated by detailed real time dynamic simulation.

The structure of the chapter is as follows: Section 5.2 describes general system model used later in the chapter for steady state analysis. Section 5.3 demonstrates the feasibility of distributed, distribution voltage support scheme using phasors, while in section 5.4, reliability of distributed voltage support is demonstrated. In Section 5.5, SVS rating of distributed, distribution voltage support is calculated and compared to the rating of lumped SVS put on the transmission side of the power delivery substation. To calculate the rating, distributed line parameters have been used. In Section 5.6 a rough estimate of the cost of two compensation methods and their impact on line losses is addressed. Section 5.7 compares steady state loadability limit for two compensation schemes and, finally, in Section 5.8 detailed real time dynamic simulation of a test system is performed.

5.2 System Model for Voltage Support Analysis -

In this chapter, more general model is considered consisting of K incoming transmission lines serving N equal constant power loads.

Fig.38 illustrates the case when voltage support is provided by N distributed SVSs installed on distribution side of power delivery substation. Fig. 39 illustrates the case when one lumped SVS provides voltage support on transmission side of the power delivery substation. SVS is treated as continuous source of reactive current. It consists of switched capacitors (for economy reason) in combination with STATCOM or (Thyristor Control Reactor) TCR. Distributed parameters are used to model each line. Resistive losses are neglected.

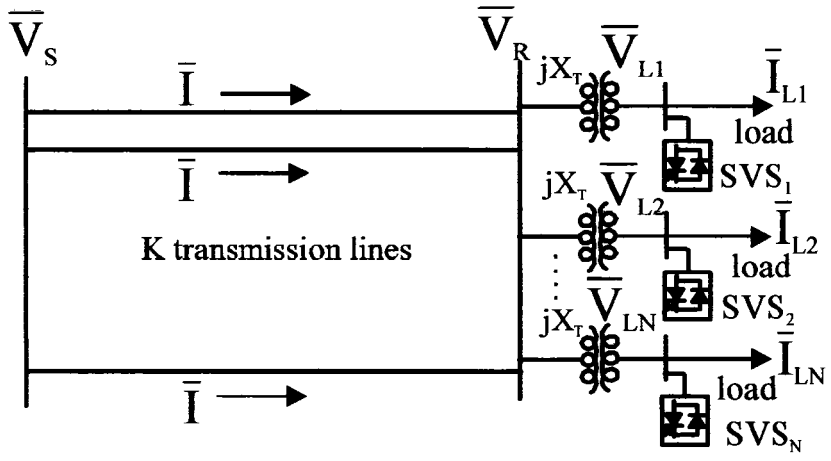

Figure 38 Single line diagram of K incoming transmission lines serving N loads over N transformers each having reactance jX_T. Each load is provided with its own SVS providing voltage support on distribution side of power delivery substation (distributed compensation).

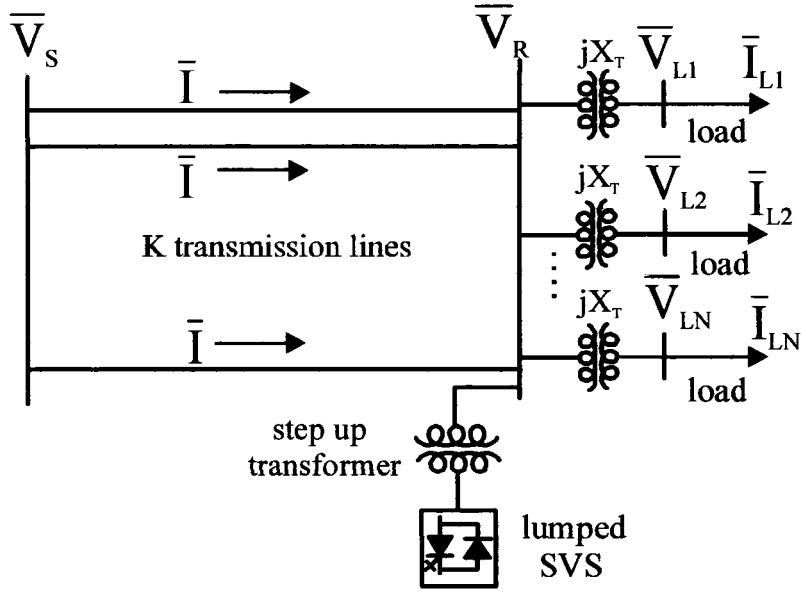

Figure 39 Single line diagram of K incoming transmission lines serving N loads over N transformers each having reactance jX_T. Voltage support is provided with one lumped SVS on transmission side of substation .

5.3 Feasibility

Before proceeding to make comparisons, it is necessary to establish that voltage support by distributed VAR compensation is mathematically feasible. This means that there are steady-state solutions for the conditions of operation. The steady-state solutions are presented here in the form of phasor diagrams. For the sake of the clarity, the number of distribution circuits is restricted to N = 3, and loads are assumed unity power factor (power factor is corrected).

5.3.1 Non-Compensated Line

The phasor diagram in Fig.40 presents the steady-state voltages and currents for non compensated line where the number of loads is N = 3. The sending end voltage $\mathbf{V_S}$ is kept at 1 p.u. due to stiffness of the system. The current $\mathbf{I} = \mathbf{I_{L1}}+\mathbf{I_{L2}}+\mathbf{I_{L3}}$ through transmission

line produces a voltage drop lowering transmission side voltage $\mathbf{V_R}$. Each load current produces additional voltage drop across transformer impedances $jX_T\mathbf{I_{Li}}$ (i=1,2 and 3)

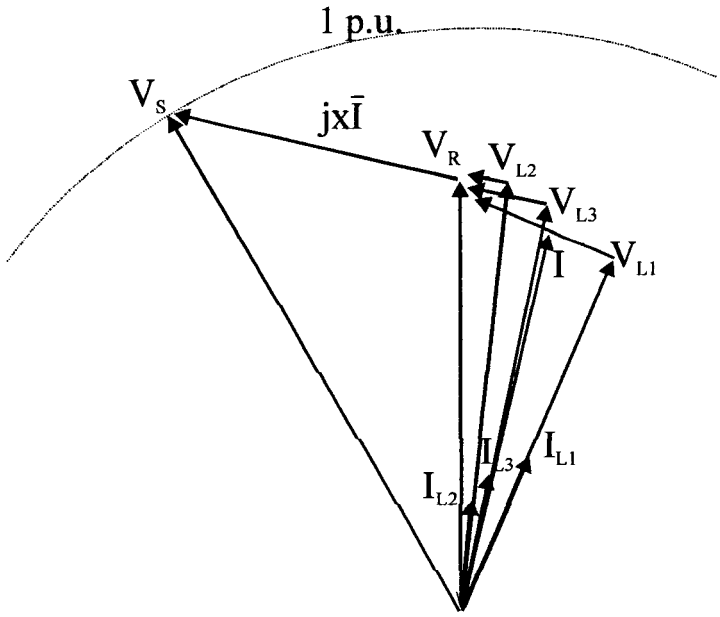

Figure 40 Phasor diagram representing current and voltages of non-compensated circuit for the case when one transmission line feeds three load centers.

5.3.2 Lumped VAR compensation

The phasor diagram in Fig.41 presents the steady-state solution for the lumped var compensation on transmission level. The sending-end voltage $\mathbf{V_S}$ and receiving-end voltage $\mathbf{V_R}$ are maintained on the circle of the 1.0 p.u. voltage radius. The closing side of the voltage triangle is the voltage phasor jXI where **I** is the current through the transmission line. The voltage triangle satisfies Kirchhoff's Voltage Law: $\mathbf{V_S} = \mathbf{V_R} + j\mathbf{XI}$. Kirchhoff's Current Law at the receiving-end bus is $\mathbf{I} = \mathbf{I_{L1}} + \mathbf{I_{L2}} + \mathbf{I_{L3}}$ where $\mathbf{I_{L1}}$, $\mathbf{I_{L2}}$ and $\mathbf{I_{L3}}$ are the load currents. For clarity, unity power factor is assumed in the loads so that the current phasors $\mathbf{I_{Li}}$ are in phase with the $\mathbf{V_{Li}}$ voltages (i=1, 2, 3). The voltage at the load

bus i is $V_{Li}=V_R - j\ X_T\ I_{Li}$, for i=1, 2, 3. It is apparent from Fig.41 that while V_R is regulated, V_{L1}, V_{L2} and V_{L3} are not.

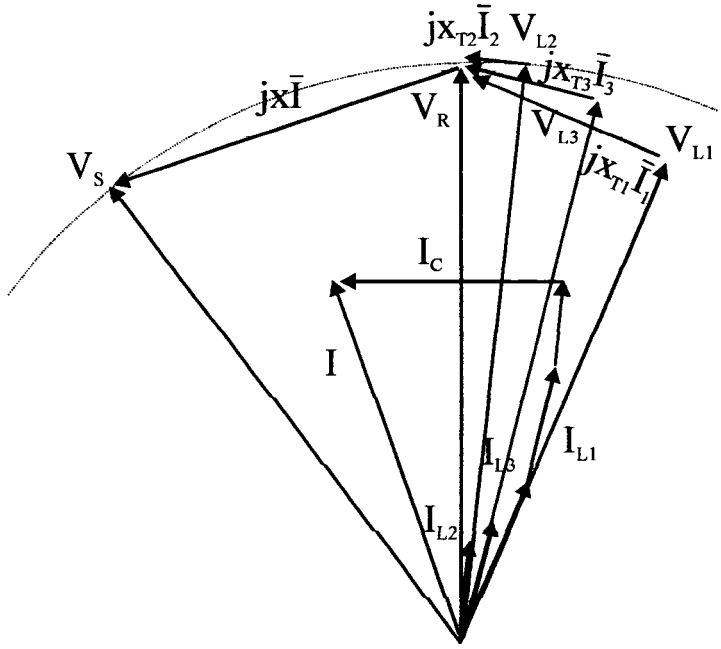

Figure 41 Phasor diagram for circuit from Fig. 39 showing voltage support from lumped compensator Compensating current I_C, injected in quadrature with voltage V_R.

5.3.3 Distributed VAR Compensation

The phasor diagram in Fig.42 presents the steady-state solution for the distributed var compensation of Fig.38 for N=3. It shows that even when the load currents I_{L1}, I_{L2} and I_{L3} are not equal (evident in the phasors j X_T I_{Li}, for i=1, 2, 3 zoomed in Fig.42), the load bus voltages V_{L1}, V_{L2} and V_{L3} can be regulated at 1.0 p.u. The receiving-end bus voltage V_R has a voltage lower than 1.0 p.u.

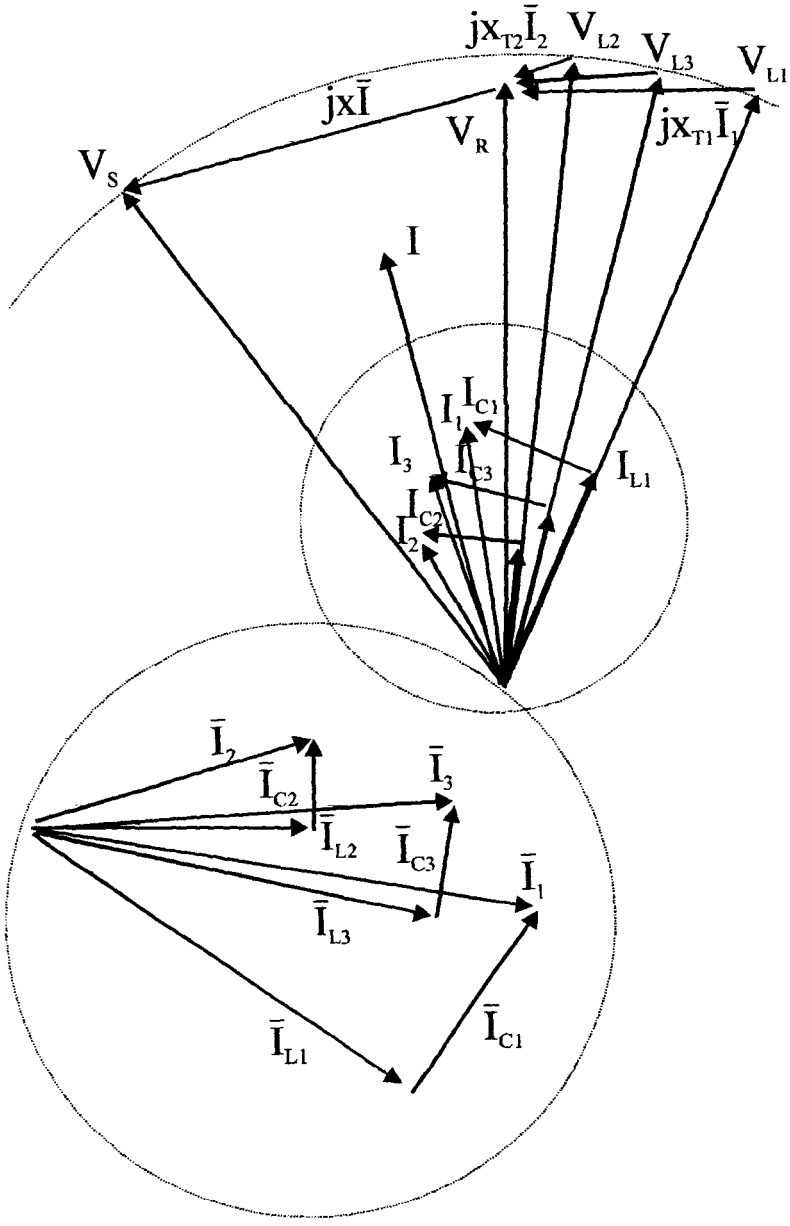

Figure 42 Phasor diagram for circuit from Fig. 38 showing voltage support from distributed compensators (SVSs or DSTATCOMs). Each SVS injects compensating current $\mathbf{I_{Ci}}$ (i=1,2 and 3), in quadrature with voltage it supports

5.4 Reliability

The loss of lumped SVS in Fig.39 (disappearance of current **Ic** on phasor in Fig.41) affects all load centers and can lead to voltage collapse. To satisfy N-1 reliability criterion there must be another stand by unit rated at the full MVAr required by the system. The loss of one of the smaller sized distributed, distribution level SVS affects only the load center that has been supported by the lost SVS and, partially, receiving end transmission voltage $\mathbf{V_R}$. However, the other distributed SVSs will indirectly support transmission voltage $\mathbf{V_R}$ and voltage on the bus where SVS has been lost.

Fig.43 describes the loss of SVS regulating load bus voltage $\mathbf{V_{L3}}$. Its loss makes compensating current I_{C3} equal to zero. As a consequence, the line current **I** decreases and rotates. The voltage $\mathbf{V_S}$ is kept at 1 pu due to stiffness of the system. Vector jX**I** (representing line voltage drop) rotates, decreasing voltage $\mathbf{V_R}$ on transmission side of the substations. Due to decrease in $\mathbf{V_R}$, distribution side voltages (load voltages) $\mathbf{V_{Li}}$ (i=1,2,3) sag. The sag of voltage $\mathbf{V_{L3}}$ is biggest because the SVS regulating it is lost. Control system of SVSs providing voltage support of load bus voltages $\mathbf{V_{L1}}$ and $\mathbf{V_{L2}}$ detect their decrease and act fast in order to restore them at 1pu. The compensating currents $\mathbf{I_{C1}}$ and $\mathbf{I_{C2}}$ increase becoming $\mathbf{I_{C1}}^{NEW}$ and $\mathbf{I_{C2}}^{NEW}$,respectively, (new SVSs compensating currents) providing additional voltage boost. The line current **I** increases rotating voltage drop jX**I**. This increases transmission voltage $\mathbf{V_R}$ but not on the same level as before the loss of the SVS, increasing load bus voltage $\mathbf{V_{L3}}$. The voltages $\mathbf{V_{L1}}$ and $\mathbf{V_{L2}}$ are restored at 1pu. Voltage $\mathbf{V_{L3}}$ stay depressed, but it is indirectly supported due to increase in transmission voltage $\mathbf{V_R}$. New steady state solution is shown in Fig.43. It is clear that the loss of one distributed SVS can be partially mitigated by the action of the other SVSs those stay into the system.

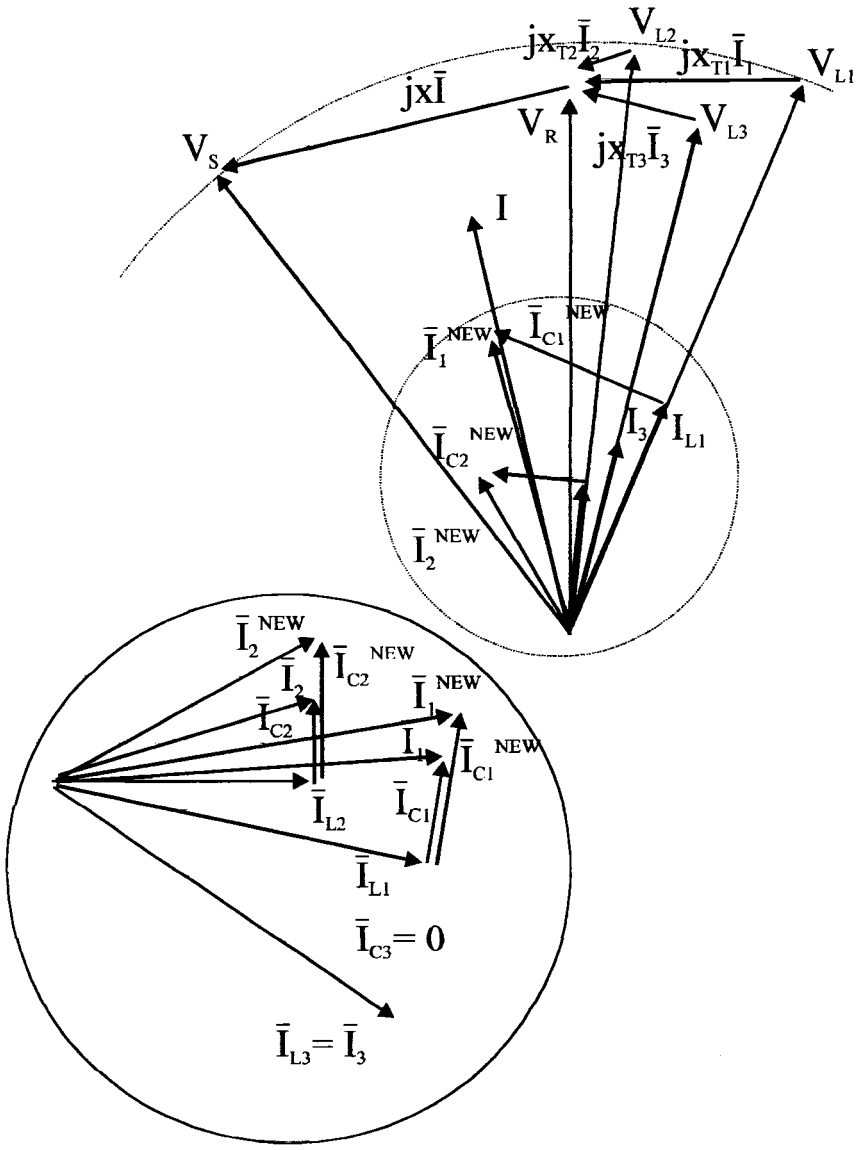

Figure 43 Phasor diagram showing steady state voltages and currents after SVS_3 is lost. Control circuits of SVS_1 and SVS_2 detect voltage drop on bus1 and bus 2 respectively. The control action of SVS_1 and SVS_2 increase its support in order to restore distribution voltages $\mathbf{V_{L1}}$ and $\mathbf{V_{L2}}$ at 1 p.u. As a consequence transmission voltage $\mathbf{V_R}$ and distribution voltage $\mathbf{V_{L3}}$ are indirectly supported.

Following example illustrates advantage of distributed, distribution side, voltage support scheme. Consider 100 km transmission line feeding three loads with powers 1.3, 0.5 and 1 p.u. over three bulk power delivery transformers. Each transformer has reactance of 0.1

p.u. and rating of 1.3 p.u. Surge impedance load P_{SIL} is used as 1 p.u.. Line reactance is $0.0013l$ where l is line length in km. When voltage support is provided with three distribution, distributed SVSs as in Fig. 42, reactive power needed to keep distribution voltages $\mathbf{V_{L1}}$, $\mathbf{V_{L2}}$ and $\mathbf{V_{L3}}$ at 1 p.u. is 0.25, 0.19 and 0.22 p.u. respectively. Transmission side voltage V_R is 0.986 p.u. If voltage support is provided with one lumped compensator on transmission side, as shown on Fig.41, reactive power Q_l needed to keep transmission side voltage $\mathbf{V_T}$ at 1p.u. is 0.755 p.u. which is 14% more. After the loss of Q_l supplied by lumped SVS on transmission side of power delivery substation, voltage collapse can happen.

If, for example, SVS_3 on distribution side is lost, as shown in Fig. 43, SVS_1 and SVS_2 respond immediately trying to restore voltages $\mathbf{V_{L1}}$ and $\mathbf{V_{L2}}$. In this case transmission side voltage $\mathbf{V_R}$ settles at 0.98 p.u., $\mathbf{V_{L3}}$ settles at 0.97 p.u. and I_{C1}^{NEW} and I_{C2}^{NEW} are 0.286 and 0.25 p.u, respectively.

5.5 SVS Rating

In this study per unit base is used and resistive losses are neglected. All loads in Fig.38 and Fig.39 are assumed equal, unity power factor. If the loads are not unity power factor then reactive power needed for power factor correction has to be accounted for separately. Each load draws the same current from the load bus. Due to unity power factor, distribution voltages $\mathbf{V_{Li}}$ and load currents $\mathbf{I_{Li}}$ are collinear. The real power supplied to each load is KP/N (K lines, each line delivering power P to N loads). The load current is $|\mathbf{I_{Li}}| = KP/N|\mathbf{V_{Li}}|$. Each SVS is represented as a source of reactive current. In the case of N distributed SVSs as in Fig.38, each SVS_i (i=1,...N) supplies reactive current $\mathbf{I_{Cdi}} = \mathbf{I_{Cd}}/N$. In the case of one lumped SVS as in Fig.39, the reactive current for voltage regulation is $\mathbf{I_{Cl}}$. For transmission lines representation, distributed parameters have been used. Transformers are assumed to have leakage reactances 10% on the transformer base, same as earlier case.

5.5.1 Per Unit Normalization

All quantities in Fig.38 and Fig.39 are normalized according to Table II so that results are general and valid for different voltage levels.

Table II

Per unit normalization

Nominal Voltage l-l [kV]V_{BASE}	230 [kV]	345 [kV]	500 [kV]	765 [kV]
$P_{SIL} = S_{BASE}$ [MW]	140	420	1000	2280
$Z_{BASE} = V^2_{BASE}/ S_{BASE} = Z_C$[Ohm]	377.8	283.4	250	256.6

Natural load P_{SIL} is 1 (p.u.). $P_{max} = MP_{SIL} = M$ (p.u.) is maximum power to be transferred over one transmission line. Bulk power delivery transformer impedance is assumed to be 10% on the transformer base. In case of one incoming line, one substation, $X_T = 0.1/M$ (pu). In case of K incoming transmission line - N outgoing distribution circuit, $X_T = 0.1N/MK$(pu). Transformer reactance changes with transformer rating. The load is assumed to be constant power. In case of K incoming lines - N outgoing distribution lines serving N loads, $R_{Li} = N|\mathbf{V_{Li}}|^2/PK$ (pu) when distribution voltages $\mathbf{V_{Li}}$ (i=1,2...N) are kept at 1pu and the power transfer over each line is assumed to be P p.u. Total power supplied to load with K transmission line is then KP p.u. The total load equivalence, as in Fig.44 a) and 44 b), is $R= |\mathbf{V_L}|^2/PK$. When voltage support is provided on distribution side as in Fig.44 a), $|\mathbf{V_L}|$ = 1p.u. and load R=1/KP. When voltage support is provided on transmission side as in Fig.44 b), the distribution voltage $|\mathbf{V_L}|$ is calculated from Fig.44 b). In this case the load current $\mathbf{I_L}=KP/\mathbf{V_L}$. Hence applying Kirchhoff's laws on circuit in Fig. 44 b), $\mathbf{V_R}=j(X_T/KM)\mathbf{I_L}+\mathbf{V_L}$:

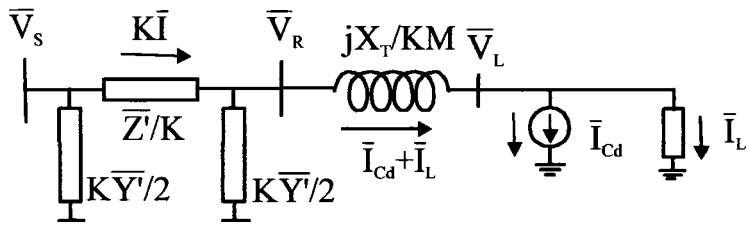

Figure 44 a) Single line diagram with N loads of Fig.38 equivalenced as a single load carrying current $\mathbf{I_L}$. Distributed SVS located at a load bus of $\mathbf{V_L}$.

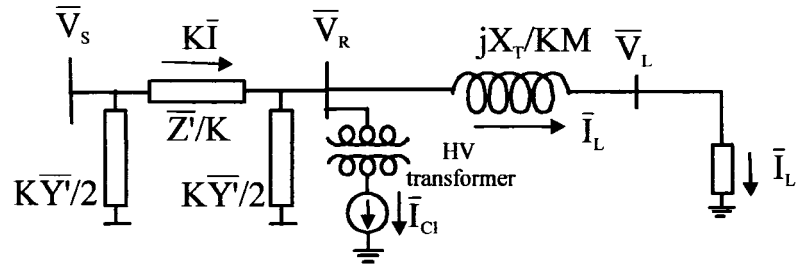

Figure 44 b) Single line diagram with N loads of Fig. 39 equivalenced as a single load carrying current $\mathbf{I_L}$. Lumped SVS connected to bus of $\mathbf{V_R}$ by additional step up transformer.

$$|\bar{V}_R|^2 = \left| \frac{X_T}{MK} \frac{KP}{|\bar{V}_L|} \right|^2 + |\bar{V}_L|^2 \tag{5.1}$$

solving (5.1) and choosing appropriate solution

$$|\bar{V}_L| = \sqrt{\frac{|\bar{V}_R|^2 M^2 + \sqrt{|\bar{V}_R|^4 M^4 - 4M^2 P^2 X_T^2}}{2M^2}} \tag{5.2}$$

Therefore, for constant power load:

$$R = \frac{|\overline{V}_L|^2}{KP} = \frac{|\overline{V}_R|^2 M^2 + \sqrt{|\overline{V}_R|^4 M^4 - 4M^2 P^2 X_T^2}}{2KPM^2} \tag{5.3}$$

Transmission lines are assumed lossless, therefore:

$$\overline{Z}' = jZ_C \sin \beta l \tag{5.4}$$

$$\frac{\overline{Y}'}{2} = j\frac{1}{Z_C} tn\frac{\beta l}{2} \tag{5.5}$$

Where, $\beta = \omega\sqrt{L'C'}$ is wave number and l is line length in km and Z_C is line characteristic impedance . When normalized, (5.4) and (5.5) become (5.6) and (5.7), respectively:

$$\overline{Z}'(p.u.) = j \sin \beta l \tag{5.6}$$

$$\frac{\overline{Y}'}{2}(p.u.) = jtn\frac{\beta l}{2} \tag{5.7}$$

5.5.2 SVS Rating

When lumped SVS provides voltage support, as in Fig.44 b), its objective is to keep transmission voltage $\mathbf{V_R}$ at 1 p.u. Then, the distribution side voltage has to be regulated, additionally, by other means. When voltage support is provided on distribution side of power delivery transformer as in Fig.44 a), distribution side voltage $\mathbf{V_L}$ is regulate at 1 p.u. and transmission side voltage does not have to be additionally regulated.

Applying Kirchhoff's laws on circuits in Fig.44 a) and 44 b) under the above cited conditions, following results are obtained:

5.5.2.1 Lumped Compensation

Reactive current provided by lumped SVS, needed to keep transmission voltage $\mathbf{V_R}$ at 1pu in Fig.44 b), is given by:

$$I_{Cl} = K\left(\frac{1}{\sin\beta l} + \frac{2P^2X_T}{M+\sqrt{M^2-4P^2X_T^2}} - tn\left(\frac{\beta}{2}l\right) - \frac{\sqrt{1-\left(P\sin(\beta l)\right)^2}}{\sin\beta l}\right) \quad (5.8)$$

Reactive power of lumped SVS is given by:

$$Q_l = |\bar{V}_R||\bar{I}_{Cl}| \quad (5.9)$$

Where $|\mathbf{V_R}|$=1pu.

Distribution side voltage $|\mathbf{V_L}|$ is obtained from (5.2) knowing that $|\mathbf{V_R}|$=1pu and is given by:

$$|\bar{V}_L| = \sqrt{\frac{M^2+\sqrt{M^4-4M^2P^2X_T^2}}{2M^2}} \quad (5.10)$$

5.5.2.2 Distributed Distribution Compensation

The magnitude of reactive current provided by distributed SVSs on distribution side of power delivery transformer in Fig.44 a) is given by:

$$I_{Cd} = K\frac{|\bar{V}_L|\left(1-\sin(\beta l)tn\left(\frac{\beta l}{2}\right)\right)}{\sin(\beta l)+\frac{X_T}{M}-\sin(\beta l)tn\left(\frac{\beta l}{2}\right)\frac{X_T}{M}} - K\frac{\sqrt{1-\frac{P^2}{|\bar{V}_L|^2}\left(\sin(\beta l)tn\left(\frac{\beta l}{2}\right)\frac{X_T}{M}-\sin(\beta l)-\frac{X_T}{M}\right)^2}}{\sin(\beta l)+\frac{X_T}{M}-\sin(\beta l)tn\left(\frac{\beta l}{2}\right)\frac{X_T}{M}} \quad (5.11)$$

The reactive power needed for distribution voltage regulation is:

$$Q_d = |\bar{V}_L||\bar{I}_{Cd}| \quad (5.12)$$

The complete derivations of equations (5.8) and (5.11) are given in the Appendix B. The equations (5.8) and (5.11) are general. They apply to all voltage levels, power transferred over the line, and line lengths. Fig. 45 a) to 45 e) show ratings of lumped SVS and distributed SVS plotted against line length in km for different ranges of power transferred over the line. Distribution side voltage $\mathbf{V_L}$ is regulated at 1 p.u. with distribution, distributed SVS. When voltage support is provided on transmission side of power delivery substation, transmission voltage $\mathbf{V_R}$ is kept at 1 p.u. The reactive power needed for load power factor correction has to be accounted for separately. Fig.45 shows how reactive power needed for voltage support varies as function of line length and power transferred over the line.

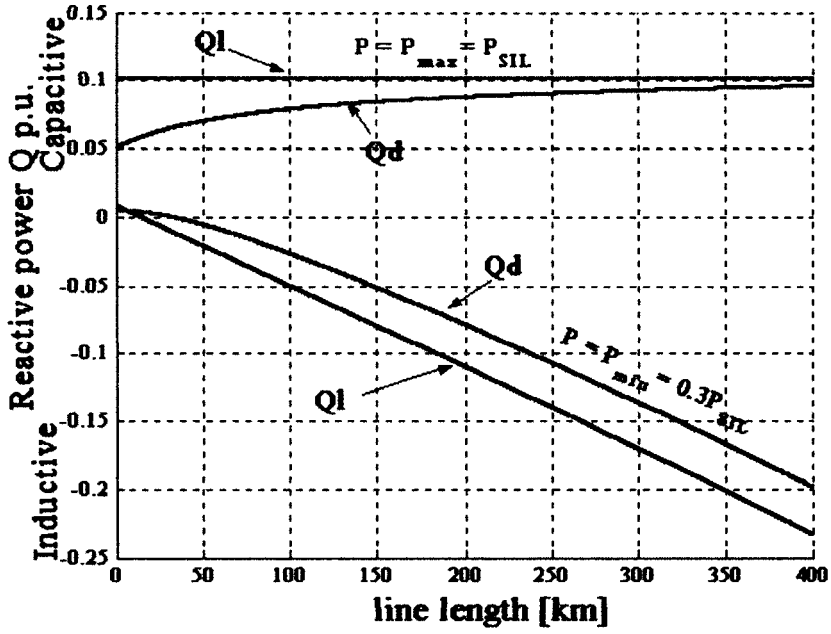

Figure 45 a) Reactive power in p.u. is plotted against line length. The power supplied to load centers vary from 0.3 p.u. to 1p.u., with unity power factor.

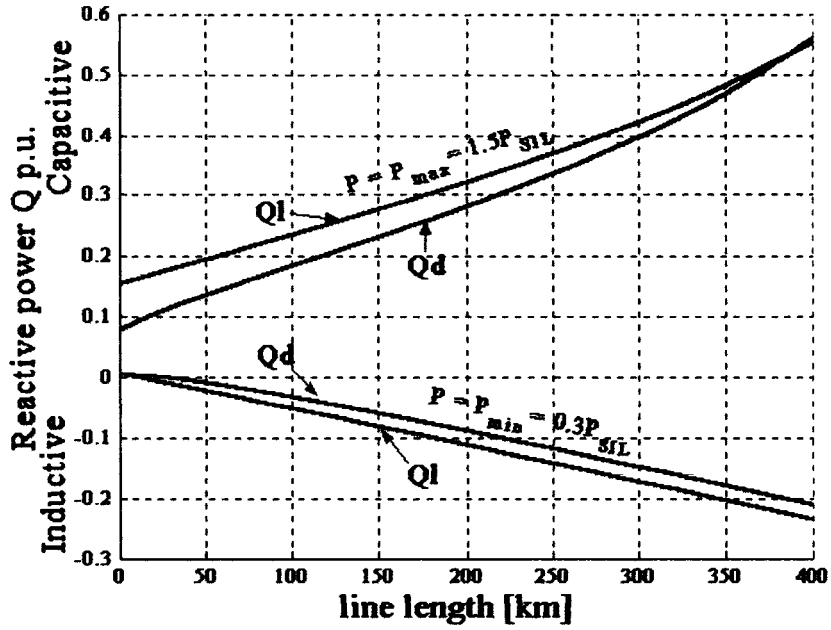

Figure 45.b) Reactive power in p.u. is plotted against line length. The power supplied to load centers vary from 0.3 p.u. to 1.5p.u., with unity power factor.

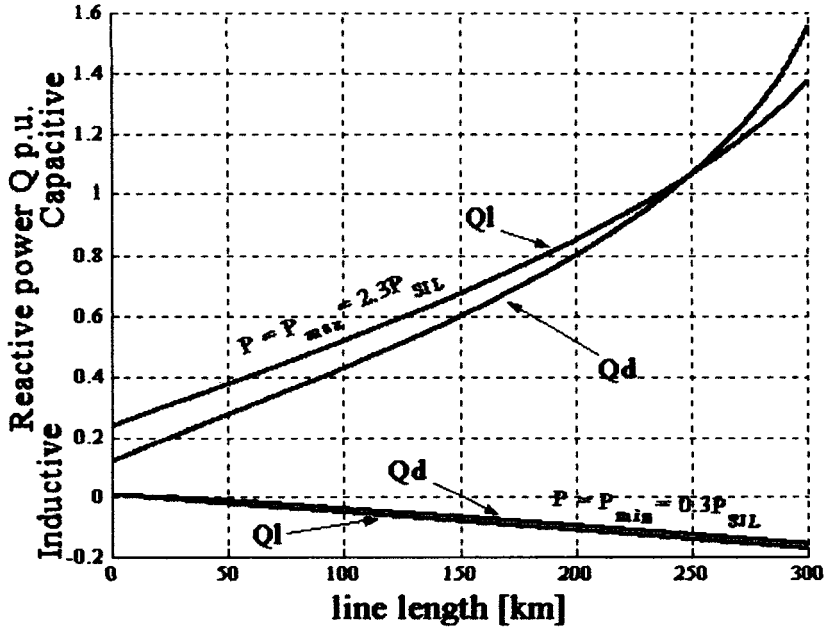

Figure 45.c) Reactive power in p.u. is plotted against line length. The power supplied to load centers vary from 0.3 p.u. to 2.3 p.u., with unity power.

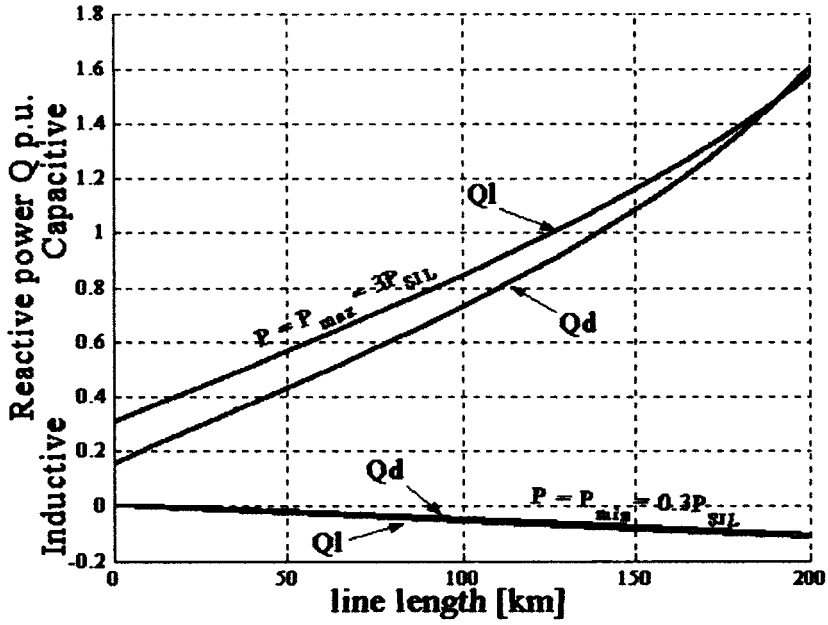

Figure 45.d) Reactive power in p.u. is plotted against line length. The power supplied to load centers vary from 0.3 p.u. to 3 p.u., with unity power factor.

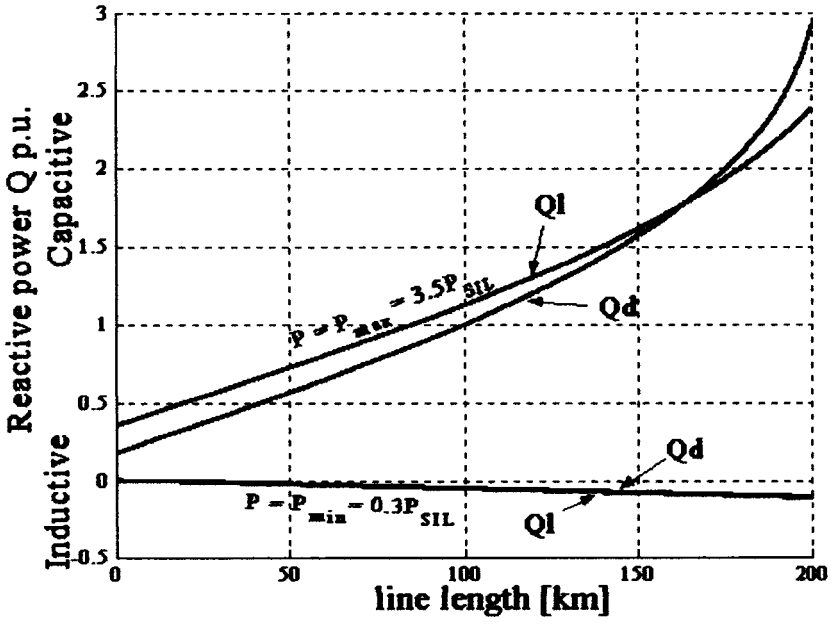

Figure 45.e) Reactive power in p.u. is plotted against line length. The power supplied to load centers varies from 0.3 p.u. to 3.5p.u. with unity power factor.

Table III

Reactive power requirements for voltage support when voltage support is provided on transmission side (TS) and on distribution side (DS)

reactive power requirements	line length [km]	position	maximum power transferred over the line [p.u.] P_{SIL} =1p.u				
			1.5	**2.0**	**2.5**	**3.0**	**3.5**
	100	TS	0.23	0.4	0.6	0.84	1.12
		DS	0.18	0.32	0.5	0.72	0.995
	200	TS	0.32	0.62	1.02	1.57	2.38
		DS	0.28	0.57	0.98	1.6	2.91
	300	TS	0.42	0.92	1.83	-	-
		DS	0.39	0.93	-	-	-
	400	TS	0.55	-	-	-	-
		DS	0.56	-	-	-	-

The results shown in Fig.45 indicate that there is a point beyond which voltage support on distribution side becomes less efficient in terms of vars than voltage support on transmission side. When compensator needed for absorption of reactive power, it is always more efficient to put it on distribution side.

5.6 Cost of Compensation

5.6.1 Cost of Mvars

The cost of compensation depends on compensation equipment used, overrating capability of compensation equipment, power transferred over the line, line length, line parameters, level of competition and overall economical situation. Cost estimates for STATCOM, SVC and Mechanical Switched Capacitors (MSC) are given in [69,70] are 50$/kVar, 40$/kVAr and 8$/kVAr, respectively. Table IV shows the difference in dollar value between two compensation methods for 500 kV line for different compensation

equipment used. Savings are calculated as difference between vars required to keep transmission side of substation voltage V_R at 1 p.u when compensator installed on transmission side of substation and vars required to keep distribution side of substation voltage V_L at 1 p.u. with compensator on distribution side of substation multiplied by dollar value of MVAr. These cost estimates are based on 1996 data. Here, they are given as a guidance only. Only the manufacturers of the equipment can give exact cost.

For costs reasons STATCOM and SVC are normally used only in situation where switched capacitors and reactors would not result in satisfactory system performance which is to be determined by detailed dynamic simulation on case basis.

Table IV

Difference in cost of voltage support for 500 kV line

500kV line	line length [km]	compensator used	Maximum power transferred over the line [p.u.] .] P_{SIL} =1p.u				
			1.5	**2.0**	**2.5**	**3.0**	**3.5**
savings[$ million] (Q_{lumped}- $Q_{distribution}$)*$/MVAR	**100**	STATCOM	2.6	3.9	5	5.75	6.2
		SVC	2.08	3.12	4	4.6	5
		MSC	0.42	0.62	0.8	0.92	1
	200	STATCOM	2	2.65	2	-1.5	-26.5
		SVC	1.6	2.12	1.6	-1.2	-21.1
		MSC	0.32	0.42	0.32	-0.24	-4.2
	300	STATCOM	1.3	-0.5			
		SVC	1.04	-0.4			
		MSC	0.21	-0.08			
	400	STATCOM	-0.35				
		SVC	-0.28				
		MSC	-0.056				

5.6.2 Cost of Transformer

When voltage support is provided on transmission side of substation with one lumped SVS, step up transformer has to be used to couple it with substation. Cost of transformer can be up to 20% of total cost of SVC. When voltage support is provided on distribution side of substation with few smaller units, there is no need for additional transformer, although, if STATCOMs are used, there is still need for coupling reactor between converter and grid.

5.6.3 Cost of Redundancy

In order to comply with N-1 reliability criterion, the rating of each SVS on distribution side has to be N/(N-1) Qd where N is number of SVS on distribution side and Qd is MVAr of all N SVSs lumped together. When voltage support is provided with one lumped SVS on transmission side of substation, loss of this unit would lead to loss of entire system. For reliability, a spare unit of the full rating should be added with its own step up transformer, doubling the cost of SVS. Even if lumped SVS is divided in few blocks of same ratings to decrease MVAr standby requirement of lumped SVS, it does not eliminate needs for additional step up transformer.

5.6.4 Line Losses

Line losses are proportional to square of the current flowing through the line.

5.6.4.1 Line Losses with Voltage support on Distribution Side of Substation

Applying Kirchhoff's current law on Fig.44 a), line current can be expressed as:

$$\bar{I} = \bar{I}_L + \bar{I}_{Cd} \tag{5.13}$$

Compensation current $\mathbf{I_{Cd}}$ is in quadrature with load current $\mathbf{I_L}$,. Therefore, using load current as reference phasor, (5.13) can be rewritten as:

$$\bar{I} = I_L + jI_{Cd} \tag{5.14}$$

Reactive current $\mathbf{I_{Cd}}$ needed for distribution voltage regulation has been calculated in (5.11), and load current I_L can be calculated as:

$$I_L = \frac{P}{|V_L|} \tag{5.15}$$

where $\mathbf{V_L}$ is distribution side voltage regulated at 1 p.u. Finally, square of line current $|\mathbf{I}|^2 = |I_{Cd}|^2 + |I_L|^2$ can be computed from (5.13),(5.14),(5.15) and (5.11).

5.6.4.2 Line Losses with Voltage support on Transmission Side of Substation

When voltage support is provided on transmission side of substation, the line current **I** can be calculated from Fig.44 b). Applying Kirchhoff's current law, it can be written:

$$\bar{I} = \bar{I}_L + \bar{I}_{Cl} \tag{5.16}$$

Compensating current I_{Cl} is given by (5.8). Load current I_L can be calculated as in (5.15), but now distribution side voltage $\mathbf{V_L}$ is not regulated at 1 p.u., but it is given by (5.10). Using transmission side voltage $\mathbf{V_R}$ as reference, load current phasor $\mathbf{I_L}$ can be represented as sum of two components, one in phase with transmission side voltage $\mathbf{V_R}$ and the second one in qudrature with it. Load current component in quadrature with

transmission side voltage is $|\mathbf{I_L}|\sin\delta$ while load current component in phase with transmission side voltage is $|\mathbf{I_L}|\cos\delta$, where δ is power angle between transmission side voltage $\mathbf{V_R}$ and distribution side voltage $\mathbf{V_L}$. Power angle δ can be calculated from:

$$P = \frac{|\bar{V}_T||\bar{V}_D|}{X_T/M}\sin\delta \tag{5.17}$$

Here V_R is regulated at 1 p.u.

Compensating current $\mathbf{I_{CI}}$ is in quadrature with transmission voltage $\mathbf{V_R}$. Finally, line current $\mathbf{I}$ can be expressed as:

$$\bar{I} = |I_L|\cos\delta + j\left(I_{CI} + |I_L|\sin\delta\right) \tag{5.18}$$

and square of line current is given by:

$$|\bar{I}|^2 = \left(|I_L|\cos\delta\right)^2 + \left(I_{CI} + |I_L|\sin\delta\right)^2 \tag{5.19}$$

Ratio of the line current squared when voltage support provided on distribution side of power delivery substation, to the line current squared when compensation provided on transmission side of substation plotted against power transferred over the line for 100, 200, 300 and 400 km transmission line is given on Fig.46. From Fig.46 it can be seen that line losses are mostly lower when voltage support is on distribution side.

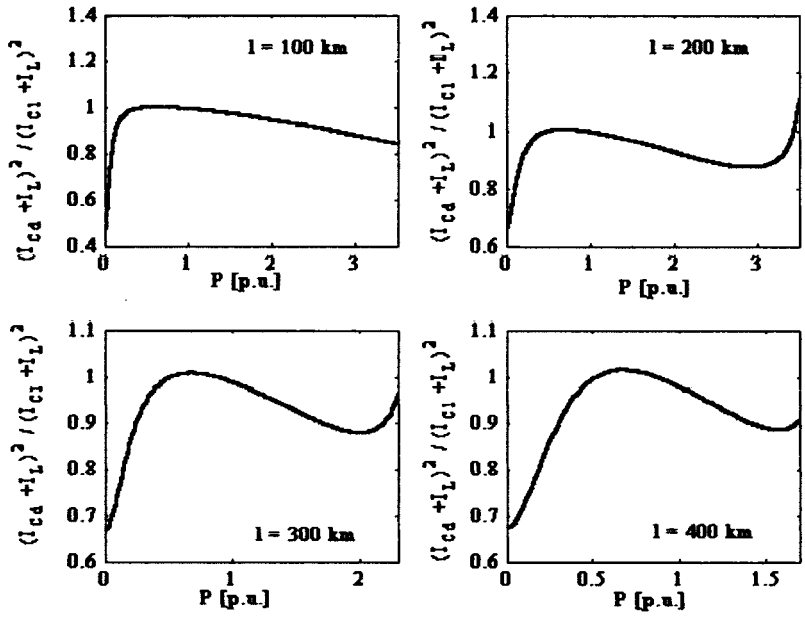

Figure 46 Ratio of the line losses when voltage support provided on distribution side of power delivery substation to losses when voltage support provided on transmission side of power delivery substation plotted against power transferred over the line for different line lengths.

5.7 Steady-State Loadability Limit

5.7.1 Uncompensated Line

Steady state loadability limit of the transmission line is determined by wave equation:

$$\overline{V}_S = \overline{V}_R \cos(\beta l) + jZ_C \sin(\beta l)\frac{P - jQ}{\overline{V}_R} \tag{5.20}$$

Where V_S is sending end voltage fixed at 1p.u. This quadratic equation can be solved for V_R. A result is shown in Fig.47 for unity power factor (Q=0). The transformer reactance is not accounted for. Therefore, the loadability limits are even lower. Loadability limits are

3.92, 2.03, 1.44 and 1.17 p.u for 100, 200, 300 and 400 km line lengths, respectively. Surge impedance load P_{SIL} = 1p.u.

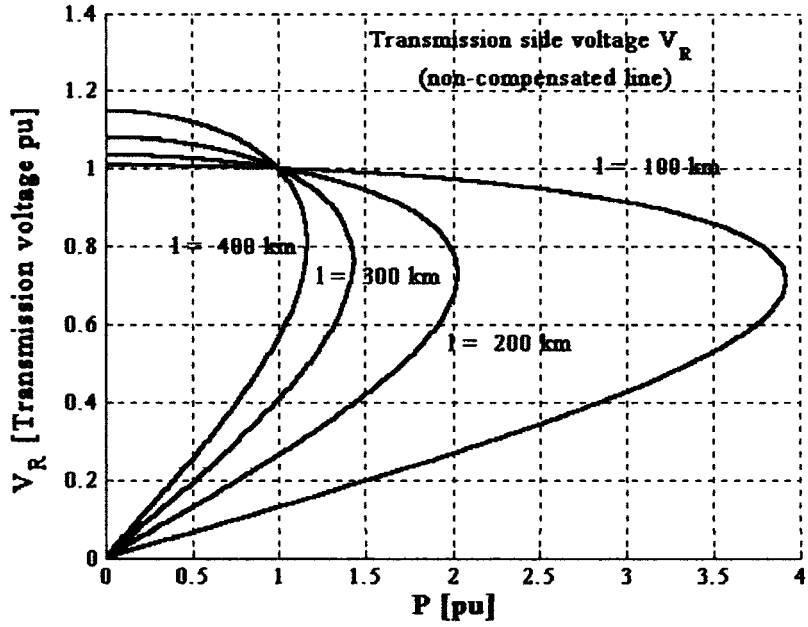

Figure 47 P-V curves for non compensated line. Surge impedance load P_{SIL} =1p.u. The effect of the transformer reactance X_T is not considered.

5.7.2 Compensated Line

5.7.2.1 Distributed SVS on Distribution Side of Substation

When distributed SVSs are sat on distribution side of power delivery substation, as in Fig. 38 (Fig.44.a)), Qd required for distribution side voltage regulation V_L is given by equations (5.11) and (5.12). Fig. 48 shows reactive power Qd needed to regulate distribution side voltage $|V_L|$ at 1.p.u. plotted versus active power P transferred over the line. The coefficient $\Delta Q/ \Delta P$ (reactive power injected into the system needed to maintain distribution voltage V_L at 1p.u. for increase in power transferred over the line) is the

measure of the system degradation. For theoretical loadability limit in steady state, $\Delta Q/\Delta P$ tends to infinity. It marks the point beyond which voltage regulation by shunt compensation becomes impossible (turning point on P-V curve). For practical application it is suggested that $\Delta Q/\Delta P$ should not exceed 0.9. From Fig. 48 it can be seen that steady state loadability limit is significantly increased compared to non-compensated line.

Before proceeding further, some explanations regarding Fig. 48 are required. The transformer reactance changes with transformer rating. In our calculation we assumed transformer impedance 10% on the transformer base. The maximum power delivered across the transformer is its rating. Loadability of lines changes with line lengths. For 400 km line, transformer rating is assumed to be $P_{MAX}=S_{MAX}$ = 1.5 p.u., for 300 km line P_{MAX} = S_{MAX} = 2.5p.u., and for 200 km and 100 km line P_{MAX} = S_{MAX} = 3.5 p.u., where P_{SIL} = 1p.u.. 3.5 P_{SIL} is considered to be the thermal limit of the line (X_T= 0.1/M(p.u.) where M = S_{MAX}/ P_{SIL}).

5.7.2.2 Lumped SVSs on Transmission Side of Substation

When lumped SVS is situated on transmission side of power delivery substation as in Fig.39 (Fig.44 b)), Ql required for transmission voltage regulation with lumped SVS (given by equations (5.8) and (5.9)) is plotted against active power transferred over the line for different line lengths as shown in Fig.5.49. It can be seen that loadability of the lines is further increased comparing to case when voltage regulation is provided on distribution level, but not considerably. Moreover, the loading of 200 km line and shorter, is already extended to thermal limits with distribution, distributed SVS.

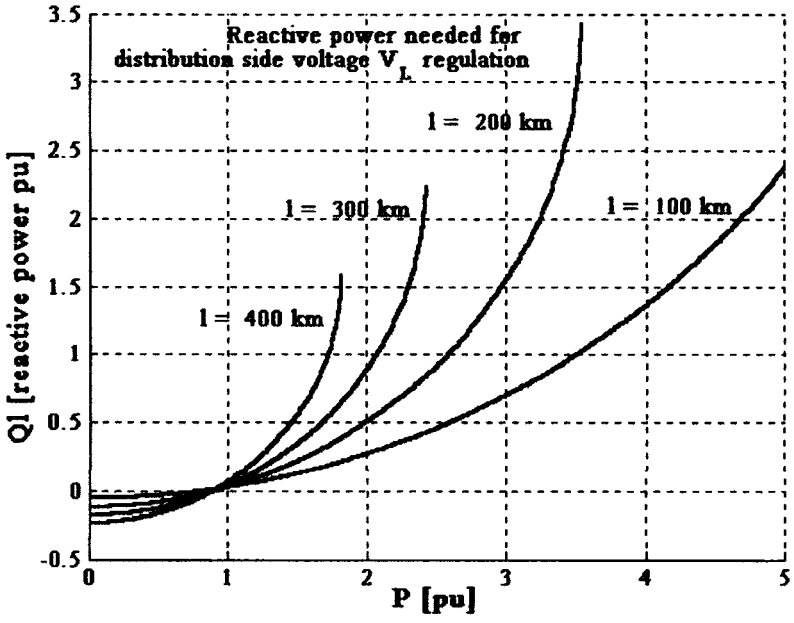

Figure 48 Qd - P curves for line compensated with distributed SVS on distribution side of power delivery substation. Surge impedance load P_{SIL} =1p.u. The effect of the transformer reactance is included.

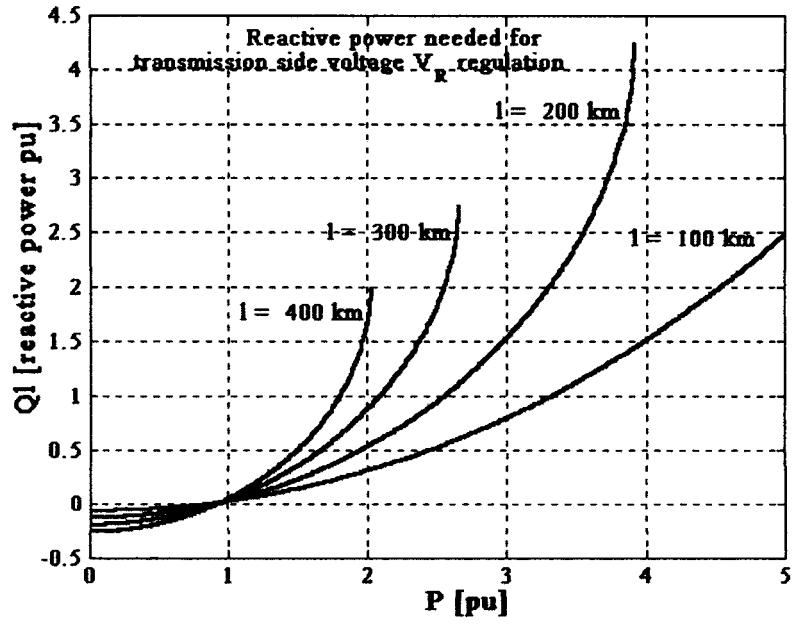

Figure 49 Ql - P curves for line compensated with lumped SVS on transmission side of power delivery substation. Surge impedance load P_{SIL} =1p.u. The effect of the transformer reactance is included.

5.8. Hypersim Digital Simulation

To demonstrate feasibility and reliability, a detailed numerical, real time simulation has been performed. Hypersim was used for this study. HYPERSIM is based on EMTP software mostly. The main advantage of HYPERSIM is availability of high precision models of lines, loads and SVCs based on experience of many years of R&D at IREQ. Importance of real time dynamic simulation is in fact that long term dynamic stability study can be performed to insure that there are no long term instabilities following contingency situations.

5.8.1 Studied System

The studied system consists of 315/25 kV, 200 km double circuit, radial transmission line delivering power to three load centers (as in Fig.38 with K=2 and N=3) shown in Fig.50. Line is transposed and each 50 km of the line is modeled with its Π nominal circuit. Load is fed over three power transformers, each rated at 400 MVA. Loads of the test system are modeled in detail. Each load is an aggregate of induction motor, static load available as default model in Hypersim, and resistive load. The active and reactive powers consumed by static load are functions of the voltage level and frequency according to (5.21) and (5.22).

$$P = P_0\left(\frac{V}{V_0}\right)^{np}\left[1 + kp\frac{f - f_0}{f_0}\right] \tag{5.21}$$

$$Q = Q_0\left(\frac{V}{V_0}\right)^{nq}\left[1 + kq\frac{f - f_0}{f_0}\right] \tag{5.22}$$

Load power factor is mostly corrected with switched and fixed capacitors connected on distribution buses. The principal parameters of test system are listed in the Appendix C. Motor parameters are taken from [1]. Detailed model description is given in [72].

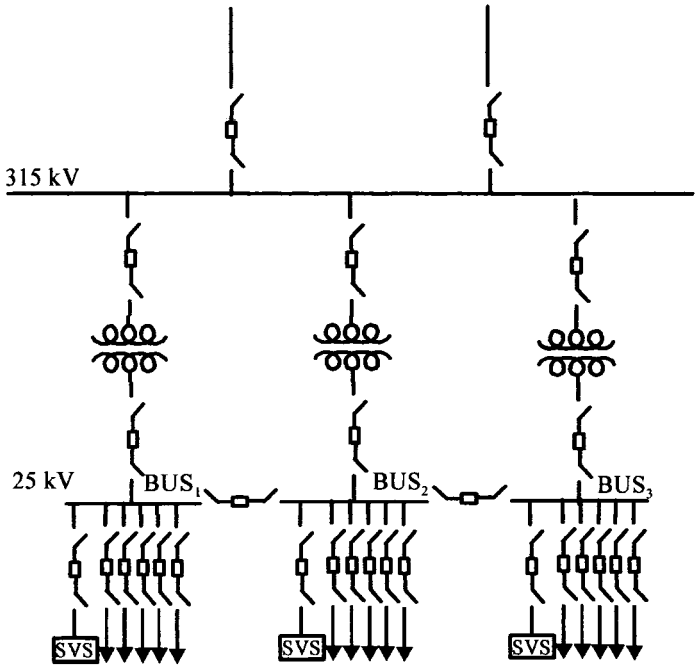

Figure 50 Test System

5.8.2 Lumped vs. Distributed Distribution SVS

First, voltage support is provided with lumped SVC consisting of three Thyristor-Switched Capacitors (TSC) circuits Y- connected and Thyristor-Controlled Reactor (TCR) delta connected. Default model of SVC with complete control and measurement system is available in Hypersim. Its detailed description is given in [72]. SVC is connected on transmission side of substation on 315 kV bus via step up transformer. Each TSC can supply 75 MVAr for total of 225 MVAr. Each branch is tuned with series reactor

to 5^{th} harmonic. Additional filtering is provided with fixed capacitor tuned to 5^{th} and 7^{th} harmonic. High pass filter is also added. Total power transferred over the line is 750 MW.

5.8.2.1 Loss of SVS

Fig. 51 shows the simulated waveforms of the power transferred over the lines, transmission side voltage of substation seen by SVC measurement circuit, phase ab current of one TCR and phase a currents of each TSC branch. The SVC is suddenly lost at 0.1 ms. The loss of SVC is apparent in disappearance of its currents. It can be seen that voltage drops instantaneously for about 20% and then continues to decay, leading to complete voltage collapse. It is clear that additional unit is needed as stand by with its own step up transformer to assure reliability. The same happens if SVC's transformer is lost to fault.

The same test, under the same conditions of operation is performed when voltage support is provided with three distributed, distribution SVC. Each load bus has its own SVC providing voltage support. Each SVC consists of one TCR delta connected and three branches of TSC Y-connected. Each SVC can provide total of 75 MVAr. Fig.52. a), b), and c) shows simulated waveforms for the loss of SVC_3. From Fig.52 it can be seen that voltage on load buses do not drop more then 5% and recover after 100 ms. The SVC_1 and SVC_2 respond to loss of SVC_3 with switching on their third TSC branch to compensate for the lost SVC_3. This shows the superiority of distributed, distribution voltage support scheme.

5.8.2.2 Loss of the line

The most onerous system contingency is loss of one transmission circuit. Outage of one line increases reactive and resistive voltage drop increasing reactive needs of system as it can be seen from Table III. If system is not designed with enough reactive reserve, line

tripping can lead towards complete voltage collapse. Fig. 53 shows response of lumped SVC on transmission side of substation after the line tripping at 0.1 sec. Immediately after the fault, SVC undervoltage protection disconnect SVC and system voltage collapses instantaneously.

Fig. 54 shows response on same fault when voltage support is provided with three distribution side SVC, each having 75 MVAr capacity. Fig. 54 shows voltage seen by SVC measurement circuit, TCR phase current and a phase currents of each TSC branch. Each SVC responds immediately after the fault turning off TCR and switching in all TSC branches. Total power transferred over the line before line tripping is 730 MW or 2.1 p.u. After the line outage, this power is redirected over the remaining line. System is designed to support 1.5 p.u power transfer over each line for a total of 1000 MW. Due to lack of reactive power, voltage decays and stabilizes at about 0.65 p.u.. Reactive power provided by SVC decreased as a square of the voltage, clearly indicating disadvantage of impendence type compensators. They provide the least when they are most needed, showing that nameplate rating of SVCs has to be increased. After 1 sec. line is re-closed and voltage recovers but never at 1 p.u. It is worth noting that even after the line re-closing and voltage recovery the post fault conditions are not equal to pre-fault conditions as it can be seen from lowest trace of Fig. 54 a) to c). Each TSC branch of every SVC stays on and TCRs are off. This is due to increase reactive power demand from accelerating induction motors.

5.8.3 STATCOM vs SVC

The same system is simulated with the difference that all three SVCs are replaced by three lower rating STATCOMs. Each STATCOM consists of voltage controlled Voltage Source Converter and its control circuit. The control circuit is described in detail in [63] and is not available as default model in Hypersim.

Each STATCOM rating is 60 MVAr with 50% short-term overload capability. The system is subjected to line loss due to three phase short circuit fault at 0.1 sec. Each STATCOM responds immediately increasing its output current. At 1 sec.(900 msec. after the fault) the line is re-closed. Fig.55 shows the simulated waveforms of the currents of the a-phase of each distributed STATCOM and power transferred over the line. The simulated instantaneous voltage at each ac bus has been converted to rms value and displayed at Fig.56. The post-fault conditions are equal to pre-fault conditions indicating that there is no motor stalling. It can be clearly seen that lower rated STATCOMs with overload capability can perform better than SVCs.

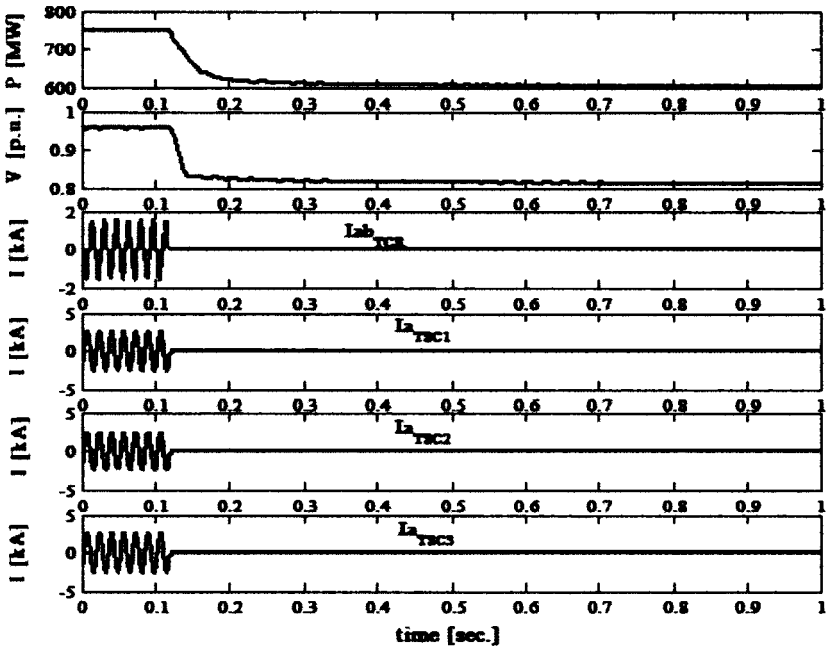

Figure 51 Transient response of studied system for loss of lumped SVC. Fig. shows power transferred over the line, transmission side substation voltage, TCR phase current and phase a currents of each SVC's branch.

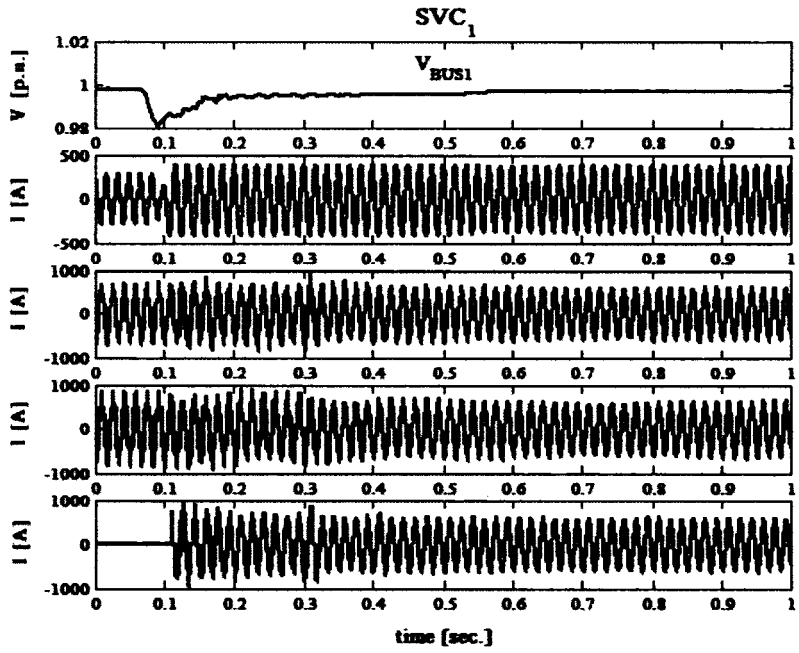

(a) SVC_1 dynamic response for the loss of SVC_3.

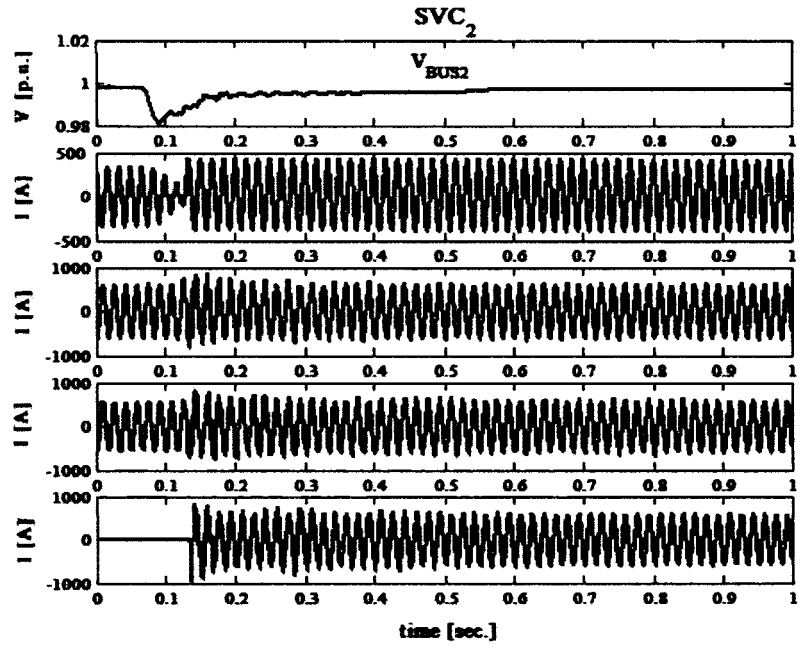

(b) SVC_2 dynamic response for the loss of SVC_3.

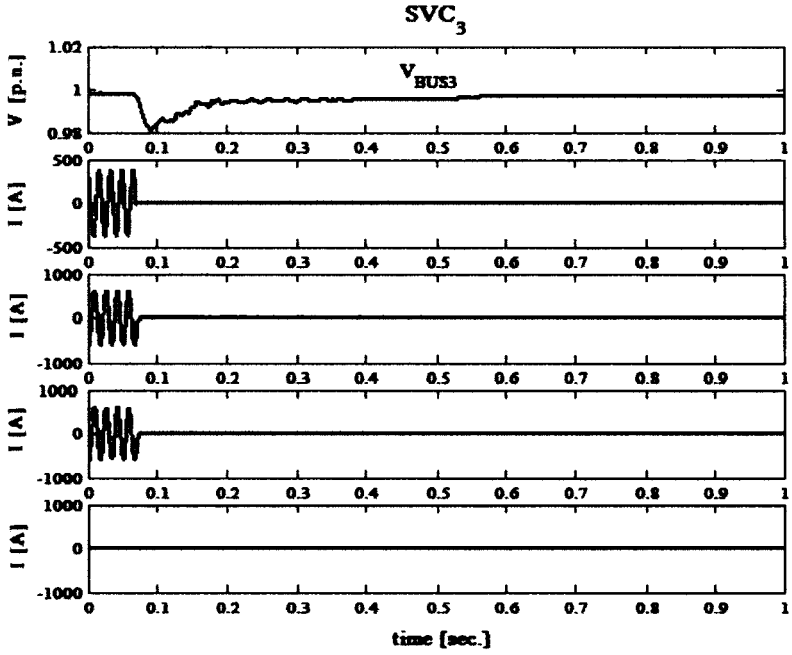

(c) SVC_3 dynamic response for the loss of SVC_3.

Figure 52 Transient response of studied system for the loss of SVC

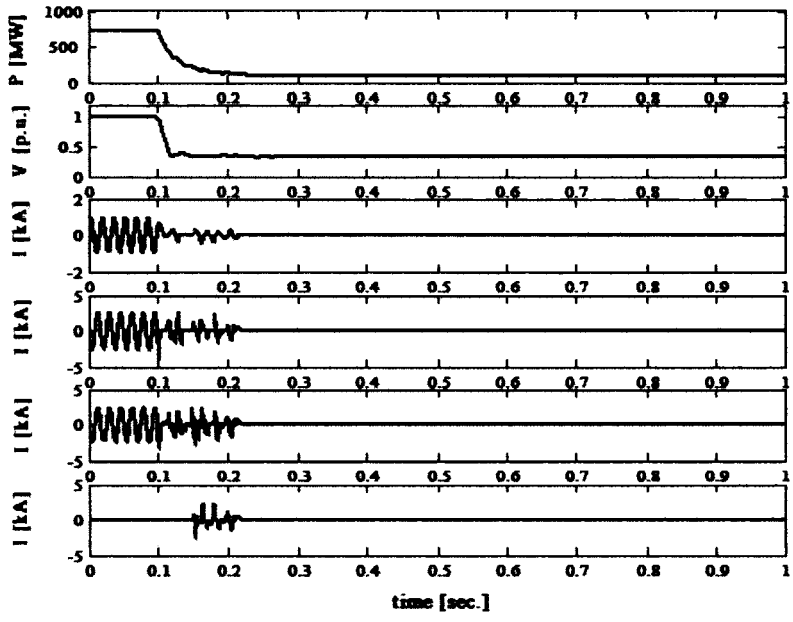

Figure 53 System transient response for one line tripping at 0.1 sec when voltage support provided with one lumped SVC on transmission side of substation.

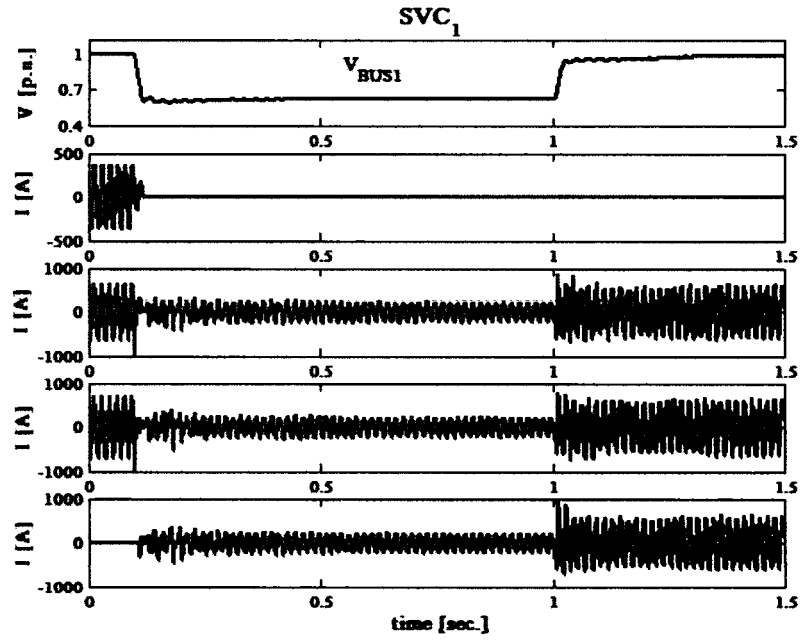

Figure 54 a) The SVC_1 dynamic response. (Bus voltage, TCR phase current and phase current of each branch of TSC).

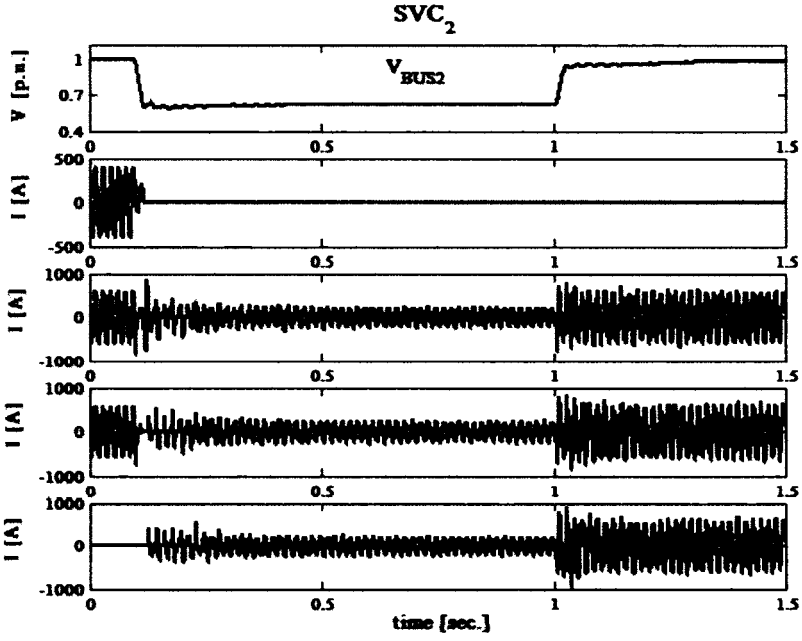

Figure 54 b) The SVC_2 dynamic response. (Bus voltage, TCR phase current and phase current of each branch of TSC).

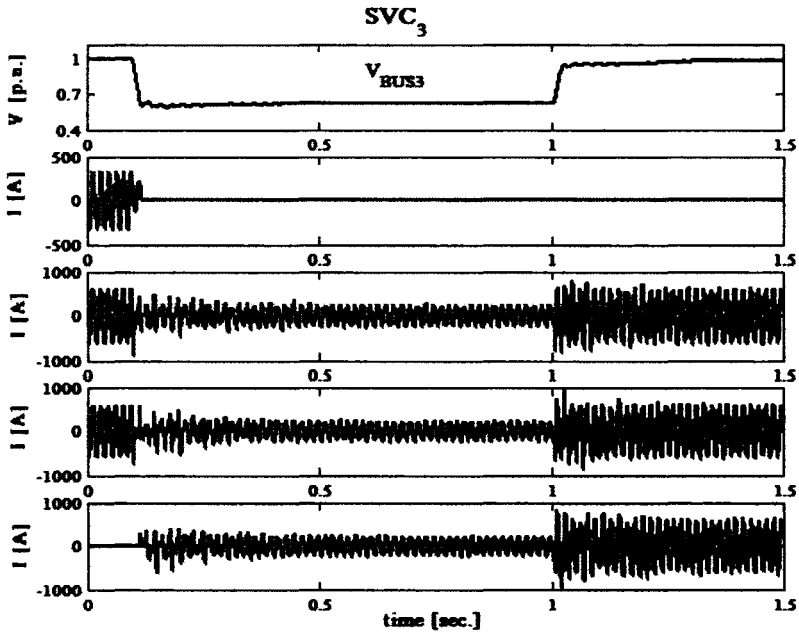

Figure 54 c) The SVC_3 dynamic response. (Bus voltage, TCR phase current and phase current of each branch of TSC). Line is lost at 0.1 sec. and re-closed at 1 sec. when voltage support provided with three distribution SVCs.

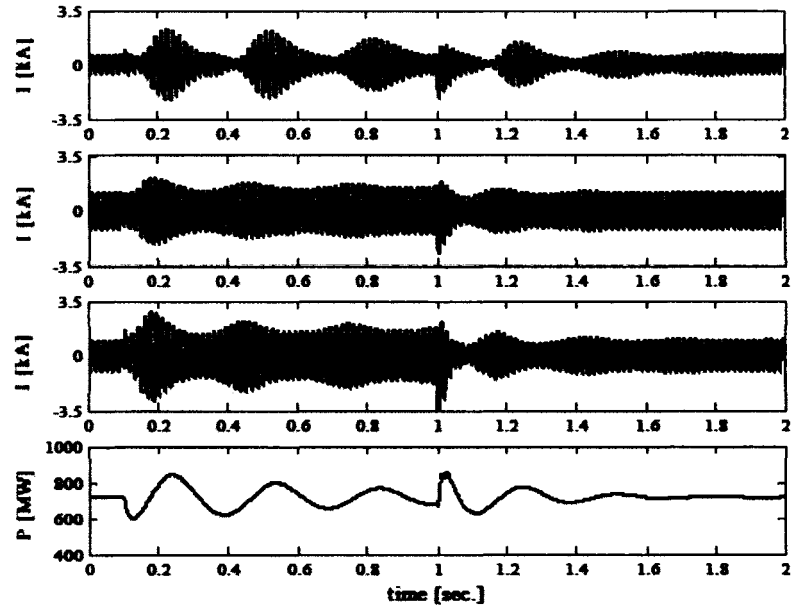

Figure 55 A system transient response when one transmission line lost at 0.1 sec. due to three phase fault. The fault is cleared and line is re-closed 900 msec. after the fault.

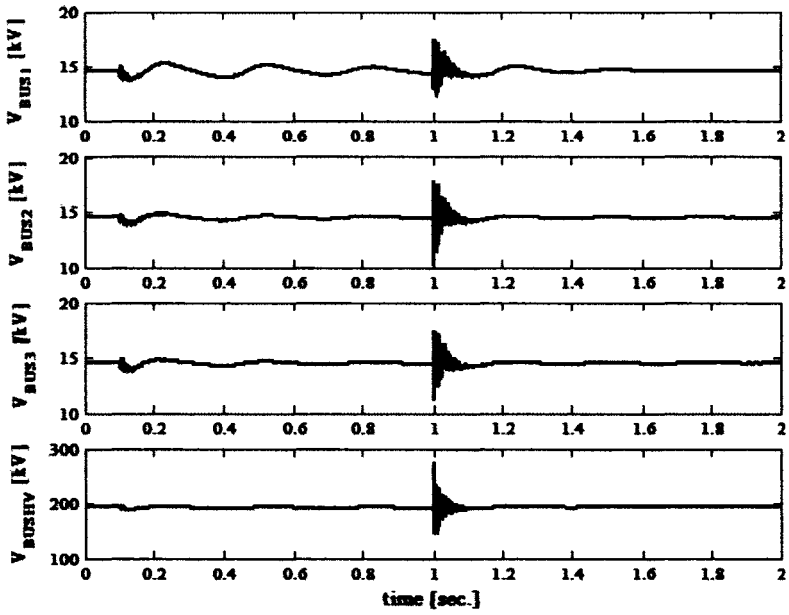

Figure 56 System transient response when one line lost at 0.1 sec. Voltage support is provided with three distribution STATCOMs. (Phase voltages (rms) of 25 kV buses and phase voltage of 315 kV bus). The faulted line is successfully re-closed at 1 sec.

5.9 Conclusions

In this chapter two voltage support schemes i) distributed, distribution compensation with large number of similarly sized SVSs providing voltage support at load centers on distribution level, versus ii) lumped compensation on transmission level with one large SVS installation, are compared. Results based on steady state analysis and detailed dynamic simulation of one equivalent test system showed a series of benefits emerging from distributed, distribution voltage support scheme. The benefits include: 1) lower VAr requirement to support load voltages, 2) better voltage regulation at load centers because each SVS regulate voltage where it is connected, 3) possibility of elimination of LTC transformers for voltage control of loads which, as consequence, decreases overall maintenance concerns, 4) not needing step up transformer to raise SVS output voltage if

SVS is installed on distribution level, 5) enhanced reliability, 6) lower standby requirement in order to satisfy N-1 reliability criterion and 7) lower line losses.
However, for each line, depending on line length and loading, there is point beyond which distribution side compensation becomes inefficient in terms of VARs needed for voltage support and line losses. Although distribution side compensation increases transmission capacity of the line, if further increase is needed, it can be obtained by transferring voltage support on transmission level. Loadability of 200 km and shorter lines can be extended to thermal limits with distribution side voltage support.

Detailed dynamic simulation of one test system has demonstrated feasibility and advantages of proposed voltage support method. Moreover, it has been shown that lower nameplate rating STATCOMs with short time overload capability can perform better then impedance based compensator devices.

CHAPTER 6

REACTIVE POWER REQUIREMNTS EVALUATION-PHASOR APPROACH

6.1 Introduction

In this chapter, a step further is undertaken toward generalization of the proposed concept. Two load centers, spaced along the transmission line are considered and two proposed voltage support approaches are compared. In order to generalize the proposed concept, general equations for reactive power requirement for voltage regulation are deduced. The advantage of deduced equations over traditional power flow equations is in lower number of iterations because, for some cases, reactive requirement of compensator can be deduced explicitly, not implicitly, as in classical power flow calculation. Moreover, the proximity to voltage collapse can be monitored from deduced equations.

6.2 Reactive Power Requirement Calculation

In this section the equations that enable calculation of compensator rating and reactive power needs of power systems are deduced. Transformer reactances are also considered. Objective is to deduce general equations applicable to general distribution of compensator and meshed network.

6.2.1 One Load Center, Voltage Support Provided on Transmission Side of Substation

Fig. 57.a) illustrates the case of one line feeding one load center over the transformer having leakage reactance jX_T. Fig.57.b) represents corresponding vector diagram showing steady state solution for the circuit in Fig.57.a).

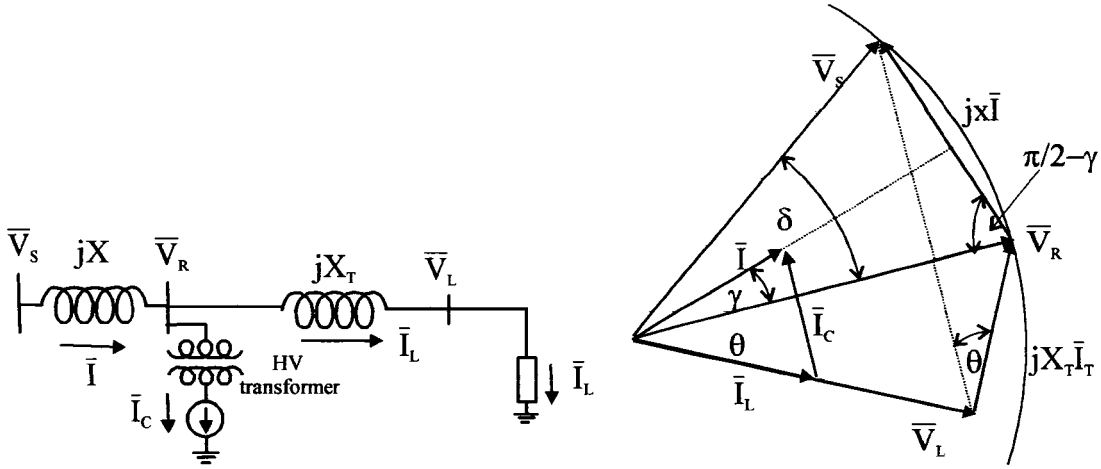

Figure 57 a) Transmission line feeding one load center. Voltage support is provided on transmission level, b) corresponding phasor diagram showing steady state solution

The active power through the node having voltage $\mathbf{V_R}$ is scalar product of voltage $\mathbf{V_R}$ and line current **I** or the load current $\mathbf{I_L}$:

$$P = \vec{I} \bullet \vec{V}_R = \vec{I}_L \bullet \vec{V}_R \tag{6.1}$$

Projection of vector **I** on V_R axe is equal to sum of projection of vector $\mathbf{I_L}$ and $\mathbf{I_C}$ on the same axe. Physically, it means that active power transferred from $\mathbf{V_S}$ to $\mathbf{V_R}$ is equal to active power transferred from $\mathbf{V_R}$ to $\mathbf{V_L}$.

$$|I|\cos\gamma = |I_L|\cos\theta \tag{6.2}$$

Equation (6.2) represents active power balance.

The reactive power required for regulation of voltage $\mathbf{V_R}$ is given by the vector product:

$$Q = |\vec{V}_R||\vec{I}_C| = |\vec{I} \times \vec{V}_R| + |\vec{I}_L \times \vec{V}_R| \tag{6.3}$$

$$|I|\sin\gamma + |I_L|\sin\theta = |I_C| \tag{6.4}$$

Equation (6.4) represents reactive power balance for circuit in Fig.57.a).

Projection of vector **I** on axe in quadrature with voltage $\mathbf{V_R}$ plus projection of vector $\mathbf{I_L}$ on the same axe is equal to compensating current I_C.

From phasor in Fig. 57.b), it can be written:

$$\cos\left(\frac{\pi}{2}-\gamma\right) = \sin\gamma = \frac{|V_R| - |V_S|\cos\delta}{|XI|} \tag{6.5}$$

$$|I \times V_R| = |I||V_R|\sin\gamma = |I||V_R|\frac{|V_R| - |V_S|\cos\delta}{|XI|} \tag{6.6}$$

$$|I \times V_R| = |V_R|\frac{|V_R| - |V_S|\cos\delta}{X} \tag{6.7}$$

$$\sin\theta = \frac{|V_R| - |V_L|\cos\theta}{|X_T I_L|} \tag{6.8}$$

$$|I_L \times V_R| = |V_R|\frac{|V_R| - |V_L|\cos\theta}{X_T} \tag{6.9}$$

combining (6.3),(6.7) and (6.9)gives reactive requirement for regulation of $\mathbf{V_R}$.

$$I_C = \frac{|V_R| - |V_S|\cos\delta}{X} + \frac{|V_R| - |V_L|\cos\theta}{X_T} \tag{6.10}$$

The equation (6.10)) can be obtained applying law of conservation of reactive power through the node having the voltage $\mathbf{V_R}$. It can be stated that total reactive power sent from the node having the voltage $\mathbf{V_R}$ is zero.

The reactive power sent from receiving end voltage $\mathbf{V_R}$ to sending end voltage V_S is :

$$Q_{RS} = \frac{|V_R|^2 - |V_S||V_R|\cos\delta}{X} \tag{6.11}$$

The reactive power send from receiving end voltage $\mathbf{V_R}$ to load is:

$$Q_{RL} = \frac{|V_R|^2 - |V_L||V_R|\cos\theta}{X_T} \tag{6.12}$$

and finally, the reactive power send from node with voltage V_R to compensator is:

$$Q_C = -|V_R|I_C \tag{6.13}$$

Summing (6.11),(6.12) and (6.13) yields (6.10).
Voltage V_L can be calculated using Pithagora's theorem as:

$$|V_R|^2 = |X_T I_L|^2 + |V_L|^2 \tag{6.14}$$

and knowing that $P = |V_L||I_L|$

$$|\overline{V}_L| = \sqrt{\frac{|\overline{V}_R|^2 + \sqrt{|\overline{V}_R|^4 - 4(X_T P)^2}}{2}} \tag{6.15}$$

and

$$P = \frac{|V_S||V_R|}{X}\sin\delta \quad \Rightarrow \sin\delta = \frac{PX}{|V_S||V_R|} \Rightarrow \cos\delta = \sqrt{1-\sin^2\delta} \tag{6.16}$$

$$\Rightarrow \sin\delta = \frac{PX}{|V_S||V_R|} \Rightarrow \cos\delta = \frac{\sqrt{|V_S|^2|V_R|^2 - P^2X^2}}{|V_S||V_R|} \tag{6.17}$$

Similarly, angle θ can be calculated.

6.2.2 N Load Centers, Voltage Support Provided on Transmission Side of Substation:

If we have N loads in parallel then reactive power needed for support of voltage V_R is:

$$Q = |\vec{V}_R||\vec{I}_C| = |\vec{I} \times \vec{V}_R| + |\vec{I}_{L1} \times \vec{V}_R| + |\vec{I}_{L2} \times \vec{V}_R| + \ldots + |\vec{I}_{LN} \times \vec{V}_R| \tag{6.18}$$

$$I_C = \frac{|V_R| - |V_S|\cos\delta}{X} + \frac{|V_R| - |V_{L1}|\cos\theta_1}{X_{T1}} + \ldots + \frac{|V_R| - |V_{LN}|\cos\theta_N}{X_{TN}} \tag{6.19}$$

In case voltage $\mathbf{V_R}$ is kept at 1 p.u, and voltage $\mathbf{V_S}$ is kept at 1 p.u., voltages V_{Li} can be expressed as function of $\mathbf{V_R}$ using Pythagoras's theorem as in (6.15), angles θi can be expressed in terms of active powers as in (6.17) and compensating current I_C can be deduced explicitly.

6.2.3 Two Load Centers in Parallel with Independent Voltage Support on Distribution Side

Fig. 58.a) illustrates the case of two load centers having independent voltage support on distribution level and Fig. 58.b) illustrates the phasor for the same circuit. To calculate reactive requirements for distribution voltage regulation, first transmission voltage $\mathbf{V_R}$ has to be calculate. The receiving end voltage $\mathbf{V_R}$ can not be expressed explicitly.

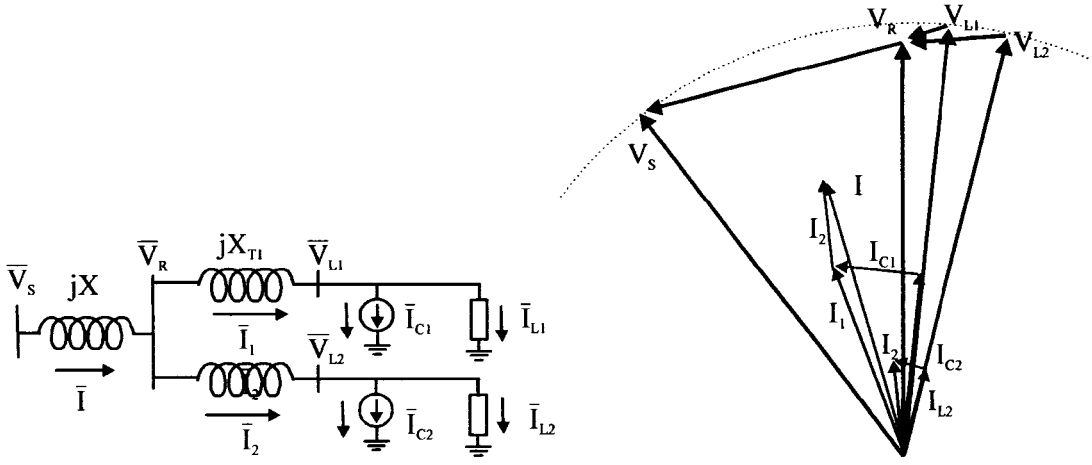

Figure 58 a)Two load centers having voltage support on distribution level, b) corresponding phasor diagram.

The line current **I** can be decomposed into two components; one in quadrature with voltage $\mathbf{V_R}$ and the other in phase with voltage $\mathbf{V_R}$.

$$|I|\sin\gamma = |I_1|\sin\gamma_1 + |I_2|\sin\gamma_2 \tag{6.20}$$

Equation (6.20) represents balance of reactive powers.

$$|I|\cos\gamma = |I_1|\cos\gamma_1 + |I_2|\cos\gamma_2 \tag{6.21}$$

Equation (6.21) represents balance of active powers. The γ, γ_1 and γ_2 are the angles the currents I, I_1 and I_2 formed with voltage V_R, respectively. For the sake of the clarity the phasor of Fig.58 b) is decomposed into two parts as shown in Fig.59.a) and 59 b).

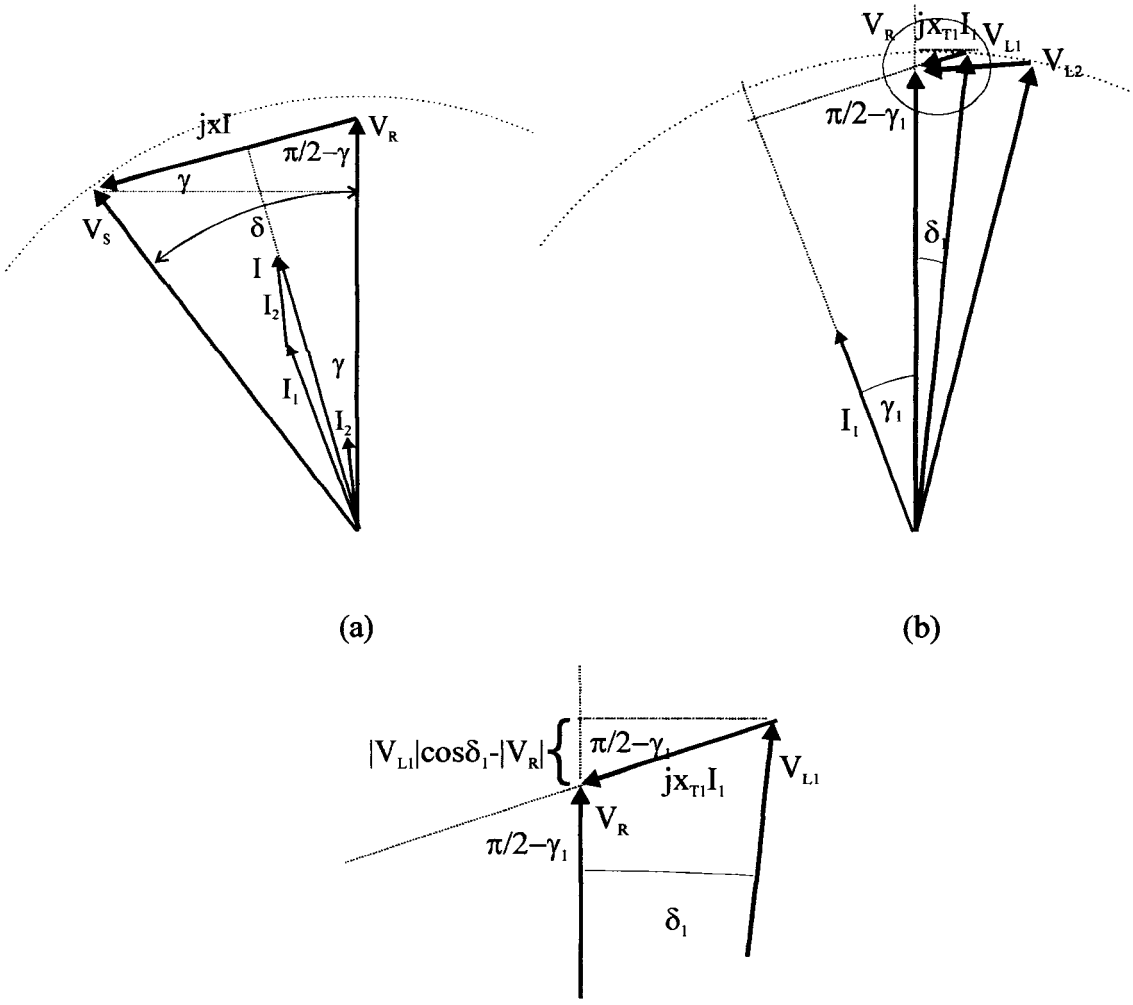

Figure 59 a) First part of phasor from Fig 58.b) second part of phasor from Fig.58.b), c)zoomed part in circle from Fig.59 b)

From phasor diagram in Fig.59.a) it can be written:

$$\sin\gamma = \frac{|V_R| - |V_S|\cos\delta}{XI} \tag{6.22}$$

$$|I|\sin\gamma = \frac{|V_R| - |V_S|\cos\delta}{X} \tag{6.23}$$

From Fig.59.b) and 59.c) it can be written:

$$\sin\gamma_1 = \frac{|V_{L1}|\cos\delta_1 - |V_R|}{X_{T1}I_1} \tag{6.24}$$

$$|I_1|\sin\gamma_1 = \frac{|V_{L1}|\cos\delta_1 - |V_R|}{X_{T1}} \tag{6.25}$$

substituting in (6.20) yields (6.26)

$$\frac{|V_R| - |V_s|\cos\delta}{X} + \frac{|V_R| - |V_{L1}|\cos\delta_1}{X_{T1}} + \frac{|V_R| - |V_{L2}|\cos\delta_2}{X_{T2}} = 0 \tag{6.26}$$

Equation (6.26) can be obtained applying Kirchhoff's laws on circuit from Fig 58 a).

Applying Kirchhoff's laws on circuit from Fig. 58 a).

$$\begin{aligned} \overline{V}_S &= \overline{V}_R + jXI \\ \overline{V}_R &= jX_{T1}\bar{I}_1 + \overline{V}_{L1} \\ \overline{V}_R &= jX_{T2}\bar{I}_2 + \overline{V}_{L2} \\ \bar{I} &= \bar{I}_1 + \bar{I}_2 \end{aligned} \tag{6.27}$$

$$\begin{aligned}
&\bar{V}_S = \bar{V}_R + jX(\bar{I}_1 + \bar{I}_2) \\
&\frac{\bar{V}_R - \bar{V}_{L1}}{jX_{T1}} = \bar{I}_1 \\
&\frac{\bar{V}_R - \bar{V}_{L2}}{jX_{T2}} = \bar{I}_2
\end{aligned} \tag{6.28}$$

Sending end voltage $\mathbf{V_S}$ together with load (distribution voltages) $\mathbf{V_{L1}}$ and $\mathbf{V_{L2}}$ are regulated at 1 p.u. Voltage V_R is taken as reference voltage, therefore, it can be written as:

$$\begin{aligned}
&|\bar{V}_S| = 1; |\bar{V}_{L1}| = 1; \ldots |\bar{V}_{L2}| = 1; \\
&angle(\bar{V}_S; \bar{V}_R) = \delta \\
&angle(\bar{V}_R; \bar{V}_{L1}) = -\delta_1 \\
&angle(\bar{V}_R; \bar{V}_{L2}) = -\delta_2 \\
&\bar{V}_R = |\bar{V}_R| e^{j0^o}
\end{aligned} \tag{6.29}$$

Combining (6.28) and (6.29) yields (6.30)

$$\bar{V}_R = \frac{\bar{V}_S + \frac{X}{X_{T1}}\bar{V}_{L1} + \frac{X}{X_{T2}}\bar{V}_{L2}}{(1 + \frac{X}{X_{T1}} + \frac{X}{X_{T2}})} \tag{6.30}$$

Equation (6.30) can be written as (6.31)

$$|\bar{V}_R|(1 + \frac{X}{X_{T1}} + \frac{X}{X_{T2}}) = \cos\delta + j\sin\delta + \frac{X}{X_{T1}}(\cos\delta_1 - j\sin\delta_1) + \frac{X}{X_{T2}}(\cos\delta_2 - j\sin\delta_2) \tag{6.31}$$

Using only real parts of (6.31) gives:

$$|\bar{V}_R|(\frac{1}{X}+\frac{1}{X_{T1}}+\frac{1}{X_{T2}})=\frac{1}{X}\cos\delta+\frac{1}{X_{T1}}(\cos\delta_1)+\frac{1}{X_{T2}}(\cos\delta_2) \tag{6.32}$$

$$\frac{|\bar{V}_R|}{X}+\frac{|\bar{V}_R|}{X_{T1}}+\frac{|\bar{V}_R|}{X_{T2}}-\frac{1}{X}\cos\delta-\frac{1}{X_{T1}}\cos\delta_1-\frac{1}{X_{T2}}\cos\delta_2=0 \tag{6.33}$$

Equation (6.33) is the same as (6.26). The (6.26) can be interpreted as conservation of reactive power for node with the voltage V_R.

$$\begin{aligned} &Q_1+Q_2+Q=0\\ &Q_1=\frac{|V_R|^2}{X_{T1}}-\frac{|V_R||V_{L1}|}{X_{T1}}\cos\delta_1\\ &Q_2=\frac{|V_R|^2}{X_{T2}}-\frac{|V_R||V_{L2}|}{X_{T2}}\cos\delta_2\\ &Q=\frac{|V_R|^2}{X}-\frac{|V_R||V_S|}{X}\cos\delta \end{aligned} \tag{6.34}$$

Where:

Q is reactive power from bus with voltage V_R to bus with voltage V_S

Q_1 is reactive power from bus with voltage V_R to bus with voltage V_{L1}

Q_2 is reactive power from bus with voltage V_R to bus with voltage V_{L2}

Taking imaginary part from (6.31) yields:

$$\begin{aligned} &\frac{1}{X}\sin\delta-\frac{1}{X_{T1}}(\sin\delta_1)-\frac{1}{X_{T2}}(\sin\delta_2)\\ &P_1+P_2+P=0 \end{aligned} \tag{6.35}$$

which represents law of conservation of active power.

6.2.4 N Load Centers in Parallel with Independent Voltage Support on Distribution Side

In more general case when N load centers are connected in parallel as in Fig.60, it can be written:

$$\frac{|V_R|-|V_s|\cos\delta}{X}+\frac{|V_R|-|V_{L1}|\cos\delta_1}{X_{T1}}+\frac{|V_R|-|V_{L2}|\cos\delta_2}{X_{T2}}+\ldots+\frac{|V_R|-|V_{LN}|\cos\delta_N}{X_{TN}}=0 \qquad (6.36)$$

the angles δ_i (i=1,2...N) are load angles and they can be expressed through the power supplied to load centers.

$$P=\frac{|V_S||V_R|}{X}\sin\delta \quad \Rightarrow \sin\delta=\frac{PX}{|V_S||V_R|} \Rightarrow \cos\delta=\sqrt{1-\sin^2\delta} \qquad (6.37)$$

$$\Rightarrow \sin\delta=\frac{PX}{|V_S||V_R|} \Rightarrow \cos\delta=\frac{\sqrt{|V_S|^2|V_R|^2-P^2X^2}}{|V_S||V_R|} \qquad (6.38)$$

Similarly, load angles are:

$$\cos\delta_i=\frac{\sqrt{|V_{Li}|^2|V_R|^2-P_i^2X_{Ti}^2}}{|V_{Li}||V_R|} \qquad (6.39)$$

substituting (6.39) into (6.36)

$$\frac{|V_R|}{X}-\frac{\sqrt{|V_R|^2|V_S|^2-P^2X^2}}{X|V_R|}+\frac{|V_R|}{X_{T1}}-\frac{\sqrt{|V_R|^2|V_{L1}|^2-P_1^2X_{T1}^2}}{X_{T1}|V_R|}+\frac{|V_R|}{X_{T2}}-\frac{\sqrt{|V_R|^2|V_{L2}|^2-P_2^2X_{T2}^2}}{X_{T2}|V_R|}+\ldots$$
$$+\frac{|V_R|}{X_{TN}}-\frac{\sqrt{|V_R|^2|V_{LN}|^2-P_N^2X_{TN}^2}}{X_{TN}|V_R|}=0 \qquad (6.40)$$

Rearranging equation (6.40),

$$|V_R|\left[\frac{1}{X}+\frac{1}{X_{T1}}+\frac{1}{X_{T2}}+\ldots+\frac{1}{X_{TN}}\right]= \frac{1}{|V_R|}\left[\frac{\sqrt{|V_R|^2|V_S|^2-P^2X^2}}{X}+\frac{\sqrt{|V_R|^2|V_{L1}|^2-P_1^2X_{T1}^2}}{X_{T1}}+\frac{\sqrt{|V_R|^2|V_{L2}|^2-P_2^2X_{T2}^2}}{X_{T2}|V_R|}+\ldots+\frac{\sqrt{|V_R|^2|V_{LN}|^2-P_N^2X_{TN}^2}}{X_{TN}}\right] \quad (6.41)$$

$$|V_R|=\frac{1}{|V_R|\left[\frac{1}{X}+\frac{1}{X_{T1}}+\frac{1}{X_{T2}}+\ldots+\frac{1}{X_{TN}}\right]} \left[\frac{\sqrt{|V_R|^2|V_S|^2-P^2X^2}}{X}+\frac{\sqrt{|V_R|^2|V_{L1}|^2-P_1^2X_{T1}^2}}{X_{T1}}+\frac{\sqrt{|V_R|^2|V_{L2}|^2-P_2^2X_{T2}^2}}{X_{T2}}+\ldots+\frac{\sqrt{|V_R|^2|V_{LN}|^2-P_N^2X_{TN}^2}}{X_{TN}}\right] \quad (6.42)$$

The equation (6.42) is an implicit equation that can be easy solved for $\mathbf{V_R}$ using method of successive iteration. It is worth noting that voltages V_{Li} if not kept at 1 p.u. can be expressed as function of $\mathbf{V_R}$ using Pythagoras's theorem applied at triangle formed by $\mathbf{V_R}$, $\mathbf{V_{LI}}$ and $jX_{Ti}\mathbf{I_i}$ as:

$$|\overline{V}_{Li}|=\sqrt{\frac{|\overline{V}_R|^2+\sqrt{|\overline{V}_R|^4-4\left(X_{Ti}P_i\right)^2}}{2}} \quad (6.43)$$

each load is assumed to be unity power factor.

The advantage of (6.42) representation is that it can be easily seen when load voltages $\mathbf{V_{Li}}$ and voltage $\mathbf{V_R}$ approach to collapse. Voltages V_{Li} can be kept at 1 p.u. with reactive power injection only and only if $|\mathbf{V_R}| > P_iX_{Ti}$.The voltage $\mathbf{V_R}$ collapse when $|\mathbf{V_R}||\mathbf{V_S}| < PX$.The points where $|\mathbf{V_R}|^2|\mathbf{V_S}|^2 = P^2X^2$ or $|\mathbf{V_R}|^2|\mathbf{V_{Li}}|^2 = P_i^2X_{Ti}^2$ are bifurcation point on p-v curb.

Knowing voltage $\mathbf{V_R}$ and load voltages V_{Li} using law of cosines, the currents $\mathbf{I_i}$ can be calculated as:

$$|\bar{I}_i| = \frac{\sqrt{|\bar{V}_R|^2 + |\bar{V}_{Li}|^2 - 2|\bar{V}_R||\bar{V}_{Li}|\cos\delta_i}}{X_{Ti}} \tag{6.44}$$

and compensating currents I_{Ci} are:

$$I_{Ci} = \sqrt{|I_i|^2 - |I_{Li}|^2} \tag{6.45}$$

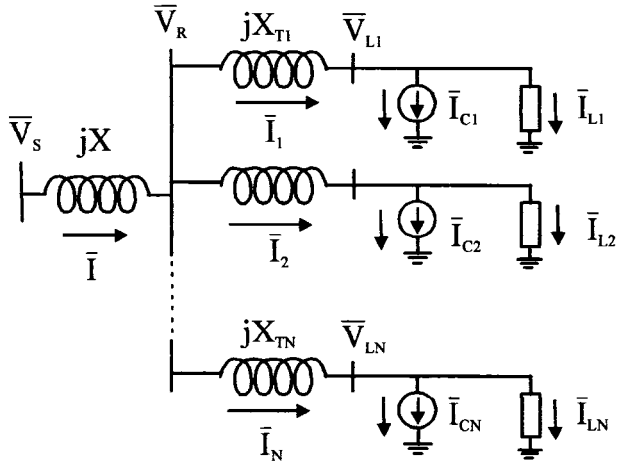

Figure 60 N load centers with independent voltage support on distribution level

6.3 Radial Line Feeding Two Load Centers Distributed Along the Line

Consider a radial transmission line of Fig.61 a) feeding two load centers over two bulk power delivery substations. Load center #1 is located on arbitrary position between two ends of the line while load center #2 is fixed where the line terminates. Voltage support can be provided on transmission level as shown on Fig.61 b) or on distribution level as shown on Fig.61 c). To underline the essentials, the simplified models and the phasor

representation are used in this study. Each segment of transmission line is represented by lumped inductive reactance whose value depends on the line segment length. The resistive losses are neglected. The power delivery substation transformers, whose leakage reactances are jX_{Ti}, bridge transmission side voltages to the distribution side voltages. The VAr compensators are treated as continues source of reactive current. The loads are assumed power factor corrected. It allows to consider only reactive requirements for voltage support.

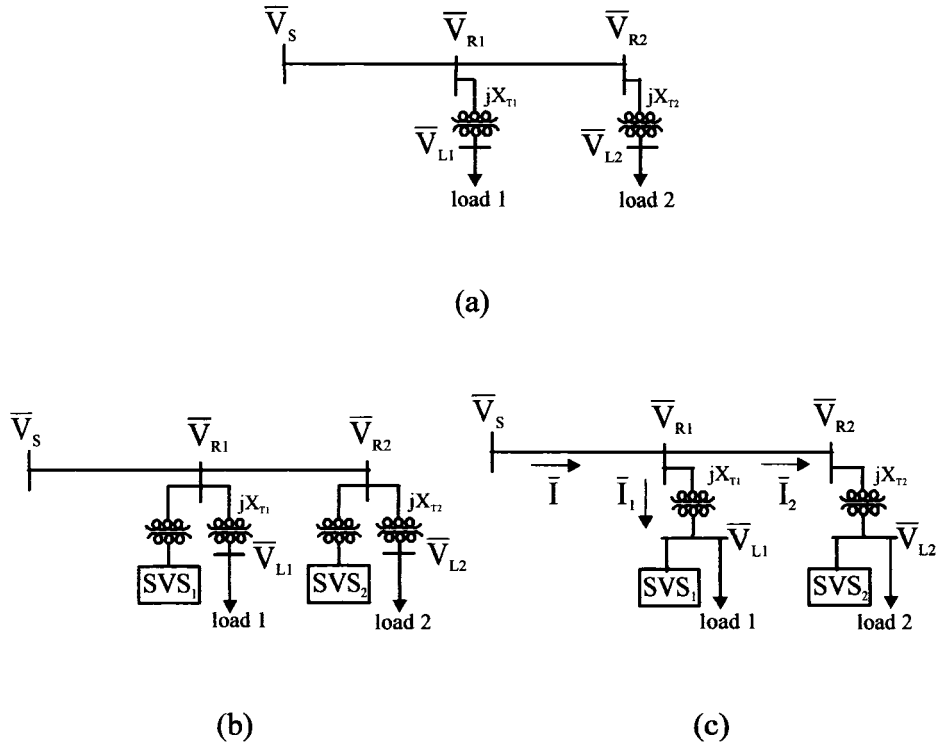

Figure 61 a) Radial transmission line feeding two load centers over two power delivery substations distributed along the line. b) Voltage support can be provided on transmission level c).or on distribution level

6.4 Feasibility

Before proceeding to make comparison, it is necessary to establish that voltage support by distributed, distribution VAr compensator of Fig. 61 c) is mathematically feasible for

different position of load centers. The steady state solutions are presented in the form of phasor diagrams. The transmission line between sending end voltage $\mathbf{V_S}$ and receiving end voltage $\mathbf{V_{R1}}$ is represented by lumped inductive reactance jX_1 and transmission line between receiving end voltage $\mathbf{V_{R1}}$ and receiving end voltage $\mathbf{V_{R2}}$ is represented by lumped reactive inductance jX_2.

6.4.1 Steady State Solution for Distribution Voltage Support

The phasor diagram of Fig.62 presents the steady state solution for the distributed, distribution side VAr compensation of Fig.61 c).

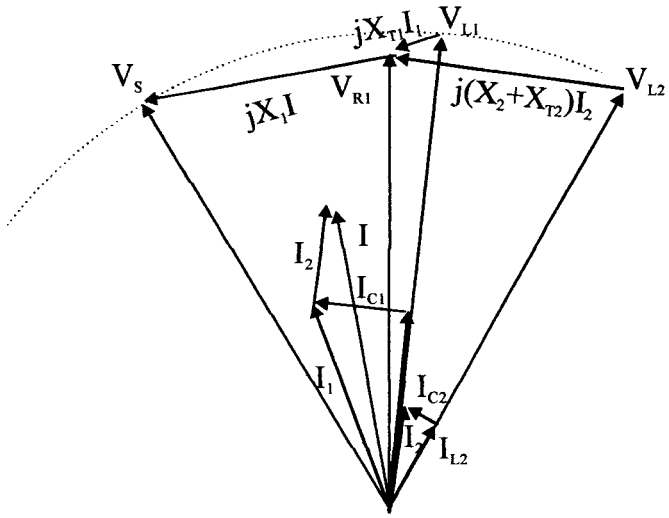

Figure 62 Phasor diagram for circuit of Fig.61. c)

The sending end voltage $\mathbf{V_S}$ and load voltages $\mathbf{V_{L1}}$ and $\mathbf{V_{L2}}$ are maintained on the circle of the 1 p.u. voltage radius. The closing side of voltage triangle $\mathbf{V_S}$, $\mathbf{V_{R1}}$ is the voltage phasor $jX_1\mathbf{I}$ where $\mathbf{I}$ is the current through the first segment of the transmission line. The sending end voltage triangle satisfies Kirchhoff's voltage law: $\mathbf{V_S} = \mathbf{V_{R1}} + jX_1\mathbf{I}$. It can be seen that the transmission level, receiving end voltage $\mathbf{V_{R1}}$ is not regulated at 1 p.u. The receiving

end voltage triangles satisfy Kirchhoff's voltage law: $\mathbf{V_{R1}} = \mathbf{V_{L1}} + jX_{T1}(\mathbf{I_{L1}} + \mathbf{I_{C1}})$ and $\mathbf{V_{R1}} = \mathbf{V_{L2}} + j(X_2+X_{T2})(\mathbf{I_{L2}} + \mathbf{I_{C2}})$ where $jX_{T1}\mathbf{I_{L1}}$ represents voltage drop caused by load current $\mathbf{I_{L1}}$ across first power delivery substation transformer, $jX_{T1}\mathbf{I_{C1}}$ represents voltage boost due to leading current flowing through transformer reactance, $\mathbf{V_{L2}}$ is regulated voltage of second substation and $j(X_2+X_{T1})(\mathbf{I_{L2}} + \mathbf{I_{C2}})$ is voltage drop/boost across the second segment of the line and power delivery substation transformer.

The Kirchhoff's current Law at the receiving ends 1 and 2 is: $\mathbf{I} = \mathbf{I_2} + \mathbf{I_1}$ where $\mathbf{I_2} = \mathbf{I_{L2}} + \mathbf{I_{C2}}$ and $\mathbf{I_1} = \mathbf{I_{L1}} + \mathbf{I_{C1}}$. It is apparent from Fig.62 that load voltages $\mathbf{V_{L1}}$ and $\mathbf{V_{L2}}$ are regulated while transmission voltages $\mathbf{V_{R1}}$ and $\mathbf{V_{R2}}$ are not.

6.5 Reactive Requirement

6.5.1 Distribution Side Compensation at Buses $\mathbf{V_{L1}}$ and $\mathbf{V_{L2}}$

The reactive requirements for regulation of load voltages $\mathbf{V_{L1}}$ and $\mathbf{V_{L2}}$ can be calculated from phasor diagram of Fig.62. using (6.42) The current through power delivery substation #1, $\mathbf{I_1}$ can be calculated from cosine theorem applied on triangle formed by load voltage $\mathbf{V_{L1}}$, receiving end voltage $\mathbf{V_{R1}}$ and voltage drop $jX_{T1}\mathbf{I_1}$ caused by the current $\mathbf{I_1}$ across substation #1 transformer:

$$|\bar{I}_1| = \frac{\sqrt{|\bar{V}_{R1}|^2 + |\bar{V}_{L1}|^2 - 2|\bar{V}_R||\bar{V}_{L1}|\cos\delta_1}}{X_{T1}} \tag{6.46}$$

The compensating current I_{C1} is in quadrature with load current I_{L1}(the load power factor is assumed corrected). These two currents form right angle triangle together with current I_1. Applying Pythagoras's theorem:

$$I_{C1} = \sqrt{|I_1|^2 - |I_{L1}|^2} \tag{6.47}$$

The receiving end voltage $|V_{R1}|$ is given by,

$$|V_{R1}| = \frac{1}{|V_{R1}|\left[\frac{1}{X_1} + \frac{1}{X_{T1}} + \frac{1}{X_2 + X_{T2}}\right]}\left[\frac{\sqrt{|V_{R1}|^2 - P^2 X_1^2}}{X_1} + \frac{\sqrt{|V_{R1}|^2 - P_1^2 X_{T1}^2}}{X_{T1}} + \frac{\sqrt{|V_{R1}|^2 - P_2^2 (X_2 + X_{T2})^2}}{X_2 + X_{T2}}\right] \tag{6.48}$$

Equation (6.48) is implicit equation that has to be solved numerically. The method of successive iterations has been used in this case. It is worth noting that from (6.48) voltage collapse can be predicted. For (6.48) to have the real solution, following conditions are imposed: $\left(|\overline{V}_{R1}| \geq |PX_1|\right) \& \left(|\overline{V}_{R1}| \geq |P_1 X_{T1}|\right) \& \left(|\overline{V}_{R1}| \geq |P_2 (X_2 + X_{T2})|\right)$.

If the above mentioned conditions are not satisfied, at least one solution is complex. The point when one of the solutions starts to become complex is bifurcation point on P-V curb.

6.5.2 Transmission Side Compensation at Buses V_{R1} and V_{R2}

Fig.63 shows the phasor for the case when voltage support is provided on transmission side of power delivery substation as illustrated on Fig.61 b).

The compensating currents I_{C1} and I_{C2} can be calculated explicitly from phasor of Fig.63. Applying (6.19) yields (6.49) and (6.50):

$$I_{C1} = \frac{|V_{R1}| - |V_S| \cos\delta}{X_1} + \frac{|V_{R1}| - |V_{R2}| \cos\delta_1}{X_2} + \frac{|V_{R1}| - |V_{L1}| \cos\theta_1}{X_{T1}} \tag{6.49}$$

$$I_{C2} = \frac{|V_{R2}| - |V_{R1}|\cos\delta_2}{X_2} + \frac{|V_{R2}| - |V_{L2}|\cos\theta_2}{X_{T2}} \tag{6.50}$$

where $|V_{R1}|=|V_{R2}|=|V_S|=1$ p.u.

and V_{L1} and V_{L2} are load voltages that can be calculated using Pythagoras's theorem as:

$|V_{Ri}|^2 = |X_{Ti} I_{Li}|^2 + |V_{Li}|^2$ and knowing that $P_i = |V_{Li}||I_{Li}|$, i=1,2.

$$|\overline{V}_{Li}| = \sqrt{\frac{|\overline{V}_{Ri}|^2 + \sqrt{|\overline{V}_{Ri}|^4 - 4(X_{Ti}P_i)^2}}{2}} \tag{6.51}$$

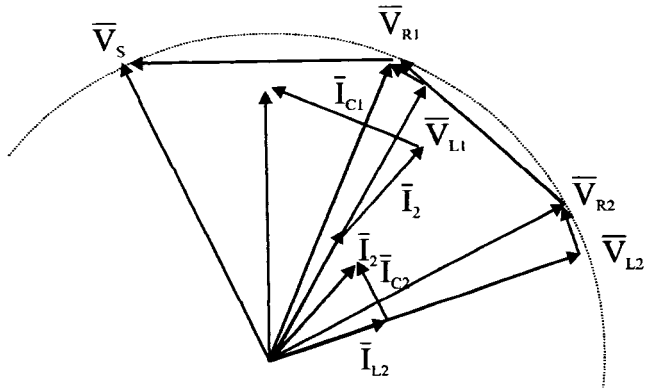

Figure 63 Phasor for transmission side voltage support

6.6 Comparison of Two Voltage Support Schema

6.6.1 Comparison of Var Requirement

Reactive power needed for voltage support depends on power transfer over the line, line length and position of load centers. Considering again the simple case of Fig.61 where radial transmission line feeds two load center. Let real power supplied to load center #1 is 2 p.u and to load center #2 is 1 p.u. Assume line length of 225 km. Surge impedance load

is used as 1 p.u. Line is assumed lossless. Line reactance is $0.0013l$ where l is line length in km. Transformer impedance is assumed 10% on transformer base . Load voltages $\mathbf{V_{L1}}$ and $\mathbf{V_{L2}}$ are regulated at 1 p.u. Load center #2 is situated at the end of the line, 225 km from sending end. Load center #1 is shifted from sending end toward load center #2 (from 0 km to 225 km). Fig. 64 shows receiving voltages $\mathbf{V_{R1}}$ and $\mathbf{V_{R2}}$ (upper trace), power angles (middle trace) (δ is angle between $\mathbf{V_S}$ and $\mathbf{V_{R1}}$, δ_1 is angle between $\mathbf{V_{R1}}$ and $\mathbf{V_{L1}}$ and δ_2 is angle between $\mathbf{V_{R1}}$ and $\mathbf{V_{L2}}$) and reactive power Q1 and Q2 (lowest trace) needed to keep load voltages $\mathbf{V_{L1}}$ and $\mathbf{V_{L2}}$ at 1 p.u., respectively, plotted against position of load center #1.

The Fig.65 compares reactive requirements for the same system when voltage support is provide on transmission level keeping voltages $\mathbf{V_{R1}}$ and $\mathbf{V_{R2}}$ at 1pu. It can be seen that most of the time reactive requirement needed for distribution, distributed voltage support are lower compared to transmission side voltage support.

6.6.2 Comparison of Transformer MVA Requirements

The Fig.66 shows MVA requirements of transformers for both cases plotted against line length. When voltage support is provided at transmission level as in Fig.61 b) transformers MVA requirements are evaluated as:

$$S_{bulk} = P_1 + Q_1 + P_2 + Q_2 = P_1 + P_2 + Q_{bulk} \tag{6.52}$$

When voltage support provided on distribution level as in Fig.6.5.c) transformer MVA are evaluated as in:

$$S_{distributed} = \sqrt{P_1^2 + Q_{1distributed}^2} + \sqrt{P_2^2 + Q_{2distributed}^2} \tag{6.53}$$

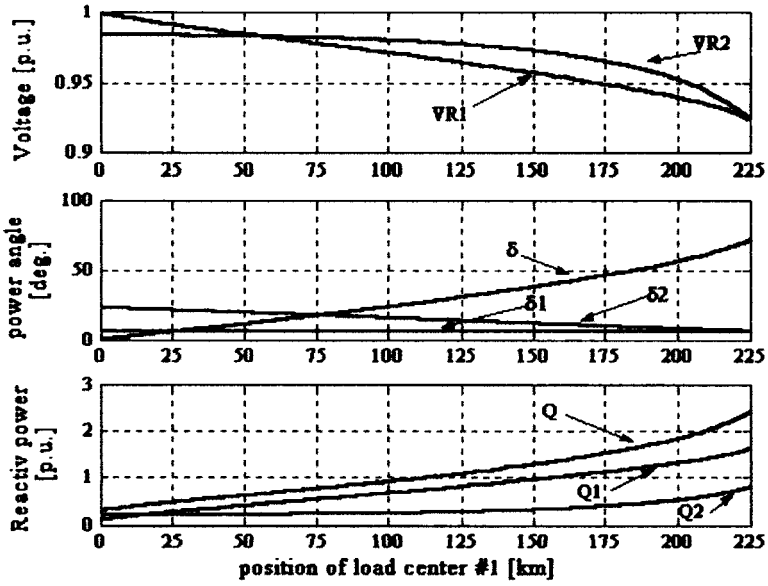

Figure 64 Power delivery substation transmission side voltages (upper trace), power angles (middle trace) and reactive power (Q = Q1+Q2) needed for voltages regulation (lower trace) on distribution side.

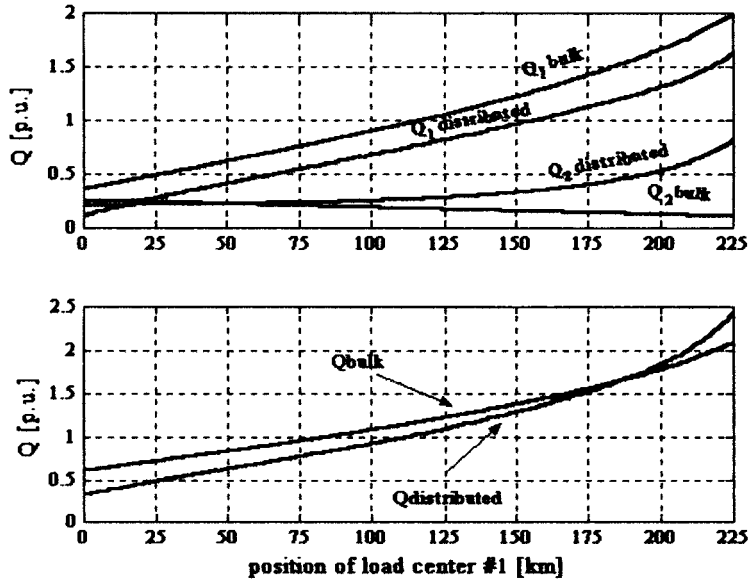

Figure 65 Comparison of reactive needs at substation #1 and #2 plotted against position of load center #1

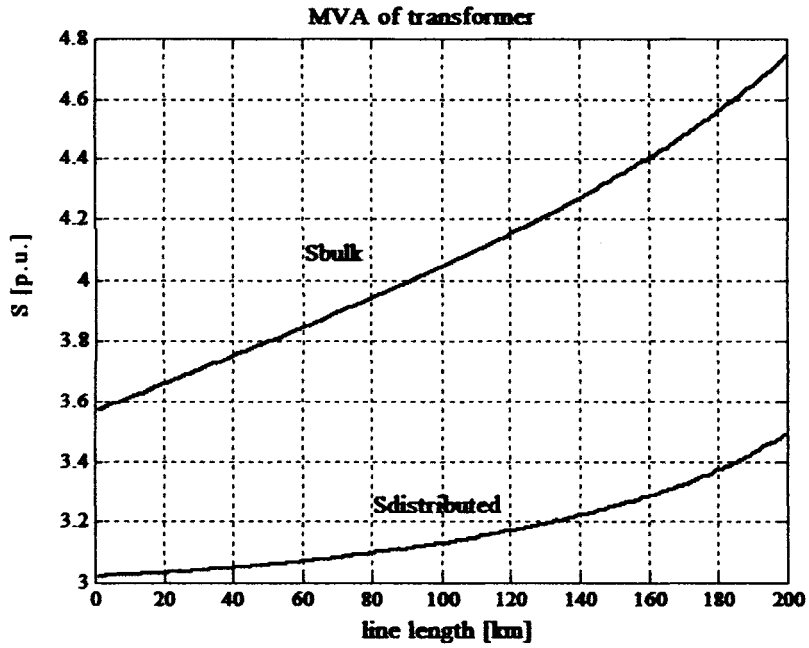

Figure 66 Transformer MVA requirements.

6.6.3 Transmission Level Voltage

In this subsection the case of two load centers, similar as shown in Fig.61 is considered. The first load center is located at line at 150th km from stiff system and the second load center is located 100 km further. Thermal limits of the line are assumed to be 3Psil so 3pu is used as P_{max}.

Fig. 67 shows variation of transmission level voltage V_{R1} (voltage on HV side of power delivery substation 1 plotted against power transferred to load center #2. The power fed to load center # 1 is fixed.

6.6.4 Comparison of Var Requirement

Fig.68 displays reactive requirement for two methods. The power fed to load center #2 is kept constant at 1 p.u. while power transferred to load center #1 is varied from 0 to 2 p.u.

Upper trace in Fig.68 shows reactive requirements for load centers #1 and #2 when voltage support is provided on transmission level. Lower trace shows reactive requirements for load centers #1 and #2 when voltage support is provided on distribution level.

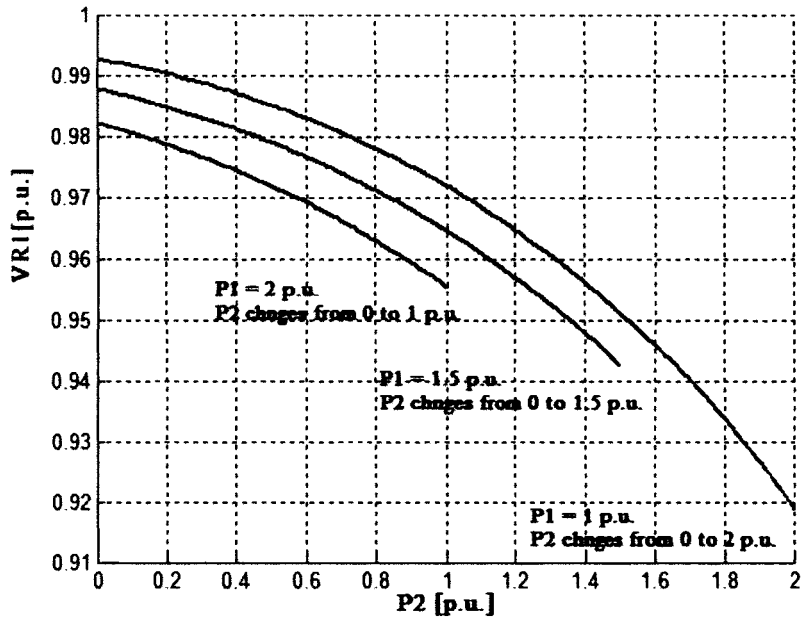

Figure 67 Variation of transmission voltage V_{R1} plotted against power P_2 fed to load center #2. $P_{1max} + P_{2max}$ = 3pu which is assumed to be thermal limit of the line.

It is worth noting that the saving in terms of $ can be considerable. Total Q for bulk case is 1.42 p.u and for distributed is 1.33. So the difference is 0.09 p.u. The savings depends upon the voltage level. In the case of 500 kV transmission line 1 p.u = 1000 MW. So the savings in MVArs are 90 MVAr. If the STATCOM is 50$/kVAr then savings are $4.5M.

Fig. 69 compares reactive needs for the case 150 km line feeding 2 p.u. load plus 100 km line feeding 1 p.u. load when compensation is provided on HV side vs. compensation on distribution voltage side. When compensation is on HV we keep V_{R1} and V_{R2} at 1p.u,

meaning the load voltages are not regulated at 1 pu. When compensation is on distribution voltage side, load voltages are kept at 1 p.u. In this graph we recover load P_2 . We can see that, even if compensation is not compared on equal footing, the Q total needed is lower for distribution side compensation. There is one other advantages too. We can see that in case of bulk compensation Q_1 is considerably bigger than in case of distributed compensation. It means that, from point of the view of system operation, is more dangerous if Q_1 is lost for bulk compensation.

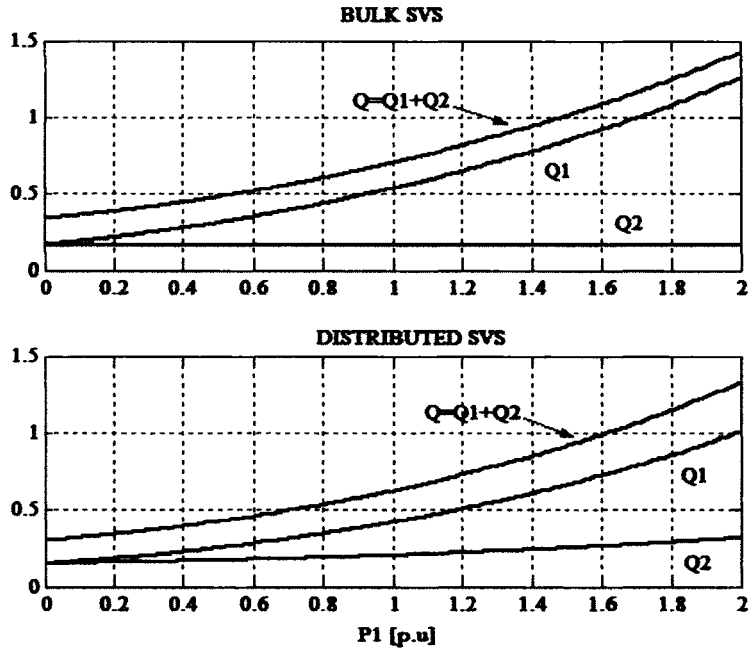

Figure 68 Comparison of reactive needs at substation #1 and #2 plotted against power transferred to load center #1. The power fed to load center #2 is kept constant at 1 p.u. while power transferred to load center #1 is varied from 0 to 2 p.u.

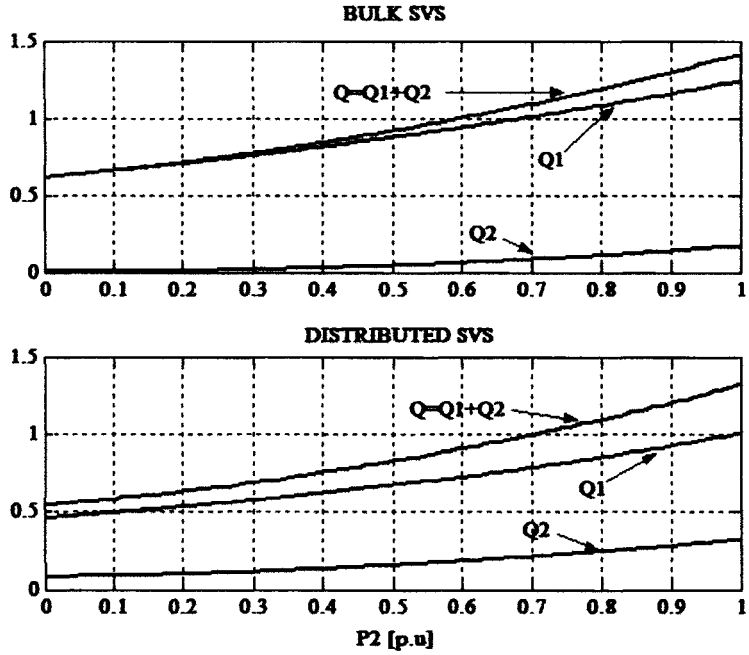

Figure 69 Comparison of reactive needs at substation #1 and #2 plotted against power transferred to load center #1. Comparison of reactive needs at substation #1 and #2 plotted against power transferred to load center #1. The power fed to load center #1 is kept constant at 1 p.u. while power transferred to load center #2 is varied from 0 to 1 p.u.

6.7 Conclusion

In this chapter two load centers spaced along radial transmission line has been considered. The equation allowing calculation of voltages and compensating currents for voltages regulation have been deduced and verified. Two methods for voltage support, namely, voltage support of transmission line with distribution level compensation and voltage support of transmission line with transmission level compensation, have been compared. It has been shown that distribution level voltage support has significant benefits over the transmission level voltage support. The benefits include lower var requirement, direct voltage regulation of distribution buses and elimination of step up transformer for voltage support.

CHAPTER 7

VOLTAGE SUPPORT OF LONG RADIAL TRANSMISSION LINES BY VAR COMPENSATION AT DISTRIBUTION BUSES

7.1 Introduction

The objective of this chapter is to bridge the gap between transmission and distribution approaches to voltage support and reactive power management. The impetus, which should bring transmission system engineers and distribution system engineers together, is the availability in the market of SVCs which can be connected directly to the distribution buses at voltages as high as 35 kV without step-up voltage transformers [68]. As it requires concrete examples to demonstrate how the innovative advance can be exploited, this chapter reviews where the potential benefits are and proceeds to substantiate the claims in a case study of a 400 km long, 230 kV radial line supplying 200 MW to each of 4 loads spaced evenly along its length.

The case study is patterned after Hydro-Quebec's 1000 km long James Bay line whose voltage profile is supported by a combination of capacitors and static var compensators at 5 intermediate points along the line. If the intermediate points are not in the Canadian wilderness but are in inhabited areas, the same concept can be applied to increase the transmissibility of real power to distant townships at intermediate points spread along the long line. As such a project falls within development and planning of transmission systems, the capacitors and static var compensators (SVC) will be installed on the transmission line buses.

One objective of this chapter is to highlight the advantages of distribution bus voltage support to transmission system engineers who are charged with the development and planning for the voltage support of long lines. In today's restructured electric utilities, the

many distribution systems and the transmission system may belong to different owners. The technical and economic advantages can still be implemented by putting voltage support as an ancillary service. The distribution system closest to the generation source is providing capacitive reactive power not only for its own load but also for the loads of distribution systems further down the line.

It is required to show that the concept is technically feasible. This is accomplished by digital simulations. The simulation tool in use has been HYPERSIM. The successful simulation firstly implies feasibility, meaning that there is a mathematical solution of the operating point. Secondly, the operating point is steady-state stable, because otherwise there is no stable convergence in the simulations. Finally, simulations have been used to demonstrate that after three-phase-to-ground faults, the transmission line automatically recovers its regulated distribution bus voltages.

In quantifying capacitive reactive power, this chapter makes a distinction between the amount required for power factor correction and the amount required for voltage support. In order to simplify bookkeeping, the amount required for power factor correction is deducted in the accounting, so that one has a realistic value of the capacitive reactive power required for voltage support. In this chapter, to provide voltage support (VS) by var compensation, the authors use Static Var Compensators(SVC) because it is proven, mature and reliable technology.

7.2 Voltage Support of Long Transmission Line

Two transmission line voltage support schemes are presented in this section: voltage support (VS) provided by SVCs on the transmission buses and VS provided by SVCs on the distribution buses. Circle phasor diagrams are given to draw attention to the fact that, unlike distribution system engineers who are concerned only with voltage support for the

loads connected to the substation, transmission system engineers have to be concerned with all the loads along the transmission line.

7.2.1 Voltage Support at Transmission Buses

Fig. 70 shows a radial transmission line made up of M sections, each of which is represented by an inductive reactance jX_i, *i=1,2,. M.* The generation source voltage is $\mathbf{V_S}$. At the i^{th} node, between two transmission line sections, the voltage is $\mathbf{V_{Ri}}$. SVC providing VS would be connected at each node to regulate the nodal transmission line voltage $|\mathbf{V_{Ri}}|$ at 1.0 pu. Because the technology of the reactive power compensation is realized at the level of distribution voltage, each installed SVC requires a step-up transformer to raise its output voltage to the transmission voltage level of $\mathbf{V_{Ri}}$. The distribution bus (voltage $\mathbf{V_{Li}}$) of the i^{th} load center is coupled to the transmission bus (voltage $\mathbf{V_{Ri}}$) by a voltage step-down transformer which is represented by its leakage reactance jX_{Ti}.

Fig.71 is a phasor diagram for the i^{th} node of Fig.70. The phasor diagram is intended as a pictorial representation of the steady-state performance of this system providing an illustration of what is happening at a glance. From Fig.71 it can be seen that, when the transmission voltages are regulated, the tips of the per-unitized transmission voltage phasors $\mathbf{V_{Ri}}$, *i=1,2..M*, lie on a circle of unit radius. The voltages of two adjacent nodes, $\mathbf{V_{Ri}}$ and $\mathbf{V_{R(i-1)}}$, form two sides of a voltage triangle in accordance to Kirchhoff's Voltage Law $\mathbf{V_{R(i-1)}}=\mathbf{V_{Ri}}+jX_i\mathbf{I_i}$ where $\mathbf{I_i}$ is the line current through jX_i, which represents the reactance of the i^{th} transmission line section. The voltage phasor $jX_i\mathbf{I_i}$ is perpendicular to the current phasor $\mathbf{I_i}$. Because of the voltage drop across the transformer leakage reactance jX_{Ti} by the load current $\mathbf{I_{Li}}$, the load voltage $\mathbf{V_{Li}} = \mathbf{V_{Ri}} - jX_{Ti}\mathbf{I_{Li}}$ is not regulated. Transformer tap changers must be employed to achieve close load voltage regulation at every node. As will be seen in Section 7.5, transformer tap changers will not be needed when the SVC regulates $\mathbf{V_{Li}}$, the distribution (load) bus voltage directly.

From Kirchhoff's Current Law at the ith node, the capacitive compensating current is: $I_{Ci}=I_i-I_{i+1}-I_{Li}$. The compensating current I_{Ci} in Fig. 71 leads the transmission bus voltage V_{Ri} by 90^0. The transmission bus voltages $V_{R(i-1)}$ and V_{Ri} lie on the unit circle. It is assumed that lagging power factor in the load has already been corrected and therefore, the load current I_{Li} is in phase with V_{Li}. The line current I_i is the vector sum of the load current I_{Li}, the current through $i+1^{th}$ segment of the line I_{i+1} and the compensating current I_{Ci}.

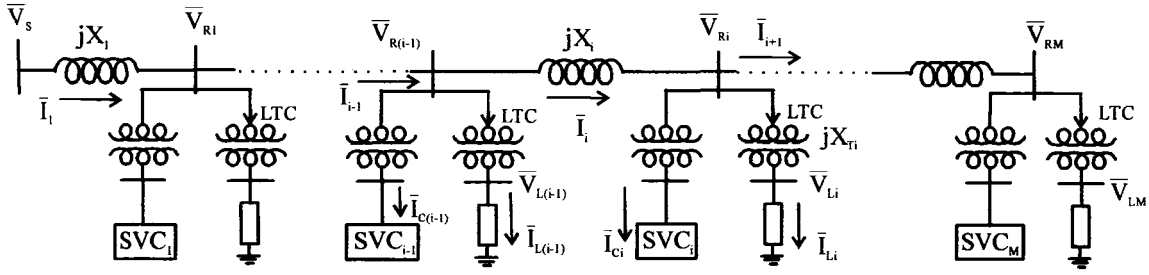

Figure 70 Single line diagram of radial transmission line feeding M load centers. Voltage support (VS) is provided on transmission buses.

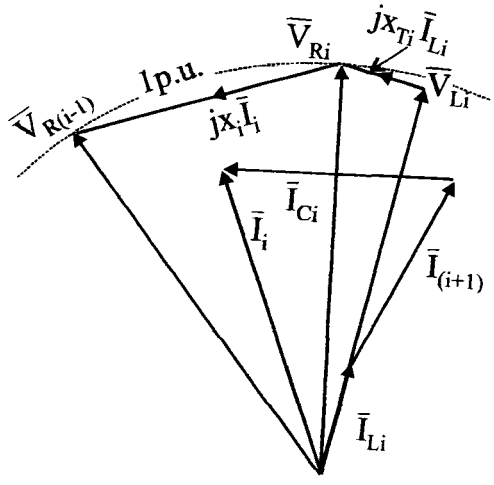

Figure 71 Phasor diagram for i^{th} node of Fig.70

7.2.2 Voltage Support at Distribution Buses

This chapter advocates connecting the SVC providing VS to the distribution buses as shown in Fig. 72. At the i^{th} node, SVS_i is set to regulate the load voltage at $|\mathbf{V_{Li}}| = 1.0$ pu.

Fig. 73 shows the distribution bus voltages, $\mathbf{V_{Li}}$ and $\mathbf{V_{L(i-1)}}$, of the i^{th} and $(i-1)^{th}$ nodes lying on the unit circle under SVC regulation. SVC_i, in providing voltage support to $\mathbf{V_{Li}}$, supports the transmission bus voltage $\mathbf{V_{Ri}}$ also. The compensating current of SVC_i, $\mathbf{I_{Ci}}$, leads the distribution voltage $\mathbf{V_{Li}}$ by 90^0. The magnitude of the transmission bus voltage, given by the formula, $|\mathbf{V_{Ri}}| = |\mathbf{V_{Li}} + jX_{Ti}(\mathbf{I_{Li}} + j\mathbf{I_{ci}})|$, is no longer at 1.0 pu. The current $\mathbf{I_{i+1}}$ further down the line joins the transmission bus to form a second node at which the current $\mathbf{I_i} = \mathbf{I_{i+1}} + \mathbf{I_{Li}} + \mathbf{I_{Ci}}$. The transmission bus voltages form a voltage triangle in accordance to Kirchhoff's Voltage Law $\mathbf{V_{R(i-1)}} = \mathbf{V_{Ri}} + jX_i\mathbf{I_i}$.

Unlike distribution system engineers who are responsible for the load current $\mathbf{I_{Li}}$, transmission system engineers have to look after the current $\mathbf{I_{i+1}}$ from further down the line also.

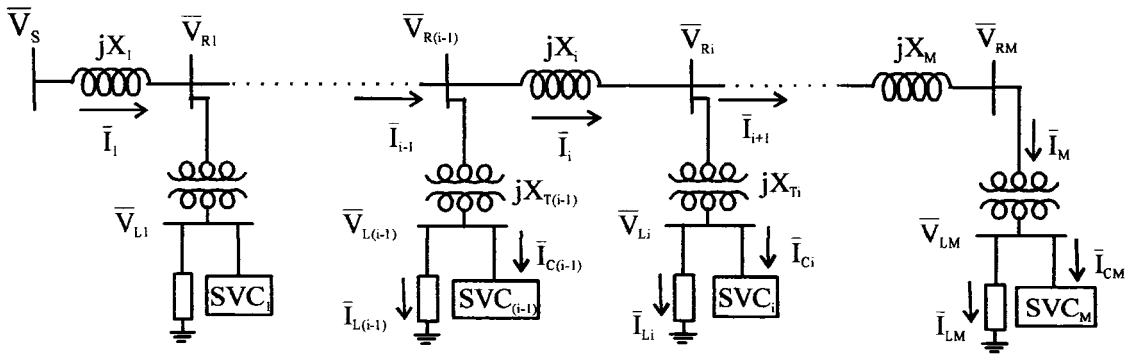

Figure 72 Single line diagram of radial transmission line feeding M load centers. Voltage support (VS) is provided on distribution buses

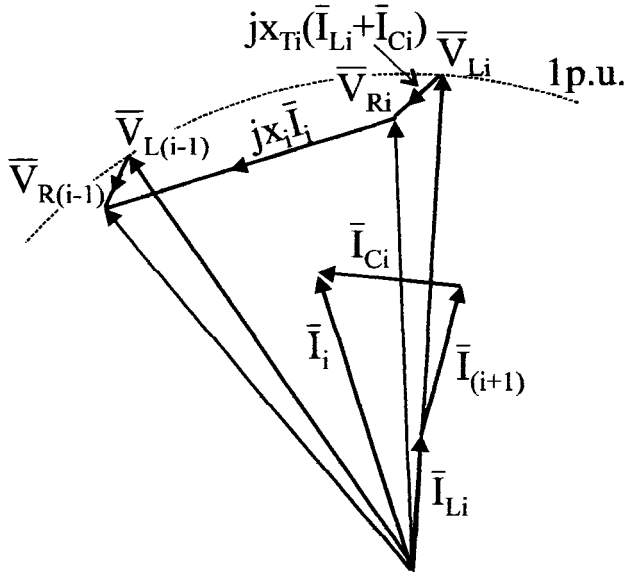

Figure 73 Phasor diagram for i^{th} node of system using distribution bus VS

7.3 Comparison of Two Voltage Support Schemes

7.3.1 Transformer Savings

At each node in Fig.70, there is one transformer for the load and another transformer for the SVC. Both the load and the SVC operate at low voltages and the objective of this chapter is to point out that there is no reason to step-up the capacitive reactive power of the SVC by one transformer to transmission voltage level and then to step it down again to the distribution voltage of the load. By connecting the SVC directly at the load bus as shown in Fig. 72, the SVC transformer can be saved.

7.3.2 Providing (N-1) Reliability

There is further saving to be gained in the planning for (N-1) reliability. (N-1) reliability

consideration requires that the voltage support be realized by N ($\neq$1) units. Should any voltage support unit fail, the remaining (N-1) units must have sufficient Mvar capacity. The cost of (N-1) reliability diminishes as N increases.

7.3.2.1 Distribution Buses Voltage Support

When Q_{iD} is the total reactive power required to provide voltage support of the ith node, (N-1) reliability requires the reactive power to be divided into N_{iD} smaller units. Upon failure of any one unit, the remaining (N_{iD}-1) units still provide the amount Q_{iD}. The (N-1) reliability requirement of reactive power is therefore $N_{iD}Q_{iD}/(N_{iD}-1)$.

Such division fits naturally in the design of distribution substations. such as shown in Fig.32. The substation consists of: high-voltage line terminations, high-voltage busbars, power transformers, low-voltage busbars and low-voltage line terminations. Breaker-and-a-half is used for both transmission and distribution voltage levels in order to fulfill the reliability of power supply.

In the example of Fig. 32, when the real power requirement is P_i, (N-1) reliability is satisfied by over-sizing each transformer to carry $P_i/(N_{iD}-1)$ watts (N_{iD}=4 in the example). In this situation, it is normal to allocate one SVC unit to each of the 25 kV buses. As the transformers carry the real and the reactive powers, their total MVA requirement is $N_{iD}(P_i^2+Q_{iD}^2)^{0.5}/(N_{iD}-1)$. As N_{iD} increases, their total MVA approaches $(P_i^2+Q_{iD}^2)^{0.5}$.

Furthermore, because $(P_i^2+Q_{iD}^2)^{0.5}<|P_i|+|Q_{iD}|$, when the ratio Q_{iD}/P_i is small, the rating of the step-down transformers is only slightly increased by the need to carry capacitive reactive power.

7.3.2.2 Transmission Buses Voltage Support

Using the same principle of dividing the reactive power Q_{iHV} required by the transmission bus SVC into N_{iHV} units, the total rating required to satisfy the (N-1) reliability criterion is: $N_{iHV}Q_{iHV}/(N_{iHV}-1)$ for: (i) the reactive power and (ii) the step-up transformers. On the load-side, the total MVA of the step-down transformers is $N_{iD}P_i/(N_{iD}-1)$.

7.3.2.3 Potential Reduction in Cost

In summary, the comparison of the two schemes are:

Reactive Power Requirements:

Distribution Bus SVC: $N_{iD}Q_{iD}/(N_{iD}-1)$

Transmission Bus SVC: $N_{iHV}Q_{iHV}/(N_{iHV}-1)$

Transformers MVA Requirements:

Distribution Bus SVC: $N_{iD}\,(P_i^2+Q_{iD}^2)^{0.5}/(N_{iD}-1)$

Transmission Bus SVC: $N_{iD}P_i/(N_{iD}-1)+N_{iHV}Q_{iHV}/(N_{iHV}-1)$

As will be seen in the next section, $Q_{iD} < Q_{iHV}$. Furthermore, usually $N_{iHV} < N_{iD}$ in engineering practice. Therefore, the equipment requirement is less for SVC on the distribution bus side than on the transmission bus side.

7.3.3 Reactive Power Savings

In general, $Q_{iD} < Q_{iHV}$, that is the reactive power required to provide voltage support is less when the SVCs are located at the distribution buses than at the transmission buses. However, there is a transmission length and a load limit beyond at which the inequality is reversed, i.e. $Q_{iHV} < Q_{iD}$. This transmission length is near to where voltage collapse occurs.

Approaching the problem by analysis, the point is close to the region where the solutions are complex and therefore infeasible. In such a case, VS by shunt compensation alone is not viable either on the transmission or the distribution buses. In such a situation, one should consider increasing the transmission voltage or using a combination of series and shunt compensation.

7.3.4 Line Losses

The transmission bus voltages $\mathbf{V_{R(i-1)}}$ and $\mathbf{V_{Ri}}$ in Fig.72 are lower than those in Fig.70. For the same real power transferred, the current $\mathbf{I_i}$ must be higher in VS on the distribution bus than on the transmission bus and consequently this applies to the line losses. But as will be seen in the case study below, the increase in losses is not substantial.

7.3.5 Benefits

To summarize, the benefits of voltage support on distribution buses by var compensation are:

i) lower transformer MVA requirements,
ii) lower var requirement for voltage support,
iii) close voltage regulation of the loads,
iv) lower cost in assuring N-1 reliability.

7.4 Proofs of Viability of Concept

The benefits will come to naught, if the system of Fig. 72 is not technically viable in the first place. This chapter presents evidences on viability in a case study based on: (i) existence of steady-state solutions; (ii) stability of steady-state solutions; (iii) ability of the system to survive faults.

7.4.1 Case Study: 400 km Long, 230 kV Radial Line

The case study relates to the single line diagram of Fig. 74. It consists of a 400 km long, radial, single circuit transmission line feeding four load centers located at 100, 200, 300 and 400 km from the generation source. The line supplies 200 MW at each load center. The transmission line voltage is rated at 230 kV. The distribution voltage is 25 kV. The source is modeled as an infinite bus.

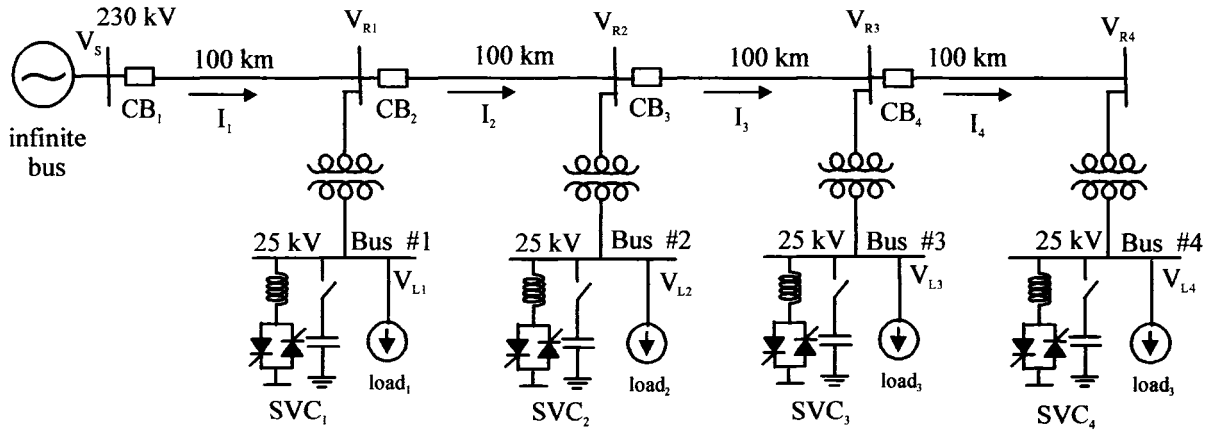

Figure 74 Case-Study of Radial line supported by SVCs connected to distribution buses

7.4.1.1 Steady-State Operation

Steady-state solutions have been obtained by 3 independent methods: (1) standard load flow studies; (2) phasor solutions of network equations using Kirchhoff's Voltage and Current Laws formulation; (3) simulation studies until the transients are damped out leaving the steady-state solutions. The solutions from the three independent methods agree.

The voltage phasors of $\mathbf{V_{Ri}}$ and $\mathbf{V_{Li}}$ are plotted in Fig. 75 The distribution voltage phasors $\mathbf{V_{Li}}$, i=1,2..4, lie on the unit circle, whereas the magnitudes of transmission bus phasors $\mathbf{V_{R1}}$ to $\mathbf{V_{R4}}$ are 0.91, 0.92, 0.96 and 0.98 pu respectively. The large angle on the sending end side and the crowding at the end reflect the fact that the line sections of currents $\mathbf{I_1}$, $\mathbf{I_2}$, $\mathbf{I_3}$ and $\mathbf{I_4}$ in Fig.6 carry powers of 800 MW, 600 MW, 400 MW and 200 MW, respectively.

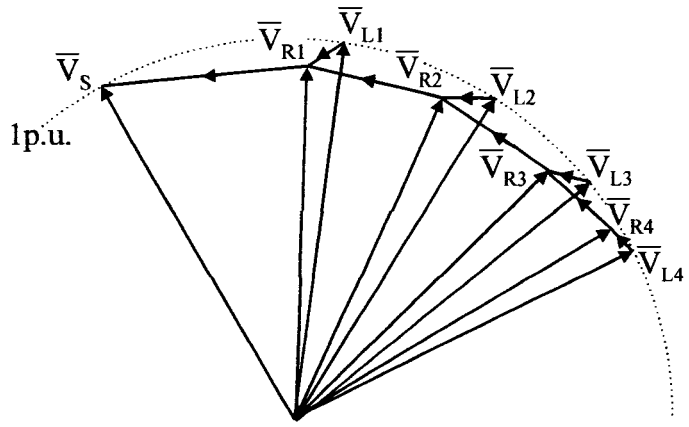

Figure 75 Steady-State Voltage Phasors

7.4.1.2 Comparisons of Two VS Schemes

The 2nd and 4th columns of Table V summarize the reactive powers $\mathbf{Q_{iD}}$ of the SVCs and the complex powers $|\mathbf{S_{iD}}|$ of the transformers at each node when VS is provided on the distribution buses. The quantities are per unitized to the surge impedance loading of the 230 kV line (P_{SIL}=211 MW).

The total requirements in Mvar and MVA are listed in the last row. For comparison, the reactive powers $\mathbf{Q_{iHV}}$ and the complex powers $|\mathbf{S_{iHV}}|$ of the transformers for SVCs on the transmission buses are listed in the 3rd and 5th columns. From the bottom row, one sees the savings coming from the step-up transformers in the first 3 nodes. The reduction of Q

(603-494) Mvar looks small but in terms of dollars capacitive Mvar is more costly than transformer MVA. The numbers in Table V do not include the requirements of (N-1) reliability.

Table V

High Voltage Bus vs Distribution bus for the test system from Fig.74

node i	Q_{iD} reactive power	Q_{iHV} reactive power	$\|S_{iD}\|$ transformer	$\|S_{iHV}\|$ transformer
1	0.904 pu	1.515 pu	1.311 pu	2.465 pu
2	0.756 pu	0.818 pu	1.214 pu	1.768 pu
3	0.429 pu	0.529 pu	1.042 pu	1.479 pu
4	0.251 pu	NIL	0.983 pu	0.95 pu
Σ	2.341 pu	2.862 pu	4.549	6.662 pu
Σ	494 Mvar	603 Mvar	959 MVA	1405 MVA

7.4.1.3 Comparison of Transmission Line Losses

As $|\mathbf{V_{Ri}}| < 1.0$ for every node in Fig. 75, it is expected that the current $\mathbf{I_i}$ in every transmission line section is higher than for the case of transmission bus VS which regulates the node voltage at $\mathbf{V_{Ri}}=1.0$. As transmission line power loss is proportional to $|\mathbf{I_i}|^2$, the power loss is expected to be higher for distribution bus VS than transmission bus VS. Fig. 76 plots the ratio of total transmission power loss (distribution bus VS)/(transmission bus VS) as a function of the real power loading at every bus.

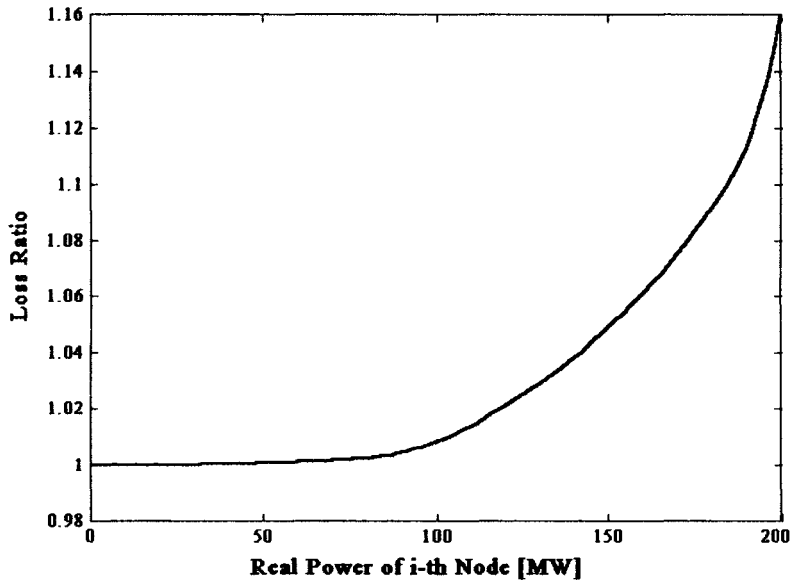

Figure 76 Ratio (distribution bus VS)/(transmission bus VS) of Transmission Line Losses

Up to 100 MW, the difference is negligible. At the peak loading of 200 MW, the increase is only around 16%. From the cost viewpoint, it is the difference in energy loss (time integral of power) which is significant. The peak load occurs only for a small fraction of the time.

7.4.1.4 Comparison of the Cost

The comparison of cost is shown in Table VI. The 2nd and 5th columns list the inductive Mvar/ capacitive Mvar requirements of the 4 nodes for distribution and transmission bus compensation respectively. The cost of thyristor switching is estimated as \$40/kVAR on the distribution level and 50 \$/kVAR at transmission level. The difference in the cost is due to the transformer that is assumed to be 20% of equipment cost [19]. Thus, the entry for node 1 under $\mathbf{Q_{iD}}$ SVC is \$10.5million=\$40x(65+195)x10^3. For comparison the same cost for high voltage bus compensation under $\mathbf{Q_{iHV}}$ is \$22m.

Table VI

Cost Estimate (SVC consisting of TCR -TSC)

node i	Q_{iD} [Mvar]	Q_{iD} [$ million]		Q_{iHV} [Mvar]	Q_{iHV} [$ million]	
		SVC	N-1		SVC	N-1
1	-65/+195	10.5	3.5	-110/+330	22	22
2	-55/+160	8.6	2.87	-60/+180	12	12
3	-30/+90	4.8	1.6	-40/+120	8	8
4	-20/+60	3.2	1.1	NIL	NIL	NIL
Σ	-170 +505	27	9	-210 +630	42	42

The 4th and 7th columns list the cost of providing (N-1) reliability. As shown in Fig. 32, each node is served by 4 SVCs. The $3.5m represents $10.5/(N-1) where N=4. Applying the (N-1) reliability practice, the authors have used N=2 for transmission voltage bus compensation. The $22m comes from $22m/(N-1) where N=2. From the bottom lines of the tables, the cost savings are $36m=$(42+42-27-9)m. Estimation figures such as $40/kvar and $50/kvar include the cost of transformers and auxiliary equipment so that the transformer savings listed in Table V become lost in this rough estimation practice. In addition, the savings in not having to use tap changers for distribution voltage regulation have not been factored in.

7.5 Fault Studies

It is necessary to show that the system of Fig.74 can survive a three-phase-to ground fault and on clearing the fault, the system is able to return to the steady-state solution that existed prior to the occurrence of the fault. Such studies are conducted using digital simulations.

7.5.1 Model of Static Var Compensator (SVC)

The distribution VS in each distribution voltage bus in Fig. 74 consists of a Thyristor Controlled Reactor - Thyristor Switched Capacitors (TCR-TSC) and switched/fixed capacitors. The capacitors are Y connected, with the neutral solidly grounded. The total amount of fixed/switched capacitors is: 500 Mvar at bus #1, 250 Mvar at the bus #2, 200 Mvar at bus #3 and 150 Mvar at bus #4. The TCRs provide for dynamic voltage control. They are delta connected. Fixed capacitors are tuned to filter out the 5th and 7th harmonics of the TCR. The simulations made use of the default model of the SVC of HYPERSIM. A description of the model is given in [72].

7.5.2 Load Models

A variety of load combinations have been studied but there is enough space in this chapter to present only one of them. This consists of a combination of:

(i) a resistive load to represent heating load

(ii) induction motor load representing industrial and/or agricultural load,

(iii) dynamic load model to represent combination of commercial and residential load

Detail descriptions of the load models are given in [72].

The dynamic load model represents reactive power and real power of the load at any instant of time as functions of voltage level according to (7.1) and (7.2) [73,74]

$$P = P_0\left(\frac{V}{V_0}\right)^{np}\left[\frac{1+T_{P1}S}{1+T_{P2}S}\right] \tag{7.1}$$

$$Q = Q_0\left(\frac{V}{V_0}\right)^{nq}\left[\frac{1+T_{Q1}S}{1+T_{Q2}S}\right] \tag{7.2}$$

where P_0 and Q_0 are respectively the nominal active and reactive power, V_0 is nominal voltage and *np* and *nq* are variation coefficients of active end reactive power as a function of the voltage. The model is valid only for fundamental frequency between 50 and 70 Hz and for voltage level greater than 0.7 p.u. If the voltage drops below 0.7 p.u., the model behaves as constant impedance. Detailed model description is given in [72].

7.5.3 Transmission Line Model

In Fig. 70 and 72, the transmission line sections have been represented by inductive reactances jX_i, i=1,2,..N. Since the model based on the more accurate telegraph equations is available in the simulation software, it is used in the simulations. The data of the distributed parameter model are:

z, impedance per km (z = 0.3 ohm/km)

y, admittance per km ($y = 5x10^{-6}$ S/km)

r, resistance per km (r = 0.04 ohm/km)

Based on the distributed model, the characteristic impedance of the line is $Z_S = \sqrt{z / y} = 250\,ohms$ and the Surge Impedance Loading (SIL) of the line $P_{SIL} = \frac{|\overline{V}_S|^2}{Z_S}$ is 211 MW. The line in use is single circuit consisting of two bundled conductors.

7.5.4 Simulation Results

7.5.4.1 Three Phase to Ground Fault

The simulation test consists of introducing a three-phase-to-ground fault in any portion of the transmission line. The composition of the load at Nodes #2 to #4 is: (i) Resistive

Load-- 30% , (ii) Induction Motor Load--35 %., (iii) Dynamic Load--35%. Load parameters are taken from [1]. To reflect the fact that industries are nearer to generation sources, the composition of the load at Node #1 is: (i) Resistive Load-- 20% , (ii) Induction Motor Load--65 %., (iii) Dynamic Load--15%.

The objectives of the simulations are: (i) to be assured that the local controls of the distributed SVCs operate harmoniously in the restoration; (ii) to ascertain that there is no voltage instability due to induction motors dynamics following the clearance of the fault [75,76].

Upon detection of the three-phase-to-ground fault, the "upstream" circuit breaker CB opens within 100 ms. Because of the great amount of fixed/switched capacitors connected across the induction motor loads, the minimum re-closing time to allow for cooling of the plasma to avoid re-striking based on the formula:

$$t = 10.5 + \frac{kV}{34.5} cycle \tag{7.3}$$

has been found to be insufficient. The formula is taken from [77]. By monitoring and waiting for the fault currents to fall to zero, the safe re-closing time is found to be 550 ms.

7.5.4.2 Results

The three-phase-to-ground fault is assumed to occur in the first transmission line section, between V_S and V_{R1} in Fig. 74. The fault is triggered at 2.1 s in Fig. 77 -80. The Circuit Breaker CB_1 opens the line at 2.16 s. All the four load centers lose the ac voltage supply V_S immediately. The Circuit Breaker re-closes in 2.71 s to allow for the 550 ms safe re-closing time. Some of the simulation results are shown in Fig.77 to 80.

Fig.77 is a record of the distribution bus voltages. Although Circuit Breaker CB_1 is open for 550 ms after the fault, the distribution bus voltages do not drop to zero immediately because of the self-excitation between the compensation capacitors and the induction motors. Upon re-closing of Circuit Breaker CB_1, the bus voltages recover, the recovery time being slowest at the remote #4 bus.

Fig. 78 shows the rms current of each load center. This current is the sum of the currents from the resistive load, the induction motor load and the dynamic load.

Fig. 79 shows the induction motor component of the load current. The large over-currents are not sources of concern because the current protection would have tripped the induction motors if their safe heating limits have been exceeded. The tripping would speed the voltage recovery.

The motor speeds in Fig. 80 are records of the deceleration upon the opening of Circuit Breaker CB_1 and the acceleration following the re-closing of CB_1. Since node #4 is separated from the infinite bus by the largest line impedance, its voltage takes the longest to recover as shown in Fig. 77. As a result, as shown in Fig. 80, the induction motor of #4 bus takes the longest time to recover rated speed.

The tests are conducted to simulate the worst case scenario when all the induction motors do not have under-voltage protection. This test shows that there is no voltage collapse and voltage recovery is accomplished by the SVCs on the distribution buses operating, harmoniously without conflict, under local control.

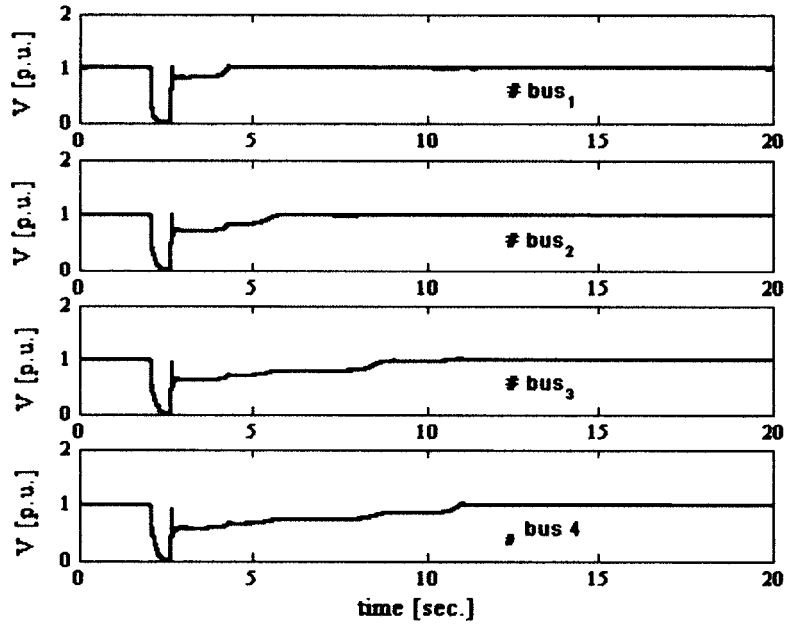

Figure 77 Load Bus Voltages (RMS) at Load Centers

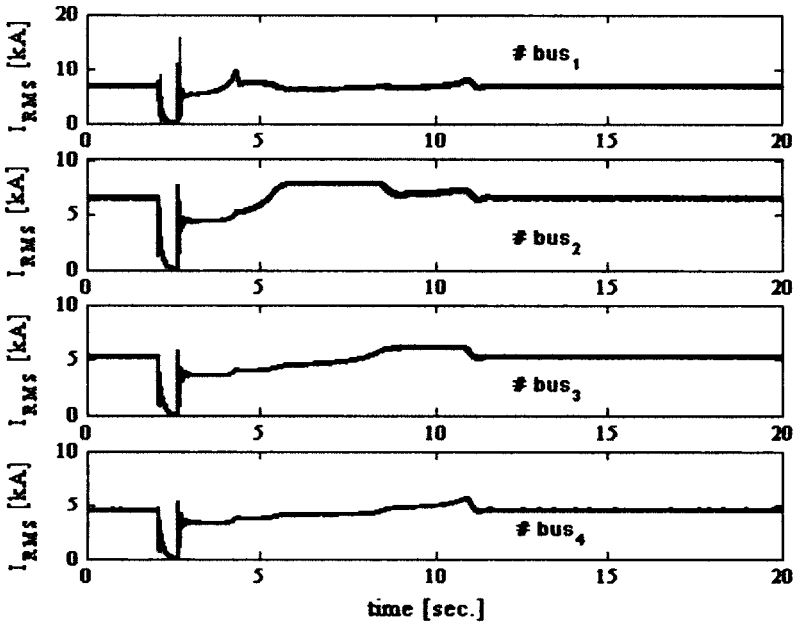

Figure 78 Currents (RMS) to the load centers

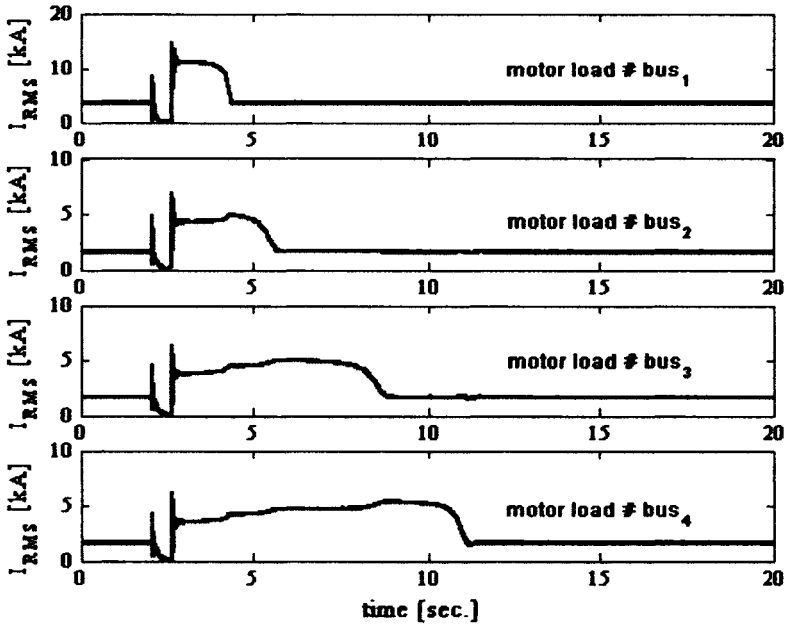

Figure 79 Currents (RMS) drawn by induction motors.

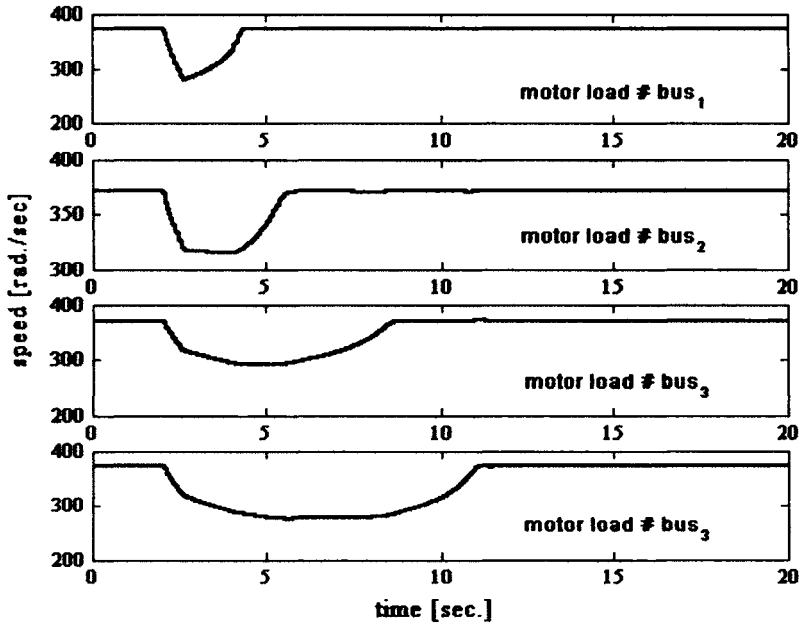

Figure 80 Speeds of Induction Motors at Load Centers. The motors slow down during fault and accelerate after fault clearing and line reclosing. Reclosing time used is 550 ms

7.5.4.3 Requirement of Longer Re-Closing Time

As capacitors, which provide voltage support, can self- excite the induction motors to feed the fault currents, a longer re-closing time has been found to be necessary. Otherwise, the system survives the short circuit fault.

7.6. Conclusion

This chapter has demonstrated that voltage support of a long transmission line, with load centers spaced along the line, can be provided on the distribution buses. The radial line has been chosen to demonstrate the concept because the radial system gives a clear insight into the proposed approach. It should be possible to extend the concept to mesh networks but more studies are required to confirm this. The benefits emerging from the proposed concept over the traditional voltage support at the transmission buses are: i) elimination of the step-up transformer for coupling the VS system to the transmission buses, ii) lower var requirements iii) lower cost in providing (N-1) reliability and iv) elimination of LTC transformers for distribution voltages regulation.

As voltage support on the distribution buses is a valuable alternative to traditional voltage support at the transmission buses, it offers distribution system engineers the opportunity to provide voltage support of transmission systems as ancillary service.

As some utilities rely on intentional, distribution voltage reductions during emergencies to obtain load reduction and transmission system relief, the proposed concept can lead to potential conflict between transmission and distribution system requirements. In this case, proper coordination of control would be required.

CHAPTER 8

CONCLUSIONS AND FUTURE WORK

8.1 Conclusion

In this thesis a new concept has been proposed, developed and analyzed. The concept is termed "Transmission lines voltage support decentralization". It consists of removing voltage support of transmission lines from transmission to distribution buses regulating, dynamically, distribution levels voltages only using larger number of smaller sized Static Var Systems.

The concrete conclusions of this work can be summarized as following:

1. Dynamic voltage support of transmission lines can be provided, economically, by regulating dynamically distribution levels voltages only, without close control of transmission voltages.
2. If distribution level voltages are regulated dynamically, the voltage quality offered by utility to consumers is improved, diminishing possibility of voltage collapse due to asynchronous motor instabilities.
3. LTC transformers regulating distribution level voltages are not required to control distribution level voltages. Knowing that LTC transformer can lead to voltage collapse and that LTC transformers require maintenance, their elimination can help improve economics of power system.
4. As power electronic industry targets higher voltage ratings of power electronic components, SVSs can be connected directly to distribution level voltages without using step-up transformers, decreasing overall cost of equipment. The step-up transformer can be up to 20% of overall installation cost of SVS.

5. Step up transformer is conceited in series with SVS. Its loss lead to loss of overall SVS. Elimination of step-up transformer for coupling of SVS with power system increases reliability of the power system because a serial element is eliminated.
6. Elimination of step-up transformer for coupling of SVS with power system eliminate needs for spare transformers to provide for the reliability.
7. When voltage support provided with large number of smaller sized SVSs on distribution level the loss of one distribution SVS affects power system less then loss of one bulk SVS on transmission level.
8. When voltage support provided on distribution level, line losses are, in most cases, lower.
9. The VAr requirements for distribution voltage regulation are lower then for transmission voltages regulation.
10. As voltage support on the distribution buses is a valuable alternative to traditional voltage support at the transmission buses, it offers distribution system engineers the opportunity to provide voltage support of transmission systems as ancillary service.
11. That voltage support of a long transmission line, with load centers spaced along the line, can be provided on the distribution buses.

8.2 Recommendations for Future Work

In this work detailed dynamic simulation has been used to evaluate performance of proposed concept under different transients. However, the lines longer then 400 km are in the region of small-signal stability limitation and not in region of voltage drop limitation. In this case SVSs installed on transmission level are traditionally used to mitigate electromagnetic oscillations and to enhance stability of the system. This subject has not been treated in this work and should be treated in the future in order to demonstrate whether the concept proposed in this work can be used to enhance small signal stability performance of very long lines. In the next step, the eigenvalue analysis of distributed,

distribution voltage support should be done to evaluate analytically small signal stability performance.

In chapter VI the original way of calculating reactive power requirement for voltage regulation are deduced. The author is of the opinion that this equation can be used to monitor proximity to voltage collapse. Further study are required to confirm.

Final proposal for the future work addresses voltage issues in modern power systems, under the deregulation and with embedded distributed generation. Based on the state of the current development and presented work in the area of voltage stability and power electronic converters, the proposal for the future work addresses application of power electronic converters in mitigation of voltage problems, while, the same, applied for incorporation of distributed generation sources into the power grid. As distributed generation sources are scattered around the main grid and embedded into power system on distribution level, the installation of large number of smaller sized power electronic converter enabling their smooth integration into power grid is required. The same can be used to provide efficient dynamic voltage control on distribution level and to provide, indirectly, transmission voltage support.

The main objective of this proposal for the future work is therefore *voltage control on distribution level and prevention of short term and long term voltage instabilities, that can lead to partial or complete black outs, using SVCs, power electronic converters based SVSs, applied for interface between power grid and distributed generation sources.*

The realization of the proposal can include:

- Development of customized, coordinated control strategies together with customized, multifunctional power electronic interface for integration of distributed energy sources enabling efficient voltage control.

- Investigating the impact of distribution level voltage control on transmission voltages when distributed generation sources are imbedded into the grid on distribution level using large number of smaller sized SVSs as interface.

The feasibility studies that can be undertaken using standard simulation packages (MATLAB) and advanced, state of the art, tools for real time simulation of power system (HYPERSIM) developed by IREQ, Hydro-Quebec's research institute. Concept validated by simulation can be prototyped in laboratory using DSP and advanced power electronic switches (IGBT).

These recommendations for the future work would make contributions to the *Environment and Sustainable Development*. The benefits that can emerge following the recommendations above are multilateral: better management of existing power system, power quality improvement, increased transmission capacity while allowing smooth integration of distributed generation sources and acquisition of new expertise and technique future development and planning of power system will be based on.

APPENDIX A

PRINCIPAL SIMULATION PARAMETERS

The principal simulation parameters are listed as:

Generator

S_B=10000 MVA, P_B=8340 W, V_B=13.8 kV, f_B=60 Hz, R_a=0.002 p.u., X_l=0.15 p.u., X_d=1.2 p.u., X_q=0.7 p.u., X'_d=0.315 p.u., X'_q=0.65 p.u., X''_d=0.2 p.u., X''_q=0.22 p.u., T_{d0}'=8 s, T_{q0}'=8 s T_{d0}''=0.07 s, T_{q0}''=0.065 s.

Hydraulic turbine

H = 4.112, K_d = 0, T_W = 1.3, T_{g0} = 0.01, β = -0.45, $\omega_{min.}$= 0.5 p.u., $\omega_{max.}$= 1.5 p.u.

Speed governor system

σ = 0.05, δ = 0.4, K_g = 1, T_1 = 0, T_2 = 0.1, T_s = 0.3, T_t = 5.2, T_{a1} = 0, T_{a2} = 1, T_p = 0.001, T_{watt} = 0.05, x_{min} = 0.005, x_{max} = 1.05, ν_{xmin} = -0.15, ν_{xmax} = 0.15.

Field excitation system

K_a = 200, K_f = 0, K_p = 12.3, T_a = 0.01, T_f = 1, T_r = 0.02, $V_{rmin.}$= -12.7, $V_{rmax..}$= 12.3, $V_{tmin.}$= 0.1, $V_{tmax..}$= 100.

Power system stabilizer

K_{ag} = 1, K_{ap} = 1, K_s = 5.289, T_1 = 0.01, T_2 = 0.66, T_3 = 0.001, T_4 = 2, T_5 = 1, T_6 = 0.001, T_{ag} = 0.0015, T_{ap} = 0.0015, T_{w1} = 1.2, T_{w2} = 0.072, V_{smin} = -0.1, V_{smax} = 0.1

Transformers

S_B=10000 MVA, 13.8/735 kV, 122.5/735 kV, Δ/Yg connection, R_1 = 0.002 p.u., X_1 = 0.16 p.u., R_2 = 0.002 p.u., X_2 = 0.16 p.u.

Transmission line

Length = 400 km, r = 0.0147 Ω/km, l = 0.0009 H/km, c = 1.308 10^{-8} F/km.

APPENDIX B

REACTIVE POWER REQUIREMENT EVALUATION

Voltage Support Provided by Lumped SVS on Transmission Side

Application of Kirchhoff's laws on circuit in Fig.44 b) with objective to keep transmission voltage $\mathbf{V_R}$ at 1pu:

Assuming constant power, unity power factor load, total power supplied to load can be written as:

$P_{TOTAL} = KP = \bar{V}_L \bar{I}_L$

where

K is number of incoming transmission lines

P is power transferred over the one line

$P_{max} = MP_{SIL}$

$\mathbf{V_L}$ is distribution side (load) voltage

$\mathbf{I_L}$ is load current

Applying Kirchhoff's laws on circuits in Fig. 44.b)

$$\bar{V}_R = j\frac{X_T}{MK}\bar{I}_L + \bar{V}_L \tag{B.1}$$

Writing,

$$\left|\bar{V}_R\right|^2 = \left|\frac{X_T}{MK}\frac{KP}{\left|\bar{V}_R\right|}\right|^2 + \left|\bar{V}_R\right|^2 \tag{B.2}$$

yields

$$\left|\bar{V}_L\right| = \sqrt{\frac{\left|\bar{V}_R\right|^2 M^2 + \sqrt{\left|\bar{V}_R\right|^4 M^4 - 4M^2P^2X_T^2}}{2M^2}} \tag{B.3}$$

The load resistance is given by:

$$R = \frac{|V|^2}{P_{TOTAL}} = \frac{\left|\bar{V}_L\right|^2}{KP} = \frac{\left|\bar{V}_R\right|^2 M^2 + \sqrt{\left|\bar{V}_R\right|^4 M^4 - 4M^2P^2X_T^2}}{2M^2KP} \tag{B.4}$$

Load current is:

$$\bar{I}_L = \frac{\bar{V}_R}{R + j\frac{X_T}{MK}} = \frac{2M^2 PK\bar{V}_T}{\left|\bar{V}_R\right|^2 M^2 + \sqrt{\left|\bar{V}_R\right|^4 M^4 - 4M^2 P^2 X_T^2} + j2MPX_T} \tag{B.5}$$

The transmission line current is:

$$K\bar{I} = \bar{V}_R \frac{K\bar{Y}'}{2} + \bar{I}_{Cl} + \bar{I}_L \tag{B.6}$$

$$\bar{V}_S = K\bar{I}\frac{\bar{Z}'}{K} + \bar{V}_R \tag{B.7}$$

Substituting from (B.1) to (B.6) at (B.7) and choosing $\bar{V}_R = 1e^{j0^\circ}$ and knowing that compensating current is injected in quadrature with $\mathbf{V_R}$, $\bar{I}_{Cl} = \pm jI_{Cl}$:

$$\bar{V}_S = 1 - \sin(\beta l)tn\left(\frac{\beta l}{2}\right) \mp \sin(\beta l)\frac{I_{Cl}}{K} + \frac{2P^2 X_T \sin(\beta l)}{M + \sqrt{M^2 - 4P^2 X_T^2}} + jP\sin(\beta l) \tag{B.8}$$

Knowing that $|\mathbf{V_S}|$ =1p.u.

$$1 = \left(1 - \sin(\beta l)tn\left(\frac{\beta l}{2}\right) \mp \sin(\beta l)\frac{I_{Cl}}{K} + \frac{2P^2 X_T \sin(\beta l)}{M + \sqrt{M^2 - 4P^2 X_T^2}}\right)^2 + \left(P\sin(\beta l)\right)^2 \tag{B.9}$$

(B.9) finally yields to

$$I_{Cl} = K\left(\frac{1}{\sin\beta l} + \frac{2\bar{P}^2 \bar{X}_T}{M + \sqrt{M^2 - 4P^2 X_T^2}} - tn\left(\frac{\beta}{2}l\right) - \frac{\sqrt{1 - \left(P\sin(\beta l)\right)^2}}{\sin\beta l}\right) \tag{B.10}$$

Voltage Support Provided by Distributed Distribution SVS

Application of Kirchhoff's laws on circuit in Fig.44 a) with objective to keep distribution side voltage at $|\mathbf{V_L}|$ p.u:

$$\bar{V}_S = K\bar{I}\frac{\bar{Z}'}{K} + \bar{V}_R \tag{B.11}$$

$$\bar{V}_R = j\frac{X_T}{K}\left(\bar{I}_{Cd} + \bar{I}_L\right) + \bar{V}_L \tag{B.12}$$

$$\bar{I}_L = \frac{KP}{\bar{V}_L} \tag{B.13}$$

$$K\bar{I} = \bar{V}_R\frac{K\bar{Y}'}{2} + \bar{I}_{Cd} + \bar{I}_L \tag{B.14}$$

Distribution voltage $\mathbf{V_L}$ is chosen as reference $\bar{V}_L = |\bar{V}_L|e^{j0^o}\,pu$ .Knowing that $X_T = 0.1\,pu$, $|\bar{V}_S| = 1\,pu$ and the compensating current $\mathbf{I_{Cd}}$ is injected in quadrature with supported voltage $\mathbf{V_L}$ so $\bar{I}_{Cd} = \pm jI_{Cd}$. Combining (B.11) to (B.14) it can be written

$$\bar{V}_R = j\frac{X_T}{KM}\left(\pm jI_{Cd} + \frac{KP}{\bar{V}_D}\right) + \bar{V}_L \tag{B.15}$$

Substituting

$$\begin{aligned}\bar{V}_S = {} & \pm\sin(\beta l)tn\left(\frac{\beta l}{2}\right)\frac{X_T I_{Cd}}{KM} \mp \frac{\sin(\beta l)}{K}I_{Cd} - |\bar{V}_L|\sin(\beta l)tn\left(\frac{\beta l}{2}\right) \\ & \mp\frac{X_T I_{Cd}}{K} + |\bar{V}_L| - j\left(\sin(\beta l)tn\left(\frac{\beta l}{2}\right)\frac{X_T P}{M|\bar{V}_L|} - \frac{P\sin(\beta l)}{|\bar{V}_L|} - \frac{X_T P}{M|\bar{V}_L|}\right)\end{aligned} \tag{B.16}$$

Knowing that $|\mathbf{V_S}|$ =1p.u.

$$1=\left[\left|\bar{V}_L\right|\left(1-\sin(\beta l)tn\left(\frac{\beta l}{2}\right)\right)\pm\frac{I_{Cd}}{K}\left(\sin(\beta l)tn\left(\frac{\beta l}{2}\right)\frac{X_T}{M}-\sin(\beta l)-\frac{X_T}{M}\right)\right]^2 + \left(\sin(\beta l)tn\left(\frac{\beta l}{2}\right)\frac{X_T P}{M\left|\bar{V}_L\right|}-\frac{P\sin(\beta l)}{\left|\bar{V}_L\right|}-\frac{X_T P}{M\left|\bar{V}_L\right|}\right)^2 \quad \text{(B.17)}$$

The current of distributed SVSs needed to regulate $\mathbf{V_L}$ is given by (B.18):

$$I_{Cd}=K\frac{\left|\bar{V}_L\right|\left(1-\sin(\beta l)tn\left(\frac{\beta l}{2}\right)\right)}{\sin(\beta l)+\frac{X_T}{M}-\sin(\beta l)tn\left(\frac{\beta l}{2}\right)\frac{X_T}{M}}-K\frac{\sqrt{1-\frac{P^2}{\left|\bar{V}_L\right|^2}\left(\sin(\beta l)tn\left(\frac{\beta l}{2}\right)\frac{X_T}{M}-\sin(\beta l)-\frac{X_T}{M}\right)^2}}{\sin(\beta l)+\frac{X_T}{M}-\sin(\beta l)tn\left(\frac{\beta l}{2}\right)\frac{X_T}{M}} \quad \text{(B.18)}$$

APPENDIX C

THE PRINCIPAL PARAMETERS OF TEST SYSTEM

The principal simulation parameters are listed as:

A. Transmission Line

R = 0.0044 Ω/km, L=0.001 H/km, C=1.167e-08 F/km

B. Power Transformers

400 MVA, 315/25 kV, YgΔ, R_1=0.0008 p.u.,X_1=0.12 p.u. R_2=0.0008 p.u., X_2=0.12 p.u.

C. Load

1) Bus1

a) Dynamic Load

P_o = 100 MW, Q_o = 48 MVAr, np =1,nq=3,kp=1,kq=-2.8

b) Motor Load

Small Industrial Motors: 60 MW

LF = 0.6, H =0.7, R_s = 0.19 Ω, X_s = 0.625 Ω, X_m = 20 Ω, R_r = 0.1125 Ω, X_r = 1.125 Ω.

Load Torque:

ω[rad/s]	0	95	188	282.	377
T[kNm]	0	10	39.8	92.7	160

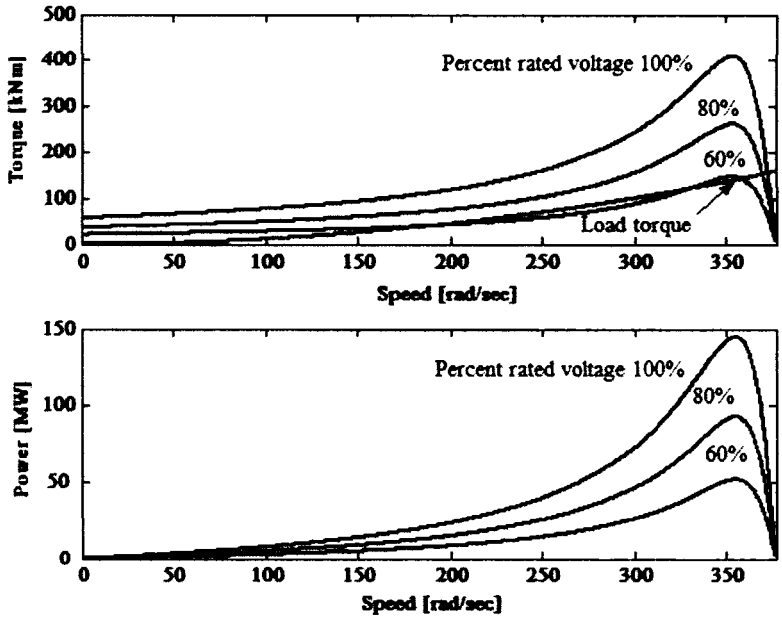

Fig.C1. Small industrial motors equivalent S=100 MVA

2) Bus2

a) Dynamic Load

P_o = 130 MW, Q_o = 80 MVAr, np=1.4, nq=1.4, kp=5.6, kq=4.2.

b) Motor Load

Agricultural water pumps: 150 MW

LF = 0.7, H =0.8, R_s = 0.07 Ω, X_s = 0.255 Ω, X_m = 9.28 Ω, R_r = 0.046 Ω, X_r = 0.5 Ω.

Load Torque:

ω[rad/sec]	0	95	188	282	377
T [kNm]	0	25.3	99.8	224	400

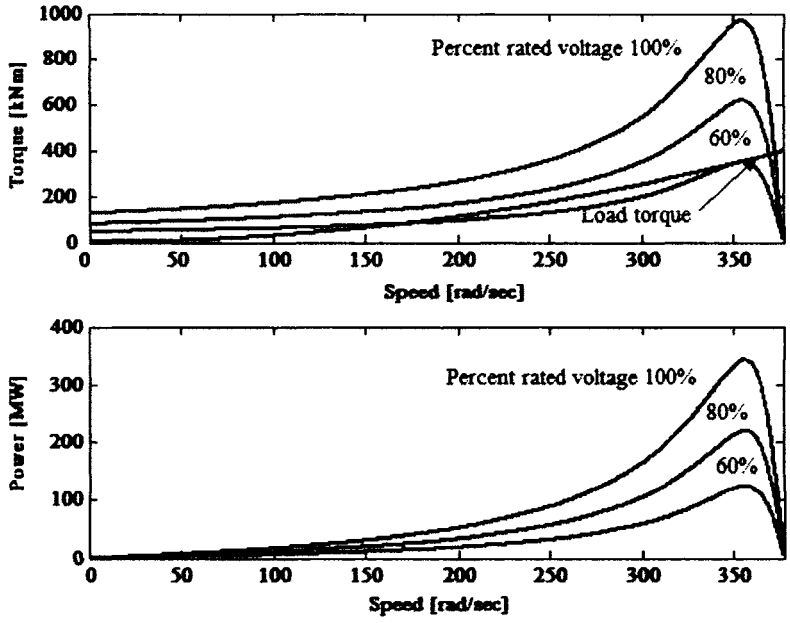

Fig.C2.Agricultural water pump

3) Bus3

a) Dynamic Load

P_o = 120 MW, Q_o = 55 MVAr, np =1.2,nq=2.8,kp=0,kq=0

b) Motor Load

Large Industrial Motors: 80 MW

LF = 0.8, H =1.5, R_s = 0.08 Ω, X_s = 0.42 Ω, X_m = 23.75 Ω, R_r = 0.056 Ω, X_r = 1.06 Ω.

Load Torque:

ω[rad/s]	0	95	188	282	377
T[kNm]	0	16.5	53.3	120	213

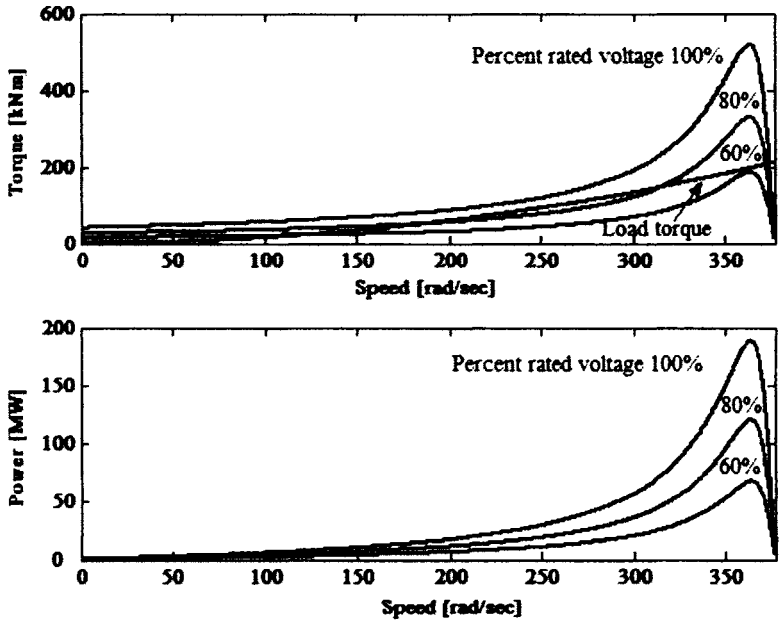

Fig. C3. Large industrial motors equivalent S=100 MVA

APPENDIX D

STEADY STATE SOLUTION FOR TEST SYSTEM

Case I

Voltage support is provided with three SVS keeping voltages V_{R1}, V_{R2} and V_{R2} at 1p.u, SVSs are connected on transmission level as shown on Fig.D.1 Compensating currents are in quadrature with supported voltages

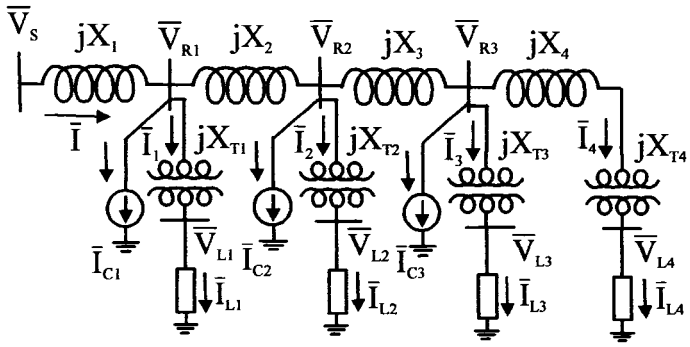

Fig.D.1

Compensating current can be found explicitly. Applying (6.19) it can be written:

$$I_{C1} = \frac{|V_{R1}| - |V_S|\cos\delta_1}{X_1} + \frac{|V_{R1}| - |V_{L1}|\cos\theta_1}{X_{T1}} + \frac{|V_{R1}| - |V_{R2}|\cos\delta_2}{X_2} \tag{D.1}$$

$$I_{C2} = \frac{|V_{R2}| - |V_{R1}|\cos\delta_2}{X_2} + \frac{|V_{R2}| - |V_{R3}|\cos\delta_3}{X_3} + \frac{|V_{R2}| - |V_{L2}|\cos\theta_2}{X_{T2}} \tag{D.2}$$

$$I_{C3} = \frac{|V_{R3}| - |V_{R2}|\cos\delta_3}{X_3} + \frac{|V_{R3}| - |V_{L4}|\cos\delta_4}{X_4 + X_{T4}} + \frac{|V_{R3}| - |V_{L3}|\cos\theta_3}{X_{T3}} \tag{D.3}$$

Knowing that $|\mathbf{V_S}| = |\mathbf{V_{R1}}| = |\mathbf{V_{R2}}| = |\mathbf{V_{R3}}| =$ 1p.u. and applying (6.15) load voltages can be calculated as(D.4) to (D.7):

$$|\overline{V}_{L1}| = \sqrt{\frac{|\overline{V}_{R1}|^2 + \sqrt{|\overline{V}_{R1}|^4 - 4(X_{T1}P_1)^2}}{2}} \tag{D.4}$$

$$|\bar{V}_{L2}| = \sqrt{\frac{|\bar{V}_{R2}|^2 + \sqrt{|\bar{V}_{R2}|^4 - 4(X_{T2}P_2)^2}}{2}} \tag{D.5}$$

$$|\bar{V}_{L3}| = \sqrt{\frac{|\bar{V}_{R3}|^2 + \sqrt{|\bar{V}_{R3}|^4 - 4(X_{T3}P_3)^2}}{2}} \tag{D.6}$$

$$|\bar{V}_{L4}| = \sqrt{\frac{|\bar{V}_{R3}|^2 + \sqrt{|\bar{V}_{R3}|^4 - 4((X_{T4} + X_4)P_4)^2}}{2}} \tag{D.7}$$

The angles δ_i between transmission level voltages V_{Ri} and $V_{R(i-1)}$, and the angles θi between load voltages V_{Li} and transmission level voltages V_{Ri} are given with(D.8) to (D.12):

$$\sin\delta_1 = \frac{PX_1}{|V_S||V_{R1}|} \Rightarrow \cos\delta_1 = \frac{\sqrt{|V_S|^2|V_{R1}|^2 - P^2X_1^2}}{|V_S||V_{R1}|} \tag{D.8}$$

$$\sin\delta_2 = \frac{(P - P_1)X_2}{|V_{R2}||V_{R1}|} \Rightarrow \cos\delta_2 = \frac{\sqrt{|V_{R2}|^2|V_{R1}|^2 - (P - P_1)^2X_2^2}}{|V_{R2}||V_{R1}|} \tag{D.9}$$

$$\sin\delta_3 = \frac{(P_3 + P_4)X_3}{|V_{R2}||V_{R3}|} \Rightarrow \cos\delta_2 = \frac{\sqrt{|V_{R2}|^2|V_{R3}|^2 - (P_3 + P_4)^2X_3^2}}{|V_{R2}||V_{R3}|} \tag{D.10}$$

$$\sin\delta_4 = \frac{P_4(X_4 + X_{T4})}{|V_{L4}||V_{R3}|} \Rightarrow \cos\delta_4 = \frac{\sqrt{|V_{L4}|^2|V_{R3}|^2 - P_4^2(X_4 + X_{T4})^2}}{|V_{L4}||V_{R3}|} \tag{D.11}$$

$$\cos\theta_1 = \frac{|V_{L1}|}{|V_{R1}|}; \cos\theta_2 = \frac{|V_{L2}|}{|V_{R2}|}; \cos\theta_3 = \frac{|V_{L3}|}{|V_{R3}|} \tag{D.12}$$

The alternative way of calculation reactive need is from phasor.

This is the case when voltages V_{Ri} are kept at 1 p.u. with SVSs that are connected with their own transformer at voltages they support. It means that the current drawn bu SVS is in quadrature with voltage where it is connected.

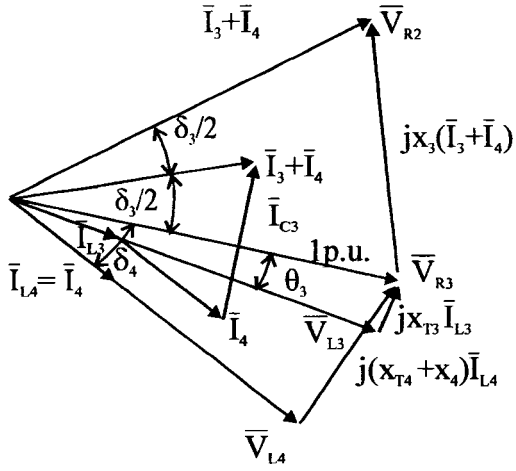

Fig.D.2 Phasor diagram showing relations among the voltages and currents from voltage V_{R2} to $V_{L4}$for circuit from Fig.D.1.

From Pythagoras theorem to the right angle triangle formed by V_{R3},V_{L4} and $j(X_{T4}+ X_4)I_{L4}$

$$\left|(X_{T4}+X_4)\right|\bar{I}_{L4}\|^2+|\bar{V}_{L4}|^2=|\bar{V}_{R3}|^2 \text{ and } P_4=|\bar{I}_{L4}\|\bar{V}_{L4}| \tag{D.13}$$

$$|\bar{V}_{L4}|=\sqrt{\frac{1+\sqrt{1-4\left((X_{T4}+X_4)P_4\right)^2}}{2}} \tag{D.14}$$

$$P_4=\frac{|\bar{V}_{R3}\|\bar{V}_{L4}|}{X_{T4}+X_4}\sin\delta_4 \tag{D.15}$$

$$\delta_4=\arcsin\frac{P_4(X_4+X_{T4})}{|\bar{V}_{L4}|} \tag{D.16}$$

$$P_3 + P_4 = \frac{|\bar{V}_{R3}||\bar{V}_{R4}|}{X_3}\sin\delta_3 \Rightarrow \delta_3 = \arcsin\left((P_3 + P_4)X_3\right),\ |\bar{I}_{L4}| = |\bar{I}_4| = \frac{P_4}{|\bar{V}_{L4}|} \tag{D.17}$$

From cosine theorem (D.18):

$$|(I_3 + I_4)X_3| = \sqrt{|\bar{V}_{R3}|^2 + |\bar{V}_{R2}|^2 - 2|\bar{V}_{R2}||\bar{V}_{R3}|\cos\delta_3} \Rightarrow |I_3 + I_4| = \sqrt{2}\frac{\sqrt{1-\cos\delta_3}}{X_3} \tag{D.18}$$

$$\frac{|\bar{V}_{L3}|}{|\bar{V}_{R3}|} = \cos\theta_3 = \ |\bar{V}_{L3}| \tag{D.19}$$

$$|\bar{I}_{L3}| = \frac{P_3}{|\bar{V}_{L3}|} \tag{D.20}$$

Reactive power supplied by SVS_3 is (D.21):

$$Q_3 = [\bar{V}_{R3}]|\bar{I}_{C3}| = |I_3 + I_4|\sin\left(\frac{\delta_3}{2}\right) + |I_4|\sin\delta_4 + |I_{L3}|\sin\theta_3 \tag{D.21}$$

Remarks:

The reactive power Q_3 can be decomposed into three terms: first term provide half reactive needs for line between voltages $\mathbf{V_2}$ and $\mathbf{V_3}$, second term represent reactive power needed for power factor correction of the load current $\mathbf{I_{L4}}$ and third is for power factor correction of load current $\mathbf{I_{L3}}$. Physicly, it can be stated that on the bus where compensator Q3 is connected (voltage $\mathbf{V_3}$) the compensator adjust reactive power so that reactive power absorbed by the line and produced by the line + compensator match . From point of view of the V_3 line is naturally loaded. Similar equations and explanation can be deduced for other voltages.

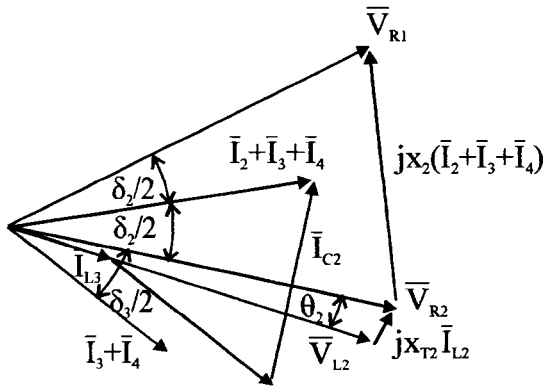

Fig.D.3 Phasor diagram showing relations among the voltages and currents from voltage V_{R1} to V_{R2} for circuit from Fig.D.1.

the rating of compensator Q_2 is (D.22)

$$Q_2 = \left[\overline{V}_{R2}\right]\bar{I}_{C2}\left| = \right|I_2 + I_3 + I_4\left|\sin\left(\frac{\delta_2}{2}\right) + \right|I_3 + I_4\left|\sin\left(\frac{\delta_3}{2}\right) + \right|I_{L2}|\sin\theta_2 \tag{D.22}$$

$$\mathbf{I_2=I_{L2}+ I_{C2}} \tag{D.23}$$

$$\left|\overline{V}_{L2}\right| = \sqrt{\frac{1+\sqrt{1-4\left((X_{T2})P_2\right)^2}}{2}} \tag{D.24}$$

$$\left|\bar{I}_{L2}\right| = \frac{P_2}{\left|\overline{V}_{L2}\right|} \tag{D.25}$$

$$\frac{\left|\overline{V}_{L2}\right|}{\left|\overline{V}_{R2}\right|} = \cos\theta_2 = \left|\overline{V}_{L2}\right| \tag{D.26}$$

From cosine theorem:

$$\left|\left(I_2 + I_3 + I_4\right)X_2\right| = \sqrt{\left|\overline{V}_{R1}\right|^2 + \left|\overline{V}_{R2}\right|^2 - 2\left|\overline{V}_{R1}\right|\left|\overline{V}_{R3}\right|\cos\delta_2} \Rightarrow \left|I_2 + I_3 + I_4\right| = \sqrt{2}\frac{\sqrt{1-\cos\delta_2}}{X_2} \tag{D.27}$$

$$\delta_2 = \arcsin\left(X_2\left(P_4 + P_3 + P_2\right)\right) \tag{D.28}$$

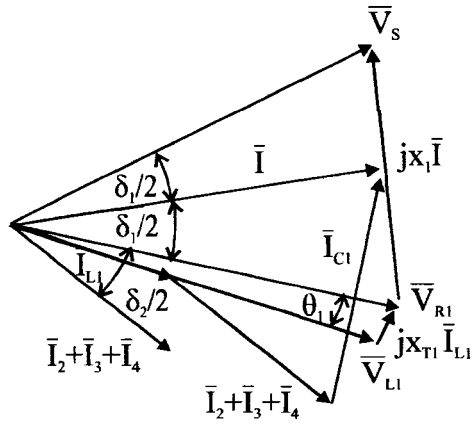

Fig.D.4 Phasor diagram showing relations among the voltages and currents from voltage V_S to V_{R1} for circuit from Fig.D.1

Finally, the rating of compensator Q_1 can be calculated from Fig. D.4 as (D.29):

$$Q_1 = \left[\overline{V}_{R1}\right]\bar{I}_{C1}\left| = \right|I_2 + I_3 + I_4\left|\sin\left(\frac{\delta_2}{2}\right) + \right|I\left|\sin\left(\frac{\delta_1}{2}\right) + \right|I_{L1}\left|\sin\theta_1\right. \tag{D.29}$$

$$\left|\bar{I}_{L1}\right| = \frac{P_1}{\left|\overline{V}_{L1}\right|} \tag{D.30}$$

$$\left|\overline{V}_{L1}\right| = \sqrt{\frac{1+\sqrt{1-4\left(\left(X_{T1}\right)P_1\right)^2}}{2}} \tag{D.31}$$

$$\frac{\left|\overline{V}_{L1}\right|}{\left|\overline{V}_{R1}\right|} = \cos\theta_1 = \left|\overline{V}_{L1}\right| \tag{D.32}$$

$$\delta_1 = \arcsin\left(X_1 P\right) \tag{D.33}$$

$$\left|IX_1\right| = \sqrt{\left|\overline{V}_{R1}\right|^2 + \left|\overline{V}_S\right|^2 - 2\left|\overline{V}_{R1}\right|\left|\overline{V}_s\right|\cos\delta_1} \Rightarrow \left|I\right| = \sqrt{2}\frac{\sqrt{1-\cos\delta_1}}{X_1} \tag{D.34}$$

and $\mathbf{I_1}=\mathbf{I_{L1}}+\mathbf{I_{C1}}$

Resume: each compensator correct power factor for the currents leaving bus where it is connected and provide the reactive needs for the half of the path between the bus where it keep voltage at 1 p.u and next bus where the next compensator keep its voltage at 1 p.u. It can be said that compensator balance reactive needs on the point of its coupling with grid.

Case 2:

Voltage support is provided on distribution level with 4 SVS as illustrated in Fig.D.5

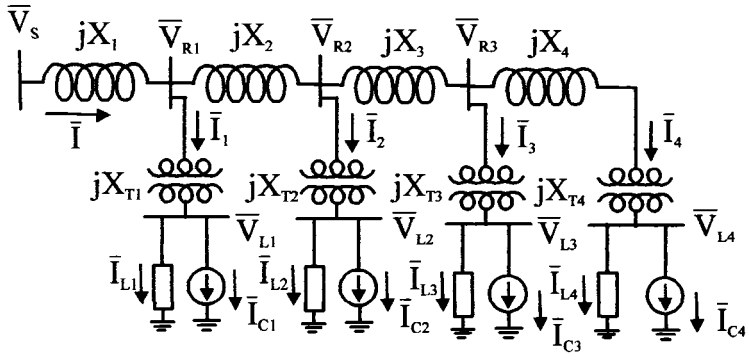

Fig.D.5

Compensation Requirement

To calculate reactive power needed for distribution side voltage regulation ($\mathbf{V_{Li}}$ =1 p.u.) first transmission side voltages $\mathbf{V_{Ri}}$ (i= 1,...N) has to be calculated. They are calculated from set of implicit equations as shown in (6.26) and for each node it can be written (D.35)

$$\frac{|V_{Ri}|-|V_{R(i+1)}|\cos\delta_{(i+1)}}{X_{i+1}}+\frac{|V_{Ri}|-|V_{R(i-1)}|\cos\delta_i}{X_i}+\frac{|V_{Ri}|-\cos\theta_i}{X_{Ti}}=0 \qquad \text{(D.35)}$$

where δi is power angle between voltages $V_{R(i-1)}$ and V_{Ri}, θ_i is power angle between voltages V_{Ri} and V_{Li}

it is known that $|V_{L1}|=|V_{L2}|=|V_{L3}|=|V_{L4}|$ 1p.u.

$|V_{R0}| = |V_S|=1$ p.u.

The power angles can be calculated from (D.36) and (D.37)

$P = \sum_{i=1}^{N} P_i$ where P is total power transferred over the line and Pi is power supplied to i-th load center. So it can be written(D.36) and (D.37):

$$P_i = \frac{|V_{Ri}||V_{Li}|}{X_{Ti}} \sin\theta_i \tag{D.36}$$

and $V_{Li} = 1$ p.u. so

$$\cos\theta_i = \frac{\sqrt{|V_{Li}|^2|V_{Ri}|^2 - P_i^2 X_{Ti}{}^2}}{|V_{Li}||V_{Ri}|} \tag{D.37}$$

The power transferred through i-th segment of the line is (C.38):

$$\sum_{k=i+1}^{N} P_k = \frac{|V_{Ri}||V_{R(i+1)}|}{X_{i+1}} \sin\delta_{i+1} \tag{D.38}$$

$$\cos\delta_{i+1} = \frac{\sqrt{|V_{R(i+1)}|^2|V_{Ri}|^2 - \left(\sum_{k=i+1}^{N} P_k\right)^2 X_{i+1}{}^2}}{|V_{R(i+1)}||V_{Ri}|} \tag{D.39}$$

substituting (D.37) and (D.39)into (D.35) we obtain (D.40):

$$|V_{Ri}| = \frac{1}{|V_{Ri}|\left[\frac{1}{X_{i+1}} + \frac{1}{X_i} + \frac{1}{X_{Ti}}\right]} \left[\frac{\sqrt{|V_{R(i+1)}|^2|V_{Ri}|^2 - \left(\sum_{k=i+1}^{N} P_k\right)^2 X_{i+1}^2}}{X_{i=1}} + \frac{\sqrt{|V_{R(i-1)}|^2|V_{Ri}|^2 - \left(\sum_{k=i}^{N} P_k\right)^2 X_2^2}}{X_i} + \frac{\sqrt{|V_{Ri}|^2 - P_i^2 X_{Ti}^2}}{X_{Ti}} \right] \tag{D.40}$$

what gives set of N algebraic implicit equations allowing to calculate voltages V_{Ri}.In this case Gauss-Seidel method has been used.

The current through each segment of the line can be computed from cosine theorem(D.41):

$$\left|\bar{I}_i\right| = \frac{\sqrt{\left|\bar{V}_{Ri}\right|^2 + \left|\bar{V}_{R(i-1)}\right|^2 - 2\left|\bar{V}_{Ri}\right|\left|\bar{V}_{R(i-1)}\right|\cos\delta_i}}{X_i} \tag{D.41}$$

the current through i-th substation can be calculated from cosine theorem applied on triangle formed by voltages V_{Ri}, V_{Li} and voltage drop across substation transformer:

$$\left|\bar{I}_{Li} + \bar{I}_{Ci}\right| = \frac{\sqrt{\left|\bar{V}_{Ri}\right|^2 + \left|\bar{V}_{Li}\right|^2 - 2\left|\bar{V}_{Ri}\right|\left|\bar{V}_{Li}\right|\cos\theta_i}}{X_{Ti}} \tag{D.42}$$

and finally compensating current I_{Ci} can be calculated from Pythagoras's theorem(C.43):

$$I_{Ci} = \sqrt{\left|I_{Li} + I_{Ci}\right|^2 - \left|I_{Li}\right|^2} \tag{D.43}$$

REFERENCES

[1] C.W. Taylor, *Power System Voltage Stability*, New York: McGraw-Hill, 1994.

[2] S.H.Horowitz and A.G. Phadke "Boosting Immunity to Blackouts", power & energy magazine, Sept./Oct. 2003, pp.47.

[3] D. Novosel, M. M. Begovic and V. Madani, "Shedding Light on Blackouts", IEEE power & energy magazine, Jan./Feb. 2004, pp.32.

[4] Bruce E. Wollenberg, "From Blackout to Blackout", IEEE power & energy magazine, Jan./Feb. 2004, pp.88.

[5] IEEE Special Publication, "Voltage Stability of Power Systems: Concept, Analytical Tools and Industry Experience", 90TH0358-2-PWR,1990.

[6] IEEE Special Publication, "Suggested Techniques for Voltage Stability Analysis", 93TH0620-5-PWR, 1993.

[7] IEEE Special Publication, "Voltage Stability Assessment: Concepts, Practices and Tools", IEEE Press 2003.

[8] R.H. Lasseter, "Control of Distributed Resources," in *Proc. Bulk Power Systems Dynamics and Control*, pp. 323-329, Greece, Aug. 23 – 28, 1998.

[9] T.J. Miller, *Reactive Power Control in Electric Systems*, New York: Wiley Interscience, 1982.

[10] L.Gyugyi, "Reactive Power Compensation and Control by Thyristor Circuits" IEEE 1976 PESC Conference Record, pp 174-184.

[11] R. Esliger, Y. Hotte and J. C. Roy, "Optimisation of Hydro Quebec's 735 kV Dynamic Shunt Compensated System Using Static Compensators on a Large Scale." PES winter Meeting, New York , Feb 1978.

[12] D. McGillis, N. Hieu Huynh and G. Scott "Role of Static Compensation in Meeting AC System Control Requirements with Particular Reference to the James Bay System", IEE Proc., Vol.128, No.6. pp. 389, Nov 1981.

[13] Ooi. B.T., Steady State Stability and Subsynchronous Resonance of Shunt Capacitor Compensated Transmission Lines", IEEE Transaction on Power Apparatus and System, vol.PAS-101, Sept.1982, no.9,pp.3269-3275.

[14] R. Mathur, " Static Compensators for Reactive Power Control", Canadian Electrical Association 1984.

[15] L. Gyugyi," Fundamentals of Thyristor Controlled Static VAr Compensators in Electric Power System application" IEEE Special Publication 87TH0187-5-PWR, 1987.

[16] N. G. Hingorani and L. Gyugyi, Understanding FACTS: Concepts and Technology of Flexible AC Transmission Systems, Wiley IEEE Press, December 1999.

[17] J. P. Ramos and H. Tyll, "Dynamic Performance of a Radial Weak Power System with Multiple Static VAr Compensators", IEEE Trans. on Power Systems Vol.4, No.4 October 1989.

[18] R. Grunbaum, M. Halonen and S. Rudin "ABB Static Var Compensator Stabilizes Namibian Grid Voltage" ABB Review, 2003, pp 43-48.

[19] H. Akagi, Y. Kanazawa and A. Nabae, "Instantaneous Reactive Power Compensators Comprising Switching Devices without Energy Storage Components," IEEE Trans. Ind. Applicat., vol. IA-20, no. 3, May./June. 1984, pp. 625-630.

[20] C.W.Edvards et al. "Advanced Static VAr Generator Employing GTO Thyristors", IEEE PES Winter Power Meeting, Paper No. 38WM109-1,1988.

[21] H.Mehta, T.W.Cease and L.Gyugyi, "Static Condenser for Flexible AC Transmission System" EPRI Flexible AC Transmission System (FACTS) conference, 18-20 May, 1992 Boston, MA.

[22] E.Larsen, N. Miller S. Nilsson and S. Lindgren. "Benifits of GTO-Based Compensations System for Electric Utility Applications, IEEE Trans. Power Delivery, vol.7, no.4 pp. 2056-2062, Oct.1992.

[23] L.Gyugyi, "Dynamic Compensation of AC Transmission Lines by Solid State Synchronious Voltage Source", IEEE Trans. Power Delivery, vol.9, no.2 pp. 904-911, April.1994.

[24] C. Schauder, M. Gerhardt, E. Stacey, T. Lemak, L. Gyugyi, T.W. Cease and A. Edris, "Development of a +/-100 MVAR Static Condenser for Voltage control of Transmission Systems" IEEE PES 1994 Summer Meeting, San Francisco, CA July24-28.

[25] K.K. Sen, "STATCOM-Static Synchronous Compensator : Theory, Modeling and Applications", IEEE, PES Winter Meeting 1999, Vol.2 pp.1177-1183.

[26] Paserba J., Larsen E., Lauby M., Leonard D., Nauman S., Miller N and Sener F.,"Feasibility Study for a Distribution-Level STATCON," FACTS Application, 1996, pp.8-22, 8-28, IEEE Catalog Number: 96TP 116-0.

[27] Koessler R, Fardanesh B., Henderson M.I. and Adapa R., "Feasibility Studies for STATCOM Application in New York State," pp. 8-46, 8-51, FACTS Application, 1996, pp.8-52, 8-58, IEEE Catalog Number: 96TP 116-0.

[28] Clark K., Doyle W.A., Sener F. and Smead M." STATCON Application Study - Potential Solution to Loss In-Feed", FACTS Application, 1996, pp.8-91, 8-96, IEEE Catalog Number: 96TP 116-0.

[29] W. McMurray, "Series Connection of Gate-Turnoff Thyristors" EPRI Report EL-5332, August 1987.

[30] A. Nabae, I. Takahashi and H. Akagi, "A New Neutral-Point-Clamped PWM Inverter," IEEE Trans. Ind. Applicat., vol. IA.17, no. 5, Sept./Oct. 1981 pp. 518-523.

[31] N. S. Choi, J. G. Cho, and G. H. Cho, A General Circuit Topology of Multilevel Inverte, IEEE 22nd Annual Power Electronic Specialist Conference, 1991, pp.96-103.

[32] P. M. Bhagwat and V. R. Stefanovic, Generalized Structure of a PWM Multilevel Inverte IEEE Trans. Ind. Applicat., vol. 19, no. 6, , Nov./Dec. 1983, pp. 1057-1069.

[33] Xiaoming Yuan and Ivo Barbi, *Fundamentals of a New Diode Clamping Multilevel Inverter* IEEE Trans. Pow. Electronics, vol. 15, no. 4, pp. 711-718, July 2000.

[34] S. Iida, S. Masukawa and Y Kubuta, et al., *Improved Voltage Source Inverter With 18-Step Output Waveformes,* IEEE Industry Applications Magazine, Jan/Feb. 1998.

[35] Lai S. and Peng F. Z., *Multilevel Converters - A New Breed of Power Converters*, IEEE Trans. Ind. Applicat., vol. 32, May/June 1996, no.3, pp 509-517.

[36] Menzies W. and Zhuang, Y.: *Advanced Static Compensation Using a Multilevel GTO Thyristor Inverter*, IEEE Transaction on Power Delivery, vol.10, April 1995, no.2, pp. 732-738.

[37] Ekanayake B. and Jenkins N.: *A Three-level Advanced Static Var Compensator*, IEEE Transaction on Power Delivery, vol.11, Jan.1996, no.1, pp. 540-545.

[38] Hochgraf C. and Lasseter R. H.: *A Transformer-less Static Synchronies Compensator Employing a Multi-level Inverter*, IEEE Transaction on Power Delivery, vol.12, April 1997 no.2, pp. 881-887.

[39] S.Kincic, A.Chandra and S.Babic "Five Level, Diode-Clamped Voltage Source Inverter and Its Application in Reactive Power Compensation" LESCOPE 2002, July 26-28, 2002, , pp.86-92, Halifax, Nova Scotia, Canada.

[40] S.Kincic, A.Chandra and S.Babic "Power Factor Correction of Single Phase and Three Phase Unbalanced Loads using Multilevel Inverter" LESCOPE 2001, July 11-13, 2001,pp.131-138, Halifax, Nova Scotia, Canada.

[41] Vijay K. Sood, " Position Paper on FACTS Technology" Canadian Electricity Association, February 1996.

[42] B. T. Ooi and X. Wang, " Boost Type PWM-HVDC Transmission System," IEEE Transaction on Power Delivery, vol.6, Oct.1991, no.4, pp. 1557-1563.

[43] X.Wang, Shu-Zu Dai and B.T.Ooi, "A series Capacitive Reactance Compensator Based on Voltage Source PWM Converter", presented at IEEE-IAS Annual Meeting, pp. 918-924, Sept./Oct 1991.

[44] B.T. Ooi, S.Z. Dai and F.D. Galiana, "A Solid State PWM Phase Shifter", IEEE Transaction on Power Delivery, vol.8, Apr.1993, no.2, pp. 573-579.

[45] B.T. Ooi and S.Z. Dai "Series Type Solid State Static Var Compensator", IEEE Transaction on Power Electronics, vol.8, Apr.1993, no.2, pp. 164-169.

[46] Mwinyiwiwa B., Wolanski Z and, Ooi B.T.: *High Power Switch Mode Linear Amplifiers for Flexible AC Transmission Systems*, IEEE Transaction on Power Delivery, vol.11, Oct.1996, no.4, pp. 1993-1998.

[47] "The Hagfors SVC Light: a world first" ABB utilities AB Power System

[48] "The Moselstahlwerk SVC light" ABB utilities AB Power System

[49] W.K.Wong, D.L.Osborn and J.L.McAvoy, "Application of Compact Static VAr Compensators to Distribution System,"*IEEE Trans. Power Delivery*, vol. 5,No.2, pp. 1113-1120, Apr. 1990.

[50] R.J.Koessler,"Dynamic Simulation of Static VAr Compensator in Distribution Systems," *IEEE Trans. Power Sysy*, vol. 7,No.3, pp. 1285-1291, Aug. 1992.

[51] A.E.Hammad and M.Z. El-Sadek," Prevention of Transient Voltage Instabilities due to Induction Motor Loads by Static VAr Compensators", *IEEE Trans. Power Systems*, vol. 4, No.3, pp.1182-1190, August 1989.

[52] Paserba J.J., Leonard D.J., Miller N.W, Nauman S.T., Lauby M.G., Lauby M and Sener F.P, "Coordination of a Distribution Level Continuously Controlled Compensation Device with Existing Substation Equipment for Long Term VAr Management" ", *IEEE Trans. Power Delivery*, vol. 9, pp. 1034-1040, Apr. 1994.

[53] J. CR. Clouston and J.H.Gurney," Field Demonstration of a Distribution Static Compensator Used to Mitigate Voltage Flicker," PES Winter Meeting 2002.

[54] S. Kolluri," Application of Distributed Superconducting Magnetic Energy Storage System (D-SMES) in the Entergy System to Improuve Voltage Stability," PES Winter Meeting 2002.

[55] John A.Diaz de Leon II and C.W. Taylor," Understanding and Solving Short-Term Voltage Stability Problems," PES Winter Meeting 2002.

[56] S.Kincic and A. Chandra, "Distribution Level STATCOMs (DSTATCOMs) for Load Voltages Support", LESCOPE 2003, 7-9 May, Montreal

[57] S.Kincic and A. Chandra, "Impact of Distributed Compensators on Power System Voltages", CCECE 2003, 5-7 May, Montreal.

[58] B.T.Ooi, S.Kincic, X.Wan, D.McGillis, A.Chandra, F.D. Galiana and G. Joos, "Distributed Static VAr Systems for Regulated Voltage Support in Load Centers, " PES General Meeting, 13-18 July,2003, Toronto.

[59] S.Kincic, X.Wan, D.McGillis, A.Chandra, B.T.Ooi, F.D. Galiana and G. Joos, "Voltage Support by Distributed Static VAr Systems " IEEE Trans. on Power Delivery, Vol.20.No.2,April 2005, pp1541-1549.

[60] Y. Chen, B. Mwinyiwiwa, Z. Wolanski and B. T. Oou," Regulating and Equalizing DC Capacitans Voltages in Multilevel Statcom," IEEE Trans. Power. Delivery, vol. 12, no. 2, April. 1997, pp. 901-907.

[61] S. Kincic "Onduleur à nivaux multiples et son application en compensation de puissance reactive" Mémoire de la maîtrise, ETS, Mai 2000

[62] S.Kincic, A.Chandra, B.N.Singh and P.Rastgoufard "Real Time Simulation With Two Novel Control Algorithms" 10th IEEE Mediterranean Conference on control Automation,. Portugal, 2002

[63] S.Kincic, A.Chandra, Z.Huang and S.Babic "Simulation Study on Enhancement of Maximum Power Transfer Capability of Long Transmission Line With Midpoint Sitting STATCOM for Voltage Support" EPE-PEMC 2002 Cavtat &Dubrovnik.

[64] B.T. Ooi and X. Wang,"Voltage Angle Lock Loop Control of Boost Type PWM Converter for HVDC Application,"IEEE Trans. power Electronics, Vol.5No.2,pp.229-235, Apr.1990.

[65] Ooi B. T., Kazerani M., Wolanski Z., Galiana F.D., McGillis D., Joos G. and Marceau G, "*Midpoint Siting of FACTS Devices in Transmission Lines*," IEEETransaction on Power Delivery, vol.12, Oct. 1997, no.4, pp.1717-1722.

[66] Z. Huang and B.T. Ooi, "Power Transfer Capability of Long Transmission Lines with Midpoint Sited Facts and HVDC," IEEE Power Engineering Review, Vol.22, No.5, pp. 51-53, May 2002.

[67] Z. Huang, B.T. Ooi, L.A. Dessaint and F.D. Galiana, "Exploiting Voltage Support of Voltage Source HVDC," IEE Proceedings-Generation, Transmission andDistribution, Vol.150, No.2, pp.252-256, Mar.2003.

[68] K. Kahle, J. Pedersen, T. Larsson and M.M de Oliveira "The New 150 Mvar kV Static Var Compensator at CERN: Background, Design and Commissioning" 17th International Conference on Electricity Distribution, Barcelona, 12-15 May 2003.

[69] R.M. Mathur and R. K. Varma, Thyristor-Based FACTS Controllers for ElectricalTransmission Systems, IEEE Press, 2002.

[70] J. Van Coevering, J. P. Stovall, R. L. Hauth, P.J. Tatro, B. D. Railing and B. K. Johnson," The Next Generation of HVDC - Needed R&D, Equipment Costs and Cost Comparisons", Proceedings of EPRI Conf. on Future of Power Delivery, Washington DC, April 1996.

[71] D. McGillis,"Principles and practice of transmission system planing",4th Int. Tesla Symp. Belgrade, Yugoslavia , Sept.1991.

[72] *Power System Simulator-HYPERSIM*: User's Manual, DMNU-5700-1.3A, TEQSIM International INC., June 1999.

[73] IEEE Task Force on Load Representation for Dynamic Performance, "Load Representation for Dynamic Performance Analysis", IEEE Trans. on Power Systems, Vol.8, No.2, May 1993.

[74] IEEE Task Force on Load Representation for Dynamic Performance, "Standard Load Models for Power Flow and Dynamic Performance Simulation", IEEE Trans. on Power Systems, Vol.10, No.3, August 1995.

[75] B. R. Williams, W. R. Schmus and D. C. Dawson, " Transmission Voltage Recovery Delayed by Stalled Air Conditioners", IEEE Trans. on Power Systems, Vol.7, No.3, pp.1173-1178, August 1992.

[76] John W. Shaffer, "Air Conditioner Response to Transmission Faults" IEEE Trans.on Power Systems, Vol.12, No.2, pp.614-621, May 1997.

[77] Walter A. Elmore, "Protective Relaying Theory and Application" ABB Power T&D Company Inc. Relay Division, Coral Springs, Florida 1994 pp.334.

[78] S.Kincic, B.T.Ooi , D.McGillis and A.Chandra,,"Voltage Support of Radial Transmission Lines by VAr Compensation at Distribution Buses", Proceedings-Generation, Transmission and Distribution Vol. 153, pp.5 -58, Jan. 2006.